HALOALKANE DEHALOGENASES IN BIOCATALYSIS

kinetic resolution and beyond

Alja Westerbeek

Cover design: Joost Groeneveld, Maarten Groeneveld and Alja Westerbeek

Printed by: Ipskamp drukkers

ISBN: 978-90-367-5569-6 (electronic)

ISBN: 978-90-367-5570-2 (printed)

This Ph.D. study was carried out in the Biotransformation and Biocatalysis Department of the Groningen Biomolecular Sciences and Biotechnology institute (GBB) of the University of Groningen and was financially supported by the B-Basic program.

rijksuniversiteit groningen

Haloalkane dehalogenases in biocatalysis

kinetic resolution and beyond

Proefschrift

ter verkrijging van het doctoraat in de
Wiskunde en Natuurwetenschappen
aan de Rijksuniversiteit Groningen
op gezag van de
Rector Magnificus, dr. E. Sterken,
in het openbaar te verdedigen op
maandag 11 juni 2012
om 12.45 uur

door

Alja Westerbeek
geboren op 20 september 1983
te Meppel

Promotores:	Prof. dr. D.B. Janssen
	Prof. dr. B.L. Feringa
Beoordelingscommissie:	Prof. dr. B.W. Dijkstra
	Prof. dr. K.U. Loos
	Prof. dr. J.G. Roelfes

CONTENTS

CHAPTER 1

General introduction and outline of the thesis

HALOALKANE DEHALOGENASES AND THEIR DISCOVERY

Haloalkane dehalogenases (EC 3.8.1.5) are hydrolytic enzymes that catalyse the cleavage of a carbon-halogen bond in haloalkanes, producing the respective alcohols. The first haloalkane dehalogenase was discovered and described by Keuning *et al* in 1985.[1] This enzyme, named DhlA, was isolated and cloned from *Xanthobacter autotrophicus* GJ10, which is able to utilise 1,2-dichloroethane for growth.[2,3] Since this discovery, various other proteins with dehalogenase activity were isolated and partially characterised.[4-6]

Nagata and coworkers described in 1993 the cloning and sequencing of haloalkane dehalogenase LinB from *Sphingomonas paucimobilis* UT26, which is able to degrade the bulky compound 1,3,4,6-tetrachloro-1,4-cyclohexadiene, as part of the degradation pathway of the insecticide γ-hexachlorocyclohexane (lindane).[7,8] In 1997, Kulakova and coworkers described a haloalkane dehalogenase (DhaA) isolated from a strain of *Rhodococcus rhodochrous*, that is able to grow on 1-chlorobutane.[9] These three enzymes, DhlA, LinB and DhaA, have been investigated in great detail, including substrate specificity and structure.

As genome sequencing became available, more putative haloalkane dehalogenases genes were assigned, cloned and the enzymes were biochemically characterised. In 2005, two rhizobial strains, *Mesorhizobium loti* MAFF303099 and *Bradyrhizobium japonicum* USDA110, were found to possess genes encoding haloalkane dehalogenases, which were named DmlA and DbjA respectively.[10] Haloalkane dehalogenase genes were also found in pathogenic *Mycobacteria*, like *M. avium* N85 (DhmA),[11] *M. bovis* (DmbA, DmbB and DmbC),[12,13] in *M. tuberculosis* (with >99% sequence identity with DmbA from *M. bovis*[14]) and in the marine bacterium *Rhodopirellula baltica* SH1 (DrbA).[13] From *Bradyrhizobium elkani* USDA94 an enzyme called DbeA was isolated.[15] More recently, haloalkane dehalogenases from the plant pathogen *Agrobacterium tumefaciens* C58 (named DatA)[16] and from the marine bacterium *Plesiocystis pacifica* SIR-1 (DppA)[17] were identified.

It can be concluded that the haloalkane dehalogenases present in various bacterial strains are involved in haloalkane biodegradation pathways. They also occur in other organisms, like *Rhizobiaceace* and in various pathogens, where their function remains unclear.[12]

TOPOLOGY OF HALOALKANE DEHALOGENASES

Haloalkane dehalogenases belong to the α/β-hydrolase fold family, which was first discovered by comparison of the crystal structures of five hydrolytic enzymes.[18] Since then, more members were added to the group,[19] which now includes among others, epoxide hydrolases,[20] proteases, lipases[21] and esterases.[22,23]

The secondary structure of these enzymes consists of a conserved basic fold of eight β-strands, where all, except the second strand, are parallel and where β-strands 3-8 are

connected to each other by five α-helices (Figure 1). At various positions inserts may be present and in most cases a so-called cap domain exists, starting from the C-terminal end of β-strand 6 (Figure 1). It closes the enzyme, shielding the catalytic residues from the environment, yet allowing substrate binding.[24]

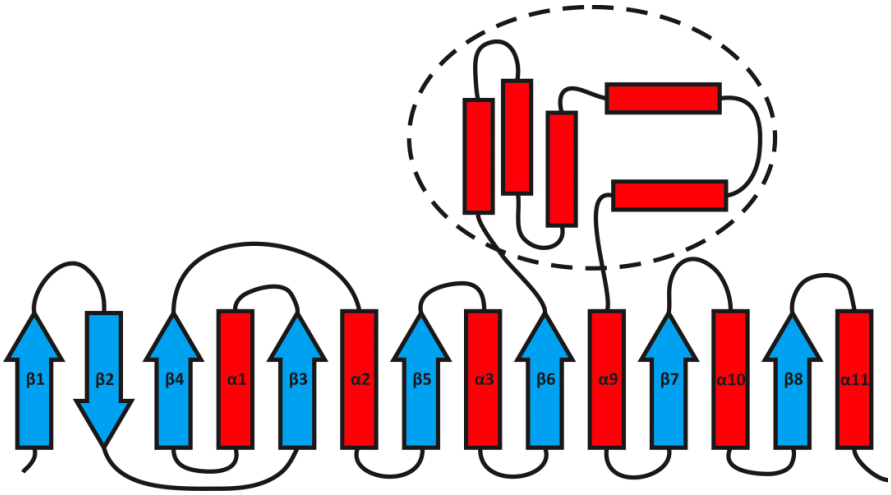

Figure 1: Topology of haloalkane dehalogenases, where a cap domain (in dashed circle) is connected to the conserved structure of the α/β-hydrolase fold.

The active site is buried between the conserved α/β-hydrolase main domain and the variable cap domain. Although the catalytic activity of the enzymes assigned to the α/β-hydrolase fold group varies, they possess a highly conserved catalytic triad which consists of a nucleophilic residue (in the loop after β-strand 5), an acidic residue (usually in the loop after β-strand 7) and a conserved histidine (in the loop after the last β-strand).[19] Furthermore, a so-called oxy-anion hole is used in the catalytic mechanism, where the negative charge, formed in the transition state, is stabilised by two backbone NH groups. One of these NH groups is donated by a residue that is always located immediately after the nucleophilic residue in the primary structure of the protein, while the position of the second residue in the sequence can vary.[19]

CATALYTIC MECHANISM

In all haloalkane dehalogenases, the nucleophile is a conserved aspartate residue, whose carboxylate group attacks the halogen-bearing carbon atom of the substrate (panel A, Figure 2), forming a covalent intermediate in an S_N2-type process. The histidine residue activates a water molecule that hydrolyses the formed ester bond (panel B, Figure 2).

Subsequently, the product and halide ion are released (panel C, Figure 2). The histidine, which is involved in the activation of a water molecule, is assisted in its function by an acidic residue, either an aspartate or a glutamate.[25]

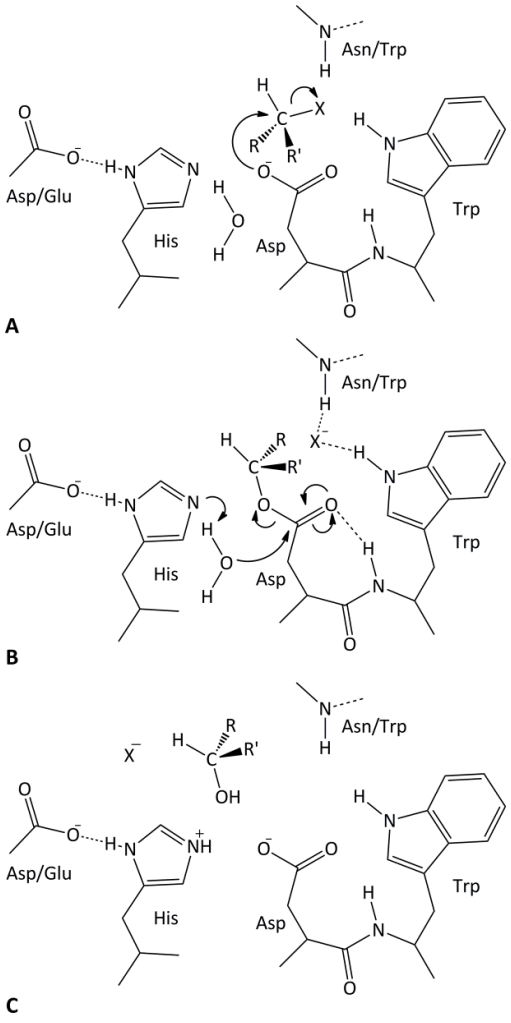

Figure 2: The catalytic mechanism of haloalkane dehalogenases, panel A to C: formation of the covalent intermediate; its hydrolysis; and the release of the product.

Two other residues activate the halogen atom and later stabilise the halide ion that is formed during the course of the reaction. One of these residues is a conserved tryptophan, flanking the nucleophilic aspartate in the sequence. The other can either be a second tryptophan or an asparagine. These two residues form, together with the catalytic triad, the so-called catalytic pentad. From the stereochemical point of view, the

haloalkane dehalogenase-catalysed reaction proceeds with inversion of configuration at the halogen-bearing carbon atom (S_N2-type nucleophilic substitution), followed by a reaction with retention of configuration (the hydrolysis of an ester). Per saldo, an inversion of configuration is observed.[25] The structure and active site of LinB are displayed in Figure 3 and 4, respectively.[26]

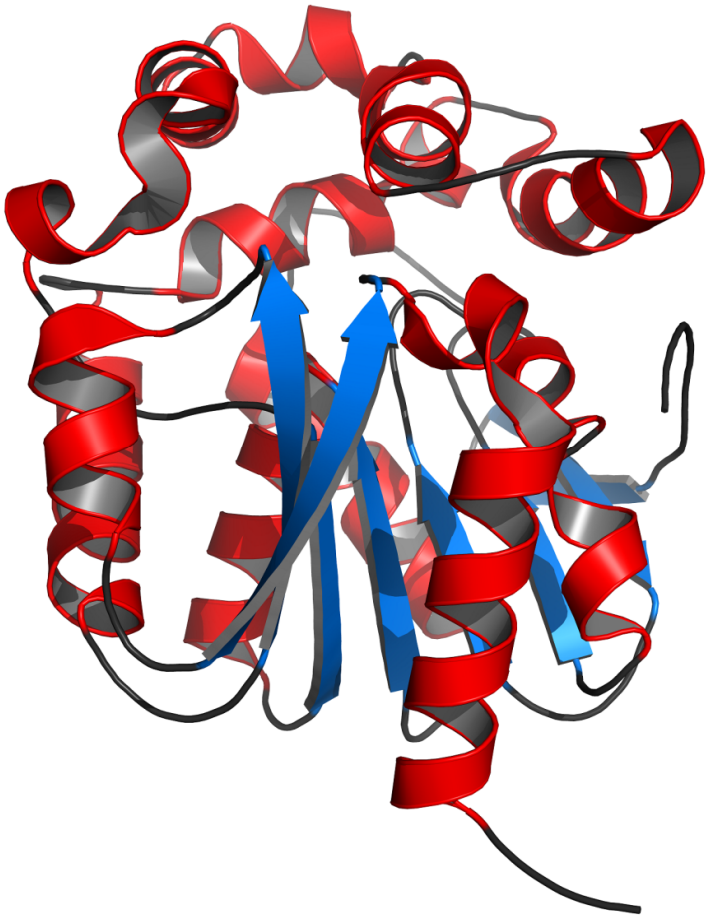

Figure 3: Crystal structure of LinB: α-helices are in red; β-sheets are in blue; loops are in grey, generated from pdb file 1MJ5.[26]

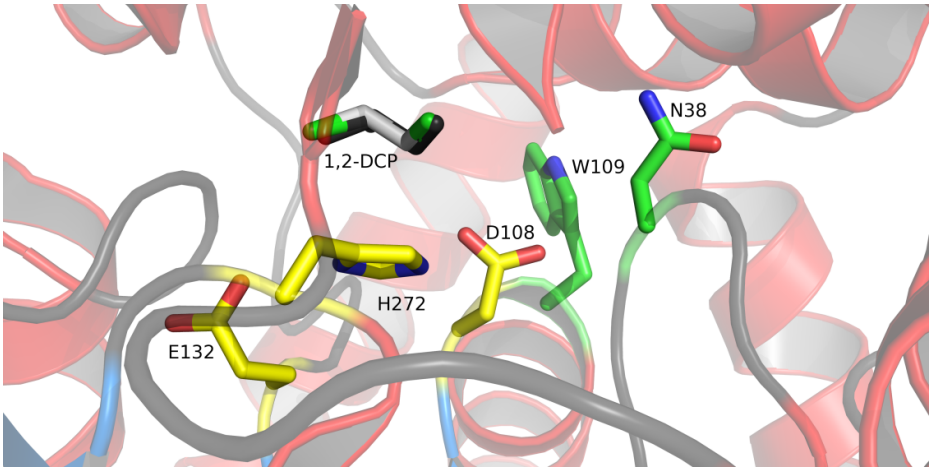

Figure 4: Active site with catalytic pentad and substrate 1,2-dichloropropane of LinB generated from pdb file 1G42.[26] In yellow is the catalytic triad with the nucleophilic aspartate (D108), the histidine (H272), which activates a water molecule and its assisting glutamate (E132). The halide-binding trypthophan (W109) and asparagine (N38) are displayed in green.

CATEGORISATION OF HALOALKANE DEHALOGENASES IN SUBFAMILIES

On basis of phylogenetic analysis, the haloalkane dehalogenases can be divided in three subfamilies. For each subfamily, the residues that form the catalytic pentad are different.[27] As described before, the nucleophilic aspartate, the histidine and the halide-stabilising tryptophan are conserved. The assisting acid can either be an aspartate in the loop after β-strand 7 or a glutamate in the loop after β-strand 6 (Figure 5). The second halide-stabilising residue can be either another tryptophan in the cap domain or an asparagine after β-strand 3 (Figure 5). Therefore, for subfamily I, the catalytic pentad is Asp-His-*Asp*-*Trp*-Trp, for subfamily II, Asp-His-*Glu*-*Asn*-Trp, and for III, Asp-His-*Asp*-*Asn*-Trp (Figure 5).[27]

Besides the variation that can be seen in the catalytic pentad, the most variable part among the different haloalkane dehalogenases is the cap domain (Figure 6). Unlike the main domain, the cap domain is a flexible region and its frequent motions, which could be involved in determining substrate specificity, were observed in MD simulations.[28] For DhlA, the most flexible region is the part of the protein that connects the rigid α/β-hydrolase fold domain and the cap domain, which is α-helix 4 in Figure 5.[28] In subfamily I, this helix is longer than in subfamily II/III. Furthermore, helix 5' is missing in subfamily I and is replaced by a loop. Helices 5, 6 and 5' form the tunnel opening for substrates. Because of the extra helix 5' in subfamily II, the entrance tunnels of DhaA and LinB are wider than of DhlA (subfamily I) and therefore allow the binding of bulkier substrates.[28,29]

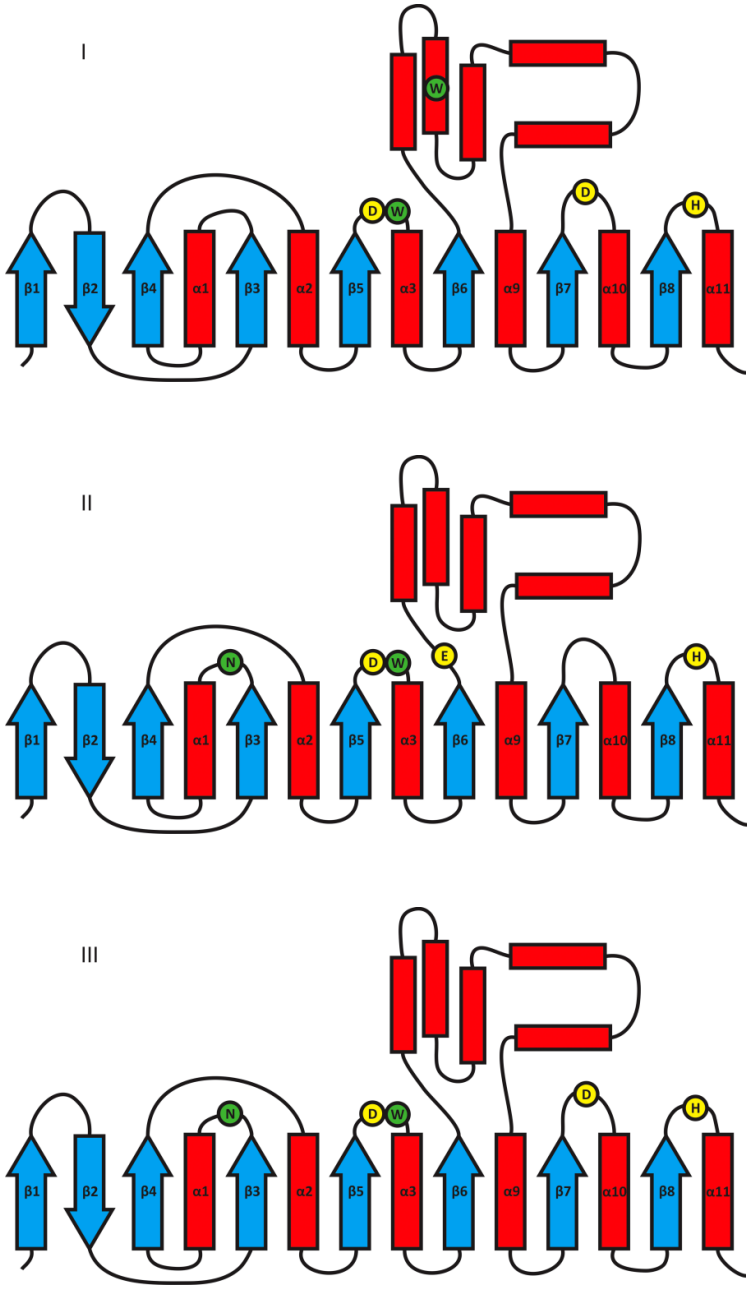

Figure 5: The topology of haloalkane dehalogenases, divided into three subfamilies. Secondary structures: α-helices and β-strands are depicted in blue and red, respectively (arrows up: parallel, arrows down: anti-parallel). The catalytic triad residues are depicted in yellow and the halide-binding residues are in green.

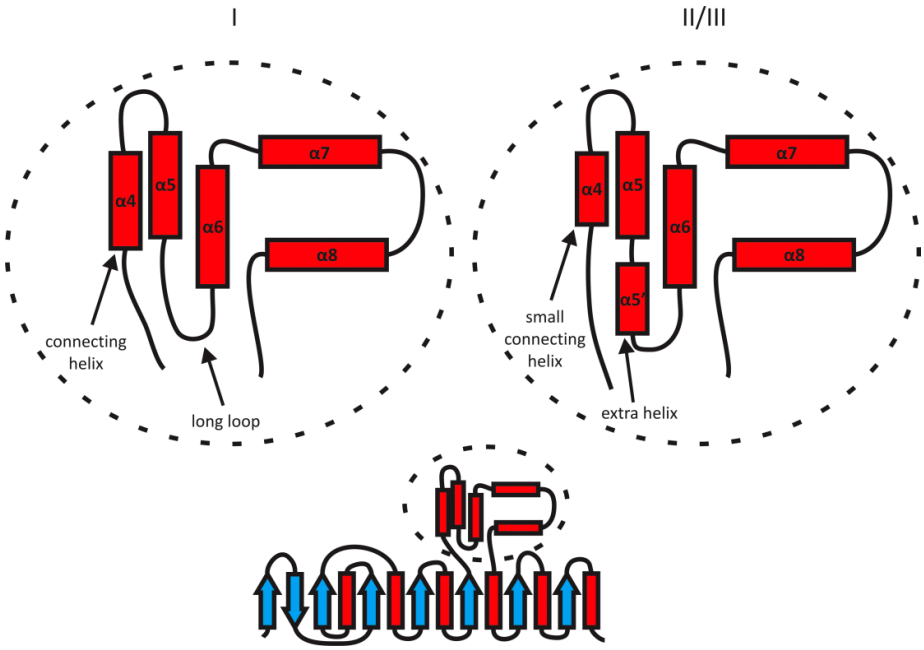

Figure 6: Structure of the cap domain, which significantly differs between subfamily I and subfamilies II/III.

The volume of the active site cavity varies among the enzymes and is determined by the cap domain. Volume calculations of the active site cavity, using a structure with 1,2-dichloroethane bound, revealed that DhlA, has the smallest cavity, with only 129 $Å^3$ volume, when compared to LinB, DmbA and DhaA with 319, 379, 261 $Å^3$, respectively.[30] The cavity and tunnel size generally determine the substrate specificity of the enzyme. Haloalkane dehalogenases with a small tunnel and small cavity are efficient in converting smaller substrates (DhlA) and haloalkane dehalogenases from subfamily II are generally better in converting bulkier substrates.[30]

To date, crystal structures were solved for five haloalkane dehalogenases (Table 1): DhlA (subfamily I),[31] DhaA (subfamily II),[32] LinB (subfamily II),[26] DbjA (subfamily II),[33] and DmbA (subfamily II).[30] No crystal structure was solved for a haloalkane dehalogenase from subfamily III yet.

Table 1: List of characterised haloalkane dehalogenases, divided into the three subfamilies

Subfamily	Enzyme	Organism	Structure available?	Reference discovery
I	DhlA	*Xantobacter autotrophicus*	Yes[31]	[1]
	DhmA	*Mycobacterium avium*	No	[11]
	DmbB	*Mycobacterium bovis*	No	[12]
	DppA	*Plesiocystis pacifica*	No	[17]
II	LinB	*Sphingomonas paucimobilis*	Yes[26]	[7]
	DhaA	*Rhodococcus rhodochrous*	Yes[32]	[9]
	DbjA	*Bradyrhizobium japonicum*	Yes[33]	[10]
	DmlA	*Mesorhizobium loti*	No	[10]
	DmbA	*Mycobacterium bovis*	Yes[30]	[12]
	DatA	*Agrobacterium tumefaciens*	No	[16]
	DmsA	*Mycobacterium smegmatis*	No	U.D.
	DbeA	*Bradyrhizobium elkani*	No	[15]
III	DmbC	*Mycobacterium bovis*	No	[13]
	DrbA	*Rhodopirellula baltica*	No	[13]

U.D.: described as unpublished data by Chovancová.[27]

The catalytic mechanism of a haloalkane dehalogenase-catalysed reaction includes four steps: binding of the substrate, formation of the alkyl-enzyme intermediate including cleavage of the carbon-halogen bond, hydrolysis of the covalent intermediate and release of the alcohol and the halide (Scheme 1).[34]

$$E + RX \underset{k_{-1}}{\overset{k_1}{\rightleftharpoons}} E.RX \xrightarrow{k_2} E\text{-}R.X \xrightarrow{k_3} E.ROH.X^- \xrightarrow{k_4} E + ROH + X^-$$

Scheme 1: Schematic overview of a haloalkane dehalogenase-catalysed reaction: binding of the substrate, formation of the alkyl-enzyme intermediate including the cleavage of the carbon-halogen bond, hydrolysis of the intermediate and release of the products.

The overall mechanism is similar for all known haloalkane dehalogenases, however the rate-limiting step varies from enzyme to enzyme and from substrate to substrate.[35] For DhlA, the release of the halide was the main rate-limiting step for 1,2-dichloroethane and 1,2-dibromoethane.[36] Two routes were described for this step, where for both enzyme isomerisation is involved. In one route the enzyme isomerisation mechanism involves

motions in the cap domain of the enzyme that create an extra space and allow water molecules to enter and the solvated halide to be released from the active site. For the other route, it was suggested that the enzyme is isomerised to a so-called collision complex, where the halide can bind on the protein surface and subsequently gets released.[36,37]

For DhaA, the release of the product 3-bromo-1-propanol was described to be the slowest step in the conversion of 1,3-dibromopropane. For 1,2-dibromopropane, the rate-limiting step was suggested to be the alcohol release, however other steps, as halide release, could not be ruled out.[34]

For LinB, the rate-limiting step for the conversion of chlorocyclohexane, bromocyclohexane and 1-chlorohexane was found to be the hydrolysis of the alkyl-enzyme intermediate. Remarkably, the release of the products (k_4) was found to be a fast process.[35]

When the structures of DhlA, DhaA and LinB are compared, it can be seen that the active site of DhlA has the smallest entrance tunnel and is more buried in the protein, and therefore is more shielded from the solvent.[29] This was suggested to be a reason for the slow halide release step.[34] The K_D for binding of chloride was found to be much lower for DhlA than for LinB.[35,38] The halide-binding residues for DhlA, two tryptophans, bind stronger to the halide than the residues in LinB, one tryptophan and one asparagine.[35] The active site of LinB is even more exposed to solvent than those of DhlA or DhaA,[29] which would allow the products to be released fast, as was confirmed by MD simulations.[28] Differences in these kinetic mechanisms are remarkable. Even for DhaA and LinB, which were both from subfamily II, the rate-limiting step is not the same.

SUBSTRATE SPECIFICITY AND BIOCATALYSIS BY HALOALKANE DEHALOGENASES

Haloalkane dehalogenases DhlA and DhaA were discovered in bacterial cultures able to grow on 1,2-dichloroethane and 1-chlorobutane, respectively. However, the substrate specificity is not restricted to these simple compounds, as other haloalkanes, haloesters or haloamides are also converted. In general, the substrate specificity is broad, but can vary strongly among the different enzymes. In this section the substrate specificity for each enzyme is described.

Subfamily I haloalkane dehalogenase DhlA has a compact active site and a narrow entrance tunnel, and therefore converts only relatively small substrates. DhlA can convert simple monohaloalkanes, such as terminally substituted bromomethane, chloromethane, 1-chloroethane, 1-chloropropane and 1-bromopentane, and dihaloalkanes, such as 1,2-dibromoethane, 1,2-dichloroethane and 1,3-dichloropropane.[1] Low activities were reported for 1-chloropentane and 1-chlorohexane. Longer chloroalkanes, from 1-chloroheptane on, are not converted.[39] Activity towards other substrates is restricted, as

with haloalcohols, haloamides and haloacids low activities or no activity was reported.[1,39] For epoxides such as epichlorohydrin and epibromohydrin good activities were reported.[2,39]

DhmA, another characterised subfamily I haloalkane dehalogenase, can also convert small compounds. Like DhlA, and unlike any other of the characterised haloalkane dehalogenases, it is able to convert 1,2-dichloroethane. Comparable activities were reported towards 1,2-dibromoethane, 1,3-dibromopropane, 1-chloropentane and 1,2,3-tribromopropane.[11]

For DppA of subfamily I, a high specific activity (4.5 U/mg) was found towards 1-bromobutane. Furthermore, conversions with 1-bromopropane, 1-bromopentane, up to 1-bromodecane were reported. However, small chloro-substituted haloalkanes, such as 1-chloropropane, 1-chlorobutane and 1-chloropentane were not converted. Remarkably, 1,2-dichloroethane, a very good substrate for DhlA and DhmA was not converted by this subfamily I haloalkane dehalogenase, neither were the tested haloacids, haloalcohols and epibromohydrin.[17]

The substrate specificity of another characterised enzyme from subfamily I, DmbB, was only briefly described. Activity was reported towards 1,2-dibromoethane (0.3 U/mg), 1,2-dibromopropane, 6-bromohexanol and epibromohydrin.[12,27]

LinB from subfamily II is known to convert large and bulky substrates, as is already suggested by its original role in lindane degradation and its relatively large active site cavity.[8] Long chloroalkanes are generally good substrates; activities were reported for compounds ranging from 1-chloropropane up to 1-chlorodecane. Also the activity towards secondary haloalkanes was reported: 2-chlorobutane, 2-chlorooctane and 3-chlorohexane. A simple compound, 1,2-dichloroethane, was not converted, but the related 1,2-dibromoethane was a good substrate.[8,39] Some cyclic compounds related to the "natural" substrate (1,3,4,6-tetrachloro-1,4-cyclohexadiene), i.e. bromocyclohexane and bromomethylcyclohexane as well as bromocycloheptane, are converted by LinB, albeit no activity was detected with bromocyclopentane.[39] High activity was reported with larger haloalcohols, 4-chlorobutanol and 6-chlorohexanol. Conversion of chlorinated acids, e.g. 2-chloropropionic acid and 3-chlorobutyric acid was not detected.[8] Activity towards β-bromoalkanes (2-bromobutane to 2-bromohexane) and α-bromoesters was reported.[33]

DhaA has a similar substrate scope as LinB. Conversion was reported with long chloroalkanes (up to 1-chlorodecane), haloalcohols, β-bromoalkanes and α-bromoesters.[33,39]

DbjA shows by far the highest activity towards 1,2-dibromoethane (~12 U/mg protein).[10] Furthermore, good activities were found for 1,3-dibromopropane and 3-chloro-2-methylpropene. DbjA also converts long α-haloalkanes up to 1-chlorodecane and bromo- and chlorocyclohexane.[10]

DmlA is active towards the same compounds as DbjA. The highest specific activity was found for 1,3-dibromopropane, albeit only 18 mU/mg of protein. Also for 1-bromobutane, bromocyclohexane and 3-chloro-2-methylpropene, a relatively high activity was found.[40]
DmbA was found to have a quite high activity with 1,2-dibromoethane (13 U/mg) as well as with 1,3-dibromopropane. Activity was also described towards 1-chlorobutane.[12]
For the very recently described DatA from the plant pathogen *Agrobacterium tumefaciens*, activity was highest for 1,3-dibromopropane (~1.4 U/mg), 1-bromohexane, 1-bromo-3-chloropropane and iodopentane. The substrate 1,2-dibromoethane, which is well converted by most of the haloalkane dehalogenases, was not a substrate for DatA. On the other hand, α-bromoesters and β-bromoalkanes, like ethyl 2-bromopropionate and 2-bromohexane were converted.[16]
The characterisation of DmsA is preliminary and data are not published yet.[27] Also for DbeA only preliminary results were published by Prudnikova *et al*. [15]
Two enzymes from subfamily III, DrbA and DmbC, and their specificity were recently described.[13] For DrbA, the highest activity was measured with 1-iodobutane, however a specific activity of only 30 mU/mg was reported. Relatively high specific activities were described for 1,3-diiodopropane (22 mU/mg) and 1-chlorobutane (17 mU/mg). No activity was detected for 1,2-dichloroethane, 1,2-propane, 1,2-pentane, 1,3-dibromopropane and 1,2,3-trichloropropane.[13]
The specific activities of DmbC were found to be in general higher than those of DrbA. Higher activities were also found with 1,3-diiodopropane (0.40 U/mg) and 1-iodobutane (0.15 U/mg). The second highest activity was reported for 1,3-dibromopropane (0.30 U/mg), where no activity was found with DrbA.[13]
Haloalkane dehalogenases were found to catalyse the cleavage of carbon-chlorine, carbon-bromine and carbon-iodine bonds. No activity was found towards carbon-fluorine bonds, known to be the strongest carbon-halogen bond.[41,42] However, a biocatalytic cleavage of a carbon-fluorine bond has been described for a haloacid dehalogenase. This enzyme also belongs to the same α/β hydrolase fold family and was found to be able to hydrolyse the carbon-fluorine bond in fluoroacetate.[41] Other haloacid dehalogenases were not found to be able to hydrolyse a carbon-fluorine bond.[43]

ENANTIOSELECTIVITY OF HALOALKANE DEHALOGENASES

Enantioselective methods for the preparation of chiral compounds are of crucial importance for medicinal chemistry, as the biological activity of the enantiomers of a drug can differ. An example of such a drug is naproxen, an anti-inflammatory drug, used in the treatment of arthritis. The (*S*)-enantiomer of this molecule gives the desired effect, whereas the (*R*)-enantiomer cause side effects, like gastro-intestinal disorders.[44]

Enzymes can play an important role in the preparation of enantiopure building blocks for medicines. They are built up of only L-amino acids and therefore are homochiral molecules themselves. The chiral catalytic center can display enantioelective recognition of a substrate and lead to enantioselective preparation of its product (Scheme 2).[45]

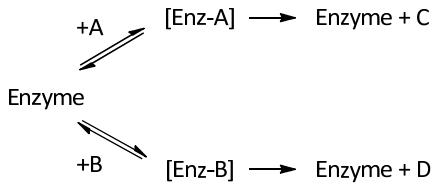

Scheme 2: General reaction scheme of an enzymatic reaction, where two enantiomers (A and B) of a substrate are converted to two enantiomers of a product (C and D).

For the reaction presented in scheme 2, the energy profile is visualised in Figure 7. The difference in Gibbs free energy (equation 1) of the transition state determines the enantioselectivity of the reaction. [45]

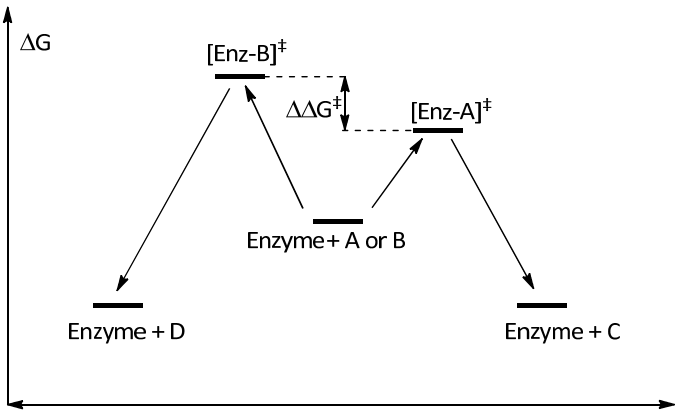

Figure 7: Energy levels during the course of a enantioselective reaction, adapted from Faber.[45]

$$\Delta\Delta G^{\ddagger} = \Delta\Delta H^{\ddagger} - T \bullet \Delta\Delta S^{\ddagger} = -RT \ln \frac{V_{max}{}^{A}}{V_{max}{}^{B}} \qquad (1)^{*}$$

** G is Gibbs free energy, H is enthalpy, T is temperature, S is entropy, R is the gas constant.*

The enantioselectivity of a reaction is represented by the E-value, which was described in an equation presented by Chen and coworkers in 1982 (equation 2).[46] From this, the E-value can be calculated when the catalytic parameters for the conversion of both enantiomers are determined.

$$E = \frac{V_{max}^{A} / K_M^{A}}{V_{max}^{B} / K_M^{B}} \qquad (2) \qquad ee_S = \frac{B - A}{A + B} \qquad (3) \qquad ee_P = \frac{C - D}{C + D} \qquad (4)$$

Enantiomeric excess (ee), which is a convenient measure of the enantiopurity of a compound, is defined by equation 3 and 4 for substrate (ee_S) and product (ee_P), respectively. For kinetic resolution processes (*vide infra*), the E-value can be determined using the ee values for the substrate and product by using equations (5 and 6). Equation 5 describes the relation between ee of the remaining substrate, the conversion (c) and the E-value, whereas equation 6 describes the relation between ee of the formed product, the conversion (c) and the E-value. [46]

$$E = \frac{\ln[(1-c)(1-ee_S)]}{\ln[(1-c)(1+ee_S)]} \qquad (5) \qquad E = \frac{\ln[(1-c)(1+ee_P)]}{\ln[(1-c)(1-ee_P)]} \qquad (6)$$

With these equations (5 and 6), the E-value can be determined when two out these three values (c, ee_S and ee_P) are known.

The enantioselectivity of haloalkane dehalogenases has been tested on various groups of halogenated compounds, which include haloalkanes (**1**-**4**), dihaloalkanes (**5**-**10**) and haloesters (**11**-**19**) (Table 2).

Most of the studied haloalkane dehalogenases exhibit very low enantioselectivity in the conversion of simple 2-haloalkanes.[16,33,47,48] This is explained by the conformational freedom of these substrates and the lack of functional groups in their structure, which would be able to form interactions (hydrogen bonds, salt bridges, π-π interactions etc.) with the residues in the active site (*vide infra*).[47] For the highly enantioselective conversion of the simple chiral haloalkane **1** no enzyme is known at this moment. Interestingly, the closely related compound **2** can be converted with high enantioselectivity by both DbjA[33,47] and DatA.[15] The best results in terms of chiral discrimination for compound **3** were also obtained with DatA.[16] This recently described enzyme can therefore be regarded as the most valuable biocatalytic tool for the enantioselective dehalogenation of simple haloalkanes. In case of DbjA the highest enantioselectivity is observed for compound **2**, which gradually drops in the series of analogs **3** and **4**.[33,47]

Table 2: Enantioselectivity (E-value) of haloalkane dehalogenases determined in the conversions of simple haloalkanes **1**-**4**, dihaloalkanes **5**-**10**, haloesters **15**-**19** and haloamides **20**-**26**.

Compound	**1**	**2**	**3**	**4**
Structure			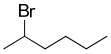	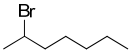
Enantioselectivity (E-value)	DhaA: 2[33] LinB: 2[33] DbjA: 1[33,47] DatA: 6[16]	DhaA: 7[33] LinB: 16[33] DbjA: 145, [33] 132(*R*)[47] DatA: >200[16]	DhaA: 4[33] LinB: 12[33] DbjA: 68[33] DatA: >200[16]	DhaA: 3[33] LinB: 3[33] DbjA: 28[33]
Compound	**5**	**6**	**7**	**8**
Structure				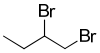
Enantioselectivity (E-value)	DhaA: 1.3[48] DhlA: 3[48]	DhlA: 4[48]	DhlA: 2[48]	DhaA: 2[48] DhlA: 2[48]
Compound	**9**	**10**	**11**	**12**
Structure	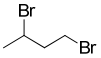	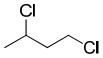		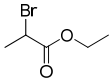
Enantioselectivity (E-value)	DhlA: 2[48]	DhlA: 3[48]	DhaA: 200[33] LinB: 52[33] DbjA: >200[33] DatA: 54[16]	DhaA: 85[33] LinB: 97[33] DbjA: 392(*R*)[47] DatA: >200[16]
Compound	**13**	**14**	**15**	**16**
Structure	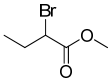	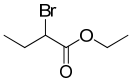	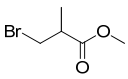	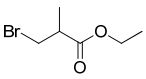
Enantioselectivity (E-value)	LinB: 28[33] DbjA: >200, [33] 209(*R*)[47]	DhaA: >200[33] LinB: >200[33] DbjA: >200[33]	DhaA: 5(*R*)[48]	DhaA: 4[48]
Compound	**17**	**18**	**19**	**20**
Structure	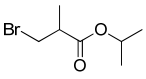	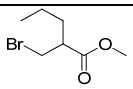	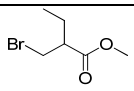	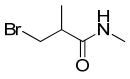
Enantioselectivity (E-value)	DhaA: 1.5[48]	DhaA: 3[48]	DhaA: 9[48]	DhaA: 3[48]

Haloalkane dehalogenases-catalysed conversions of dihaloalkanes **5**-**10** were studied only with DhaA and DhlA. Very low E-values were found. Removal of both the primary and the secondary halogens was reported.[48]

α-Haloesters **11**-**14** possess in their structure a carbonyl group that can interact *via* hydrogen bonds and electrostatic interactions with the residues in the active site of the enzyme, providing additional opportunities for chiral recognition.[33] This is reflected in the higher enantioselectivity observed in the enzymatic conversions of these compounds, with DbjA giving the best results. For compounds **11**-**13**, the (*R*)-enantiomer was determined to be preferably converted by DbjA.[33,47]

The enantioselectivity of DhaA was shown to be very low for ester **15**, in which the stereocenter is located in the α-position to the carbon bearing a halogen substituent.[47] Even lower selectivities were reported for the halogenated esters of bulkier alcohols (compounds **16** and **17**).[48] Only marginal improvement was observed upon using bulkier substituents attached directly to the stereogenic carbon (compounds **18** and **19**). Changing the ester group into an amide moiety (compound **20**) also did not result in increased enantioselectivity.[48]

To conclude, the choice of an enzyme for the enantioselective dehalogenation strongly depends on the type of substrate. For simple small aliphatic haloalkanes, the newly discovered enzyme DatA seems to be the biocatalyst of choice. More structurally diverse compounds, that include carbonyl groups in their structures (i.e. halogenated esters and amides) can be converted with the highest enantioselectivity by DbjA.

KINETIC, THERMODYNAMIC AND STRUCTURAL ANALYSIS OF THE ENANTIOSELECTIVITY OF HALOALKANE DEHALOGENASES

DhaA

Stereoselective conversion of compound **15** (Table 2) by DhaA was studied in detail,[48] revealing that the large differences in K_M between the enantiomers ($K_M^S/K_M^R > 130$) are largely compensated by the opposing differences in k_{cat} ($k_{cat}^R/k_{cat}^S > 35$). In other words, in the kinetic resolution of the racemate, the slowly converted (*R*)-enantiomer inhibits the conversion of the otherwise faster reacting (*S*)-enantiomer. This subtle interplay between binding affinity and conversion rate results in the low E-value for compounds **15** and **16**.[48]

DbjA

DbjA exhibits high enantioselectivity in the conversion of the simple β-bromoalkane **2** and bromoesters **11** and **12** (Table 2). For these compounds, the enthalpic and entropic contribution to the $\Delta\Delta G^{\ddagger}$ were determined (see Figure 5 and equation 1, *vide supra*) by the analysis of the changes of enantioselectivity as a function of temperature, in the range of 20-50°C (Table 3).[47]

Table 3: Thermodynamic analysis of the enantioselectivity of DbjA in the conversion of compounds **2**, **11** and **12**.[47]

Substrate	E at 298K	$\frac{T \bullet \Delta\Delta S^{\ddagger}}{\Delta\Delta H^{\ddagger}}$	$\Delta\Delta G^{\ddagger}$ (kJ/mol)
2	132	0.83	-11.7
11	392	0.38	-14.8
12	209	0.49	-13.2

There is a striking difference in the contribution of the entropic term for the simple haloalkane **2** (83% of the enthalpic term) and haloesters **11** and **12** (<50% of the enthalpic term). Compound **2** does not have any functional groups in its structure that may form interactions with the residues in the enzyme active site. Therefore its enantioselective conversion by DbjA stems mainly from the differences in solvation, conformational degrees of freedom and the displacement of solvent molecules present in the structure of the enzyme.[47]

In the case of haloesters, the contribution of the enthalpic term is much higher (Table 3), which is explained by the differences in binding of the two enantiomers in the active site of the enzyme.[47] This stems from the presence of functional groups in the structure of compounds **11** and **12**, which may allow additional interactions in the active site. This results in the difference in the enthalpy of binding for the two enantiomers.

The differences in the molecular interactions with DbjA, observed for simple haloalkanes and haloesters **2**, **11** and **12**, were studied further through the analysis of the enzyme structure.[47] The E-values in the conversion of compound **2** were found to be 145, 7 and 16 for DbjA, DhaA and LinB, respectively. The comparison of the protein sequences of these enzymes suggested that the high enantioselectivity of DbjA stems most likely from the presence of an additional segment located on the protein surface. DbjaAΔ, a mutant of DbjA in which the additional segment was removed, was subsequently prepared.[33]

The enantioselectivity of DbjA in the conversion of **13** stems predominantly from the enthalpic contribution and for DbjAΔ no significant difference in the enantioselectivity and the ratio of enthalpy-entropy contribution was observed. In the case of the conversion of compound **2**, the situation is strikingly different, as the enantioselectivity of DbjAΔ shows inversed temperature dependence, which is the result of the prevailing entropy contribution.[33]

To provide a structural explanation for these observations, docking and MD simulations were performed. The docking of both enantiomers of **2** into the active site of DbjA revealed that they bind in different locations in which the chiral centers for both enantiomers are not superimposable, which results in two distinct binding modes, one reactive and one non-reactive. In molecular dynamics simulation the (*R*)-enantiomer was found to bind in the reactive mode. The ratio of the binding of the (S)-enantiomer in

different modes was found to be modulated by the conformation of His139, which is influenced by the presence of the additional segment. The deletion of the additional segment causes a change in His139 conformation, which results in the increased reactivity towards the non-preferred (*S*)-enantiomer and the loss of enantioselectivity.[33]
Docking of both enantiomers of **13** into DbjA and DbjAΔ yielded structures in which the chiral centers of **13** are virtually superimposable. Therefore the rate of the conversion of both enantiomers is not influenced by the distance between the nucleophile and the carbon bearing the halogen substituent, as it was in the case of compound **2**. Instead, the enantioselectivity stems from the difference in the binding energies between the enantiomers.[33]
The structural and thermodynamic analysis of DbjA-catalysed reactions revealed different distinct molecular bases of the enantioselectivity for different classes of compounds: simple haloalkanes and haloesters.[33,47] This provides important insight into the reaction mechanism and will guide the future engineering attempts aimed at providing highly enantioselective variants of DbjA.

BEYOND KINETIC RESOLUTION

In a kinetic resolution process, the racemic mixture of the substrate is being converted in an enantioselective manner (Scheme 3). When k_1 is much higher (>200 times) than k_2, a yield of 50% and high enantiomeric excess (>99%) can be achieved for both the unconverted substrate (*ent*-**1**) and the product (**2**).

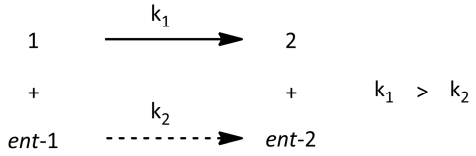

Scheme 3: General scheme of kinetic resolution, starting from racemic substrate **1**, where ideally 50% yield can be achieved for enantiopure substrate (ent-**1**) and enantiopure product **2**.

For a haloalkane dehalogenase-catalysed kinetic resolution, a general strategy is depicted in Scheme 4, where, as described earlier, an S_N2 mechanism results in an inversion of configuration. Hence, the remaining substrate and the generated product have the same absolute configuration. This maximal yield of 50% severely limits the applicability of a kinetic resolution for the preparation of enantiopure compounds. This section will focus on the possibilities of raising the yield and examples reported in literature using α/β hydrolase fold enzymes.

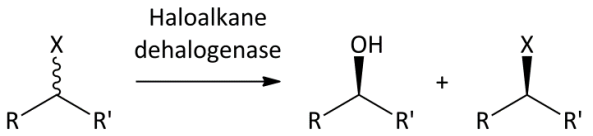

Scheme 4: Kinetic resolution using a haloalkane dehalogenase, starting from a racemic substrate.

Dynamic kinetic resolution

One of the most used methods to overcome the limitation of yield in kinetic resolution processes is the dynamic kinetic resolution (DKR), where the substrate is being racemised *in situ* (Scheme 5).[49]

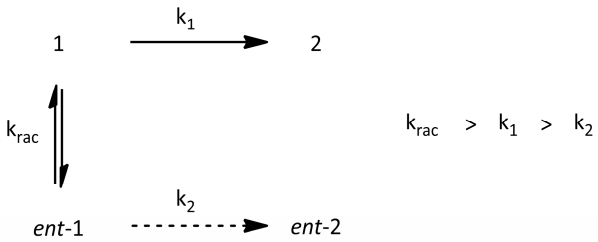

Scheme 5: General scheme of dynamic kinetic resolution.

For a perfect DKR, the high enantioselectivity of the enzyme should be combined with a fast rate of substrate racemisation. The racemisaton can be performed using synthetic catalysts[50] or an enzyme (racemase).[51] Bäckvall and coworkers published a dynamic kinetic resolution towards (*R*)-duloxetine, starting from β-hydroxynitrile (Scheme 6). A ruthenium complex catalyses the racemisation of the β-hydroxynitrile and *Candida antarctica* lipase B produces the β-cyano acetate the with high yield (87%) and 98% ee (Scheme 6).[52]

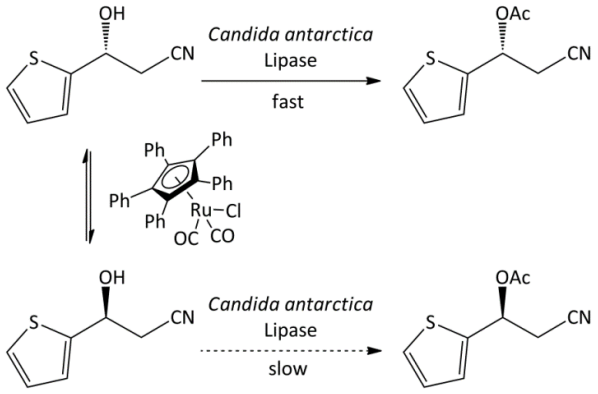

Scheme 6: Dynamic kinetic resolution towards (*R*)-duloxetine, using a lipase and a ruthenium complex for racemisation. Figure adapted from Träff *et al*.[52]

The racemisation can also be performed by an enzyme. Vongvilai and coworkers describe a striking example, where the lipase that performs the kinetic resolution of α-aminonitriles by amidation also performs the racemisation (Scheme 7). Yields of 87-90% were reported, where the enantiomeric excess is the range of 85-88%.[53]

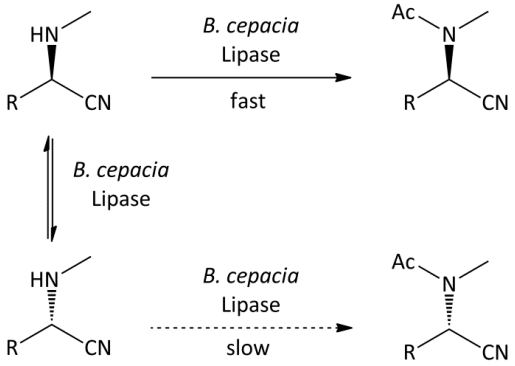

Scheme 7: Dynamic kinetic resolution of α-aminonitriles, using a single lipase.[53]

Enantioconvergent conversion

Another method to achieve higher yields and go beyond kinetic resolution is an enantioconvergent process. In such a process, the non-preferred substrate (*ent*-**1**) is converted in an alternative route into enantiopure product (**2**) (Scheme 8). Both routes should deliver a product with the same configuration.

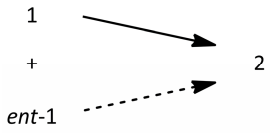

Scheme 8: General enantioconvergent process of substrate **1** and its enantiomer ent-**1**, resulting in product **2**.

The two routes (Scheme 8) can be performed by two different enzymes. For example, Cao and coworkers describe a process where two different epoxide hydrolases are used. These two enzymes possess an opposite enantiomeric preference in the conversion of styrene oxide. For the production of (*R*)-1-phenyl-1,2-ethanediol from racemic styrene oxide, a yield of 100% with an enantiomeric excess of 98% was reported (Scheme 9).[54]

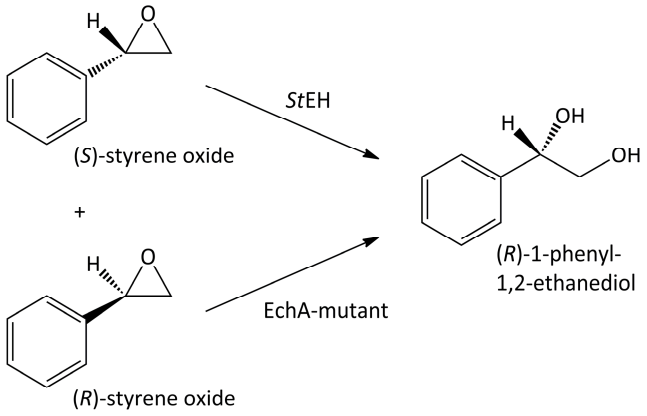

Scheme 9: Enantioconvergent reaction using two enzymes with different enantiomeric preference.[54]

Besides using two different enzymes, one of the routes can also be performed chemically, where one or more chemical follow-up reactions are performed. For example, in the synthetic pathway for the preparation of an enantiopure α-amino acid, where the racemic precursor is hydrolysed enantioselectively and with retention of configuration to the α-hydroxyamide. Subsequently, a chemo-catalytic reaction is performed with inversion of configuration (Scheme 10), by converting the product of the enzymatic reaction into tosylate and subsequent substitution with an acetate anion.[55]

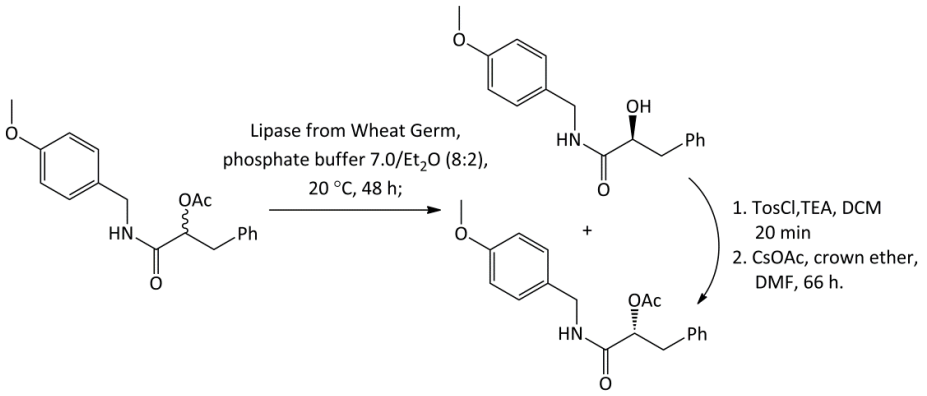

Scheme 10: Chemo-enantioconvergent route towards enantiopure precursor of α-aminoacids.[55]

Asymmetric synthesis

Another way to overcome the maximum yield of 50% in a kinetic resolution is the use of asymmetric conversion of a prochiral compound, introducing a chiral center. For example, asymmetric synthesis by a lipase was shown by Duhamel *et al* in 1993, where a prochiral diacetate was converted into an keto acetate (Scheme 11), with reported enantiomeric excess of >98%, conversion of 100%, and yield of 80%.[56]

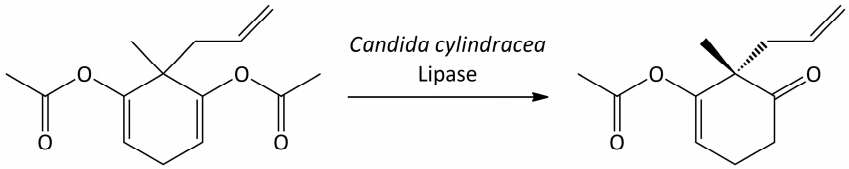

Scheme 11: Asymmetric synthesis of a keto acetate from a prochiral compound by a lipase.

Until now, these types of reactions including dynamic kinetic resolutions, enantioconvergent processes and asymmetric syntheses, were not investigated for haloalkane dehalogenases. In this thesis these reactions will be explored.

APPLICATIONS OF (HALOALKANE) DEHALOGENASES

Haloalkanes and related halogen-containing compounds are present in the environment, where they were mainly introduced by mankind, as they are used for example as solvents and as agrochemicals. The lack of microbiological degradation routes causes the persistence of these usually toxic compounds in nature.[57] Haloalkane dehalogenases were found to be valuable in the degradation of haloalkanes that are present in the groundwater.[58] Another class of dehalogenases, halohydrin dehalogenases, have been shown to be applicable for the removal of toxic compounds found in contaminated

(industrial) sites, as well as removal of haloalcohols in food industrial processes.[59] Furthermore, haloalkane dehalogenases were described to be of great potential for the recycling of coproducts 1,2-dichloropropane, 1,2,3-tribromopropane and 1,2-dichlorobutane, generated along with the industrial synthesis of propylene oxide, epichlorohydrin and butylene oxide, respectively.[57] A more bioanalytical application is the use of a haloalkane dehalogenase as a protein tag, to function as a label in cell imaging.[60] Furthermore, these enzymes were even mentioned to be promising in neutralising the warfare chemical agent sulfur mustard gas.[61]

Despite the fact that haloalkanes are toxic pollutants and unwanted site products in industrial processes, they are of great importance in synthetic chemistry as they possess a good leaving group. Therefore, they are good precursors and interesting building blocks, especially when they are available in an enantiopure form. Haloalkane dehalogenases have the potential to be of importance in processes where enantiopure compounds are desired. Halohydrin dehalogenases were already described to be good biocatalysts in the production of enantipure epoxides, starting from inexpensive haloalcohols.[57]

AIM OF THE THESIS

In this thesis, biocatalytic properties and applications of five homologous haloalkane dehalogenases are explored. In every chapter, a different aspect of the synthetic applicability of these industrially promising enzymes has been highlighted.

In **chapter 2**, asymmetric conversion of prochiral, polyhalogenated compounds and subsequent kinetic resolution using haloalkane dehalogenases is investigated. Furthermore, the enantiomeric excess of the produced haloalcohols is monitored during the course of the reactions, while the second step, a kinetic resolution of the haloalcohols towards the diol, can increase the enantiomeric excess of the haloalcohol.

In **chapter 3**, the kinetic resolution of α-haloamides is described: E-values for these conversions and yields of preparative scale reactions are reported. Also a theoretical explanation for the observed enantioselectivity is provided, using molecular dynamics.

An *in-situ* racemisation method that can be used in haloalkane dehalogenase-catalysed transformation of haloesters and haloamides is reported in **chapter 4**. Furthermore this method is used in a dynamic kinetic resolution system in which high yields of α-hydroxyamides are obtained.

In **chapter 5**, an enantioconvergent method is described for the synthesis of α-substituted amides. In this method, a haloalkane dehalogenase-catalysed kinetic resolution of α-

bromoamides with inversion of configuration is combined with subsequent chemically catalysed reactions. After the kinetic resolution, the hydroxy group of the formed α-hydroxy amides is converted with retention of configuration into a good leaving group. In a third step, the intermediates are substituted by *N*-, *O*-, or *S*- nucleophiles, resulting in high yields and high enantiomeric excess of α-substituted amides.

REFERENCES

[1] S. Keuning, D. B. Janssen, and B. Witholt. *J. Bacteriol.* **1985**, *163*, 635-639.

[2] D. B. Janssen, A. Scheper, and B. Witholt. *In E. H. Houwink and R. R. van der Meer (ed.), Innovations in biotechnology. Progress in industrial microbiology, vol 20. Elsevier Science Publishers, Amsterdam.* **1984**, 169-178.

[3] D. B. Janssen, F. Pries, P. J. van der, B. Kazemier, P. Terpstra, and B. Witholt. *J. Bacteriol.* **1989**, *171*, 6791-6799.

[4] P. J. Sallis, S. J. Armfield, A. T. Bull, and D. J. Hardman. *J. Gen. Microbiol.* **1990**, *136*, 115-120.

[5] R. Scholtz, T. Leisinger, F. Suter, and A. M. Cook. *J. Bacteriol.* **1987**, *169*, 5016-5021.

[6] T. Yokota, T. Omori, and T. Kodama. *J. Bacteriol.* **1987**, *169*, 4049-4054.

[7] Y. Nagata, T. Nariya, R. Ohtomo, M. Fukuda, K. Yano, and M. Takagi. *J. Bacteriol.* **1993**, *175*, 6403-6410.

[8] Y. Nagata, K. Miyauchi, J. Damborsky, K. Manova, A. Ansorgova, and M. Takagi. *Appl. Environ. Microbiol.* **1997**, *63*, 3707-3710.

[9] A. N. Kulakova, M. J. Larkin, and L. A. Kulakov. *Microbiology*. **1997**, *143*, 109-115.

[10] Y. Sato, M. Monincova, R. Chaloupkova, Z. Prokop, Y. Ohtsubo, K. Minamisawa, M. Tsuda, J. Damborsky, and Y. Nagata. *Appl. Environ. Microbiol.* **2005**, *71*, 4372-4379.

[11] A. Jesenska, M. Bartos, V. Czernekova, I. Rychlik, I. Pavlik, and J. Damborsky. *Appl. Environ. Microbiol.* **2002**, *68*, 3724-3730.

[12] A. Jesenska, M. Pavlova, M. Strouhal, R. Chaloupkova, I. Tesinska, M. Monincova, Z. Prokop, M. Bartos, I. Pavlik, I. Rychlik, P. Mobius, Y. Nagata, and J. Damborsky. *Appl. Environ. Microbiol.* **2005**, *71*, 6736-6745.

[13] A. Jesenska, M. Monincova, T. Koudelakova, K. Hasan, R. Chaloupkova, Z. Prokop, A. Geerlof, and J. Damborsky. *Appl. Environ. Microbiol.* **2009**, *75*, 5157-5160.

[14] A. Jesenska, I. Sedlacek, and J. Damborsky. *Appl. Environ. Microbiol.* **2000**, *66*, 219-222.

[15] T. Prudnikova, T. Mozga, P. Rezacova, R. Chaloupkova, Y. Sato, Y. Nagata, J. Brynda, M. Kuty, J. Damborsky, and I. K. Smatanova. *Acta Crystallogr. Sect. F. Struct. Biol. Cryst. Commun.* **2009**, *65*, 353-356.

[16] K. Hasan, A. Fortova, T. Koudelakova, R. Chaloupkova, M. Ishitsuka, Y. Nagata, J. Damborsky, and Z. Prokop. *Appl. Environ. Microbiol.* **2011**, *77*, 1881-1884.

[17] M. Hesseler, X. Bogdanovic, A. Hidalgo, J. Berenguer, G. J. Palm, W. Hinrichs, and U. T. Bornscheuer. *Appl. Microbiol. Biotechnol.* **2011**,

[18] D. L. Ollis, E. Cheah, M. Cygler, B. Dijkstra, F. Frolow, S. M. Franken, M. Harel, S. J. Remington, I. Silman, J. Schrag,J. L. Sussman, K. H. G. Verschueren and A. Goldman. *Protein Eng*. **1992**, *5*, 197-211.

[19] M. Nardini and B. W. Dijkstra. *Curr. Opin. Struct. Biol.* **1999**, *9*, 732-737.

[20] M. Nardini, I. S. Ridder, H. J. Rozeboom, K. H. Kalk, R. Rink, D. B. Janssen, and B. W. Dijkstra. *J. Biol. Chem.* **1999**, *274*, 14579-14586.

[21] A. Roussel, S. Canaan, M. P. Egloff, M. Riviere, L. Dupuis, R. Verger, and C. Cambillau. *J. Biol. Chem.* **1999**, *274*, 16995-17002.

[22] D. Ghosh, M. Erman, M. Sawicki, P. Lala, D. R. Weeks, N. Li, W. Pangborn, D. J. Thiel, H. Jornvall, R. Gutierrez, and J. Eyzaguirre. *Acta Crystallogr. D. Biol. Crystallogr.* **1999**, *55*, 779-784.

[23] Y. Wei, J. L. Schottel, U. Derewenda, L. Swenson, S. Patkar, and Z. S. Derewenda. *Nat. Struct. Biol.* **1995**, *2*, 218-223.

[24] P. D. Carr and D. L. Ollis. *Protein Pept. Lett.* **2009**, *16*, 1137-1148.

[25] D. B. Janssen. *Curr. Opin. Chem. Biol.* **2004**, *8*, 150-159.

[26] A. J. Oakley, Z. Prokop, M. Bohac, J. Kmunicek, T. Jedlicka, M. Monincova, I. Kuta-Smatanova, Y. Nagata, J. Damborsky, and M. C. J. Wilce. *Biochemistry*. **2002**, *41*, 4847-4855.

[27] E. Chovancova, J. Kosinski, J. M. Bujnicki, and J. Damborsky. *Proteins*. **2007**, *67*, 305-316.

[28] M. Otyepka and J. Damborsky. *Protein Sci.* **2002**, *11*, 1206-1217.

[29] J. Marek, J. Vevodova, I. K. Smatanova, Y. Nagata, L. A. Svensson, J. Newman, M. Takagi, and J. Damborsky. *Biochemistry*. **2000**, *39*, 14082-14086.

[30] P. A. Mazumdar, J. C. Hulecki, M. M. Cherney, C. R. Garen, and M. N. James. *Biochim. Biophys. Acta*. **2008**, *1784*, 351-362.

[31] K. H. Verschueren, S. M. Franken, H. J. Rozeboom, K. H. Kalk, and B. W. Dijkstra. *J. Mol. Biol.* **1993**, *232*, 856-872.

[32] J. Newman, T. S. Peat, R. Richard, L. Kan, P. E. Swanson, J. A. Affholter, I. H. Holmes, J. F. Schindler, C. J. Unkefer, and T. C. Terwilliger. *Biochemistry*. **1999**, *38*, 16105-16114.

[33] Z. Prokop, Y. Sato, J. Brezovsky, T. Mozga, R. Chaloupkova, T. Koudelakova, P. Jerabek, V. Stepankova, R. Natsume, J. G. van Leeuwen, D. B. Janssen, J. Florian, Y. Nagata, T. Senda, and J. Damborsky. *Angew. Chem. Int. Ed. Engl.* **2010**, *49*, 6111-6115.

[34] T. Bosma, M. G. Pikkemaat, J. Kingma, J. Dijk, and D. B. Janssen. *Biochemistry*. **2003**, *42*, 8047-8053.

[35] Z. Prokop, M. Monincova, R. Chaloupkova, M. Klvana, Y. Nagata, D. B. Janssen, and J. Damborsky. *J. Biol. Chem.* **2003**, *278*, 45094-45100.

[36] J. P. Schanstra and D. B. Janssen. *Biochemistry*. **1996**, *35*, 5624-5632.

[37] G. H. Krooshof, R. Floris, A. W. Tepper, and D. B. Janssen. *Protein Sci.* **1999**, *8*, 355-360.

[38] J. P. Schanstra, J. Kingma, and D. B. Janssen. *J. Biol. Chem.* **1996**, *271*, 14747-14753.

[39] J. Damborsky, E. Rorije, A. Jesenska, Y. Nagata, G. Klopman, and W. J. Peijnenburg. *Environ. Toxicol. Chem.* **2001**, *20*, 2681-2689.

[40] T. Kaneko, Y. Nakamura, S. Sato, E. Asamizu, T. Kato, S. Sasamoto, A. Watanabe, K. Idesawa, A. Ishikawa, K. Kawashima, T. Kimura, Y. Kishida, C. Kiyokawa, M. Kohara, M. Matsumoto, A. Matsuno, Y. Mochizuki, S. Nakayama, N. Nakazaki, S. Shimpo, M. Sugimoto, C. Takeuchi, M. Yamada, and S. Tabata. *DNA Res.* **2000**, *7*, 331-338.

[41] T. Kamachi, T. Nakayama, O. Shitamichi, K. Jitsumori, T. Kurihara, N. Esaki, and K. Yoshizawa. *Chem. – Eur. J*. **2009**, *15*, 7394-7403.

[42] G. Glockler. *J. Phys. Chem*. **1959**, *63*, 828-832.

[43] T. Kurihara. *Biosci. Biotechnol. Biochem*. **2011**, *75*, 189-198.

[44] W. J. Quax and C. P. Broekhuizen. *Appl. Microbiol. Biotechnol*. **1994**, *41*, 425-431.

[45] K. Faber. *5th edition, Springer-Verlag Berlin Heidelberg New York*. **2004**,

[46] C. S. Chen, Y. Fujimoto, G. Girdaukas, and C. J. Sih. *J. Am. Chem. Soc*. **1982**, *104*, 7294-7299.

[47] R. Chaloupkova, Z. Prokop, Y. Sato, Y. Nagata, and J. Damborsky. *FEBS J*. **2011**, *278*, 2728-2738.

[48] R. J. Pieters, J. H. L. Spelberg, R. M. Kellogg, and D. B. Janssen. *Tetrahedron Lett.* **2001**, *42*, 469-471.

[49] H. Pellissier. *Tetrahedron*. **2011**, *67*, 3769-3802.

[50] N. J. Turner. *Curr. Opin. Chem. Biol.* **2004**, *8*, 114-119.

[51] B. Schnell, K. Faber, and W. Kroutil. *Adv. Synth. Catal.* **2003**, *345*, 653-666.

[52] A. Traff, R. Lihammar, and J. E. Backvall. *J. Org. Chem*. **2011**, *76*, 3917-3921.

[53] P. Vongvilai, M. Linder, M. Sakulsombat, M. S. Humble, P. Berglund, T. Brinck, and O. Ramstrom. *Angew. Chem. Int. Ed. Engl.* **2011**, *50*, 6592-6595.

[54] L. Cao, J. Lee, W. Chen, and T. K. Wood. *Biotechnol. Bioeng.* **2006**, *94*, 522-529.
[55] W. Szymanski and R. Ostaszewski. *Tetrahedron Asymmetry*. **2006**, *17*, 2667-2671.
[56] P. Duhamel, P. Renouf, D. Cahard, A. Yebga, and J. M. Poirier. *Tetrahedron Asymmetry*. **1993**, *4*, 2447-2450.
[57] P. E. Swanson. *Curr. Opin. Biotechnol*. **1999**, *10*, 365-369.
[58] G. Stucki and M. Thuer. *Environ. Sci. Technol*. **1995**, *29*, 2339-2345.
[59] M. Schallmey, R. Floor, W. Szymański and D. B. Janssen, submitted.
[60] G. V. Los, L. P. Encell, M. G. McDougall, D. D. Hartzell, N. Karassina, C. Zimprich, M. G. Wood, R. Learish, R. F. Ohane, M. Urh, D. Simpson, J. Mendez, K. Zimmerman, P. Otto, G. Vidugiris, J. Zhu, A. Darzins, D. H. Klaubert, R. F. Bulleit, and K. V. Wood. *ACS Chem. Biol*. **2008**, *3*, 373-382.
[61] Z. Prokop, F. Oplustil, J. DeFrank, and J. Damborsky. *Biotechnol. J.* **2006**, *1*, 1370-1380.

CHAPTER 2

Haloalkane dehalogenase catalysed desymmetrisation and tandem kinetic resolution for the preparation of chiral haloalcohols

Alja Westerbeek, Jan G. E. van Leeuwen, Wiktor Szymański,
Ben L. Feringa, and Dick B. Janssen

Submitted for publication to Tetrahedron

ABSTRACT

Six different bacterial haloalkane dehalogenases were recombinantly produced in *Escherichia coli*, purified and used to catalyse the conversion of prochiral dihaloalkanes and a *meso* dihaloalkane, yielding enantioenriched haloalcohols. Kinetic parameters for the conversion of substrates were measured and k_{cat} values of up to 1.6 s^{-1} were found. A two-reactions-one-enzyme process was established in which the desymmetrisation of a dihaloalkane is followed by kinetic resolution of the chiral haloalcohol that is produced in the first step. In case of 1,3-dibromo-2-methylpropane and 1,3-dibromo-2-phenylpropane, an improvement of the enantiomeric excess of the respective haloalcohol was observed in time, leading to e.e. values of >97%, with analytical yields of 24 and 52%, respectively. The results show that haloalkane dehalogenases can be used for the production of highly enantioenriched haloalcohols and that in some cases product enantiopurity can be improved by allowing a one-enzyme tandem reaction.

INTRODUCTION

Enantiopure 1,2-haloalcohols (halohydrins) and 1,3-haloalcohols are chiral intermediates for the preparation of several important classes of compounds. Halohydrins can be converted into lactones[1] and epoxides, which are versatile intermediates in organic synthesis.[2-5] For example, indene bromohydrin is a precursor for anti-HIV protease inhibitor Indinavir.[2] 1,3-Haloalcohols are precursors of β-amino acids[6] and 1,3-aminoalcohols,[7] which are important chiral ligands.[8]

Current biocatalytic routes towards enantiopure 1,2- and 1,3-haloalcohols include enzymatic asymmetric reduction of haloketones[9], haloperoxidase-mediated conversion of unsaturated compounds to *vicinal* halohydrins[10], kinetic resolution of halohydrins by using a *Pseudomonas* strain[11] and lipase-catalysed resolution of racemic alcohols and esters.[12,13] We are interested in exploring the possibility of using isolated enzymes for the preparation of such compounds, using conversions that not rely solely on kinetic resolution. Since haloalcohols can in principle be produced by biocatalysed hydrolysis of dihaloalkanes, their preparation could be facilitated by the use of a tandem desymmetrisation/kinetic resolution process (Scheme 1).

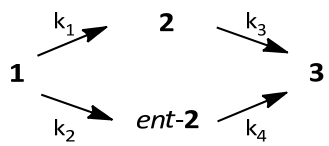

Scheme 1: Reaction scheme for the tandem conversion of a prochiral or *meso* dihaloalkane **1**. The reaction yields chiral haloalcohol **2**, which is converted to prochiral or *meso* diol **3**.

In such a system, the changes of enantiomeric excess of intermediate **2** over time depend on the ratio of the kinetic constants.[14] If one enantiomer of the intermediate is formed faster in the first reaction ($k_1 > k_2$), and consumed at lower rate in the second reaction ($k_4 > k_3$), an increase of its enantiomeric excess over time can be expected, unlike in a normal kinetic resolution, where product e.e. decreases over time, especially when the E-value is not high.[15] In the opposite case ($k_3 > k_4$), the enantiomeric excess of the intermediate will decrease, and it is possible that towards the end of the reaction the enantiomer of **2** that is not the preferred product in the first step predominates.[16]

Reported applications of such tandem reactions were mainly explored using hydrolases.[14-16] Wang and coworkers[14] have shown that porcine pancreatic lipase (PPL) and pig liver esterase (PLE) both can perform a conversion of prochiral diesters, and subsequently enhance the enantiomeric excess of the monoester product by converting it into the diol. In another study, lipase P-30 from *Pseudomonas cepacia* was used in the preparation of a cyclic monoester in a tandem reaction from the diester.[15]

The usefulness of haloalkane dehalogenases in stereoselective, biocatalytic reactions has been recently recognised and was employed in the preparation of chiral esters and bromoalkanes via kinetic resolution.[17,18] In the current study, we explored the possibilities to use haloalkane dehalogenases in a tandem reaction as described in Scheme 1. We tested the activity of haloalkane dehalogenases from five different sources for the activity and stereoselectivity with selected prochiral and *meso* compounds **1a-1e** (Figure 1).

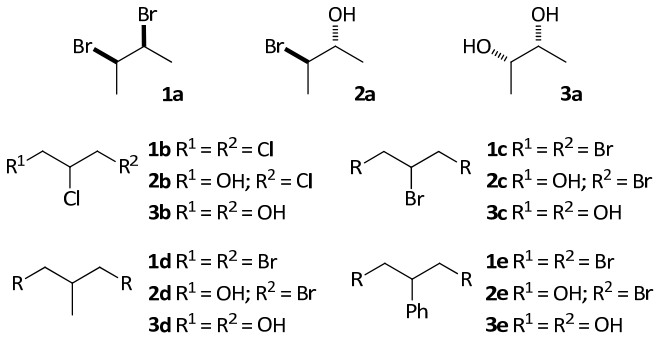

Figure 1: Prochiral and *meso* substrates (**1a**-**1e**) together with the products of their single and double dehalogenation (**2** and **3** respectively).

RESULTS AND DISCUSSION

Cloning and production of haloalkane dehalogenases

Haloalkane dehalogenases used in this study were from *Xanthobacter autotrophicus* (DhlA),[19] *Rhodococcus rhodochrous* (DhaA),[20] *Sphingomonas paucimobilis* UT26 (LinB),[21] *Bradyrhizobium japonicum* USDA110 (DbjA)[22] and *Mesorhizobium loti* MAFF303099 (DmlA).[22] DhaA31 is a mutant of DhaA with enhanced catalytic activity for 1,2,3-trichloropropane.[23] Haloalkane dehalogenase genes were expressed with an *N*-terminal His-tag under control of an L-arabinose inducible promoter in *E. coli* TOP10. Typically, around 50 mg of enzyme was obtained per liter of overnight induced cultures after purification using an AKTA purifier system using Ni-NTA columns (GE Healthcare). The purity of the isolated enzymes was > 95% as judged by SDS-polyacrylamide gel electrophoresis.

Kinetic parameters for prochiral/meso compounds

Kinetic parameters k_{cat}, K_M and catalytic efficiency (k_{cat}/K_M) for the haloalkane dehalogenase catalysed conversions of compounds **1a-1e** were determined. Due to the low substrate solubility, determination of K_M and k_{cat} values was not possible for all substrates, since saturation of the reaction rate was not obtained with all compounds. In such cases, only the catalytic efficiency is reported (Table 1).

Meso-2,3-dibromobutane (**1a**) is converted by four of the six tested enzymes. LinB possesses the highest catalytic efficiency of 2.4 $mM^{-1}s^{-1}$. Affinities of DhaA, DhaA31 and DbjA are lower, with K_m values over 1 mM. The catalytic efficiencies of DhaA and DbjA are comparable (both about 100-fold lower than LinB) and DhaA31 has a fivefold higher efficiency than DbjA and DhaA. No activity was observed with DhlA and DmlA.

1,2,3-Trichloropropane (TCP) (**1b**) is a toxic xenobiotic compound that is used in chemical synthesis and is a side-product in the synthesis of epichlorohydrin and 1,2-dichloropropene. Improper disposal of TCP led to several cases of spreading of this pollutant into water.[24] Enantioselective conversion of TCP would allow conversion of a harmful side-product into a valuable chiral building block.[25] Biodegradation of **1b** using DhaA was investigated by the group of Damborsky and activity towards TCP was improved using mutagenesis, which led to the discovery of a DhaA mutant with six mutations (DhaA31).[23,26] In our study (Table 1) we found that this improved variant possesses a 28-fold higher catalytic efficiency towards compound **1b** than DhaA, which is in agreement with data reported by Damborsky and coworkers.[23] The activity of DbjA with **1b** was very low, only an observed catalytic rate at 1 mM substrate could be given. Due to the very low activity of other studied dehalogenases with compound **1b** the reliable determination of kinetic parameters was not possible (Table 1).

The DhaA31 mutant also has by far the highest catalytic efficiency and affinity for 1,2,3-tribromopropane **1c**. The catalytic efficiencies of LinB and DhaA are both more than 10-

fold lower than those of DhaA31, but all three catalytic rates are in the same range. Both the catalytic efficiency and affinity of DbjA with **1c** are significantly lower than the values found with DhaA31. The catalytic efficiencies of DmlA and DhlA were very low, about 5 x 10^4 fold lower than of DhaA31. It can be concluded that tribromopropane (**1c**) is a better substrate than trichloropropane (**1b**) for all the studied haloalkane dehalogenases.

With 1,3-dibromo-2-methylpropane (**1d**) high affinities (K_M < 0.17 mM^{-1}) and catalytic efficiencies of >1.5 $mM^{-1}s^{-1}$ were found for DhaA, DbjA, LinB and DhaA31. DmlA and DhlA again both possess much lower affinity and catalytic efficiency.

The solubility of 1,3-dibromo-2-phenylpropane (**1e**) in the reaction medium is very low, reaching only 0.5 mM with addition of 20 vol% of DMSO. Therefore only an observed rate at this concentration could be determined. Compound **1e** was only converted by LinB (k_{cat} ≥ 0.8 s^{-1}) and DhaA31 (k_{cat} ≥ 0.4 s^{-1}). The fact that this most sterically demanding compound is only converted by these two enzymes agrees with the observation that LinB generally can react with bulkier compounds, like its natural substrate 1,3,4,6-tetrachloro-1,4-cyclohexadiene,[21] and with the fact that DhaA31 is a mutant of DhaA with enhanced activity towards 1,2,3-trichloropropane.[23]

Table 1: Kinetic parameters for conversion of prochiral/*meso* compounds with purified dehalogenases, measured in 50 mM Tris.SO_4, pH 8.2, at room temperature

enzyme	kinetic parameters	1a	1b	1c	1d	1e
DhaA	K_M	> 2.0	4.8	0.34	< 0.15	-
	k_{cat}	> 0.07	0.047	1.6	0.36	< 0.015
	k_{cat}/K_M	0.031	0.01	4.7	> 2.3	-
DbjA	K_M	> 2.2	-	> 1.0	0.17	-
	k_{cat}	> 0.05	k_{obs}= 0.005	> 0.9	0.76	-
	k_{cat}/K_M	0.025	-	0.87	4.5	< 0.002
LinB	K_M	0.41	-	0.19	0.17	-
	k_{cat}	0.97	-	1.4	1.4	≥ 0.8
	k_{cat}/K_M	2.4	< 0.002	7.3	8.4	-
DhaA31	K_M	> 1.1	1.7	0.021	< 0.15	-
	k_{cat}	> 0.19	0.47	1.6	0.22	≥ 0.4
	k_{cat}/K_M	0.14	0.28	77	> 1.5	-
DhlA	K_M	-	-	> 1.1	>1.3	-
	k_{cat}	-	-	> 0.017	0.06	-
	k_{cat}/K_M	< 0.002	< 0.002	0.015	0.050	< 0.002
DmlA	K_M	-	-	> 1.0	> 1.3	-
	k_{cat}	-	-	>0.015	>0.4	-
	k_{cat}/K_M	< 0.002	< 0.002	0.015	0.34	< 0.002

K_M in mM, k_{cat} in s^{-1} and k_{cat}/K_M in $mM^{-1}s^{-1}$. K_M and k_{cat} had RSD ≤ 20%. For compound **1e**, the reaction was performed in 20% DMSO at maximum solubility of 0.5 mM.

Summarising, LinB and DhaA31 are the best enzymes for conversion of compounds **1a-1e**. DhaA31 converts all tested compounds and has especially a very high catalytic efficiency (77 $mM^{-1}s^{-1}$) for tribromopropane (**1c**). LinB converts all compounds, except trichloropropane (**1b**), with rates of about 1 s^{-1}. DhaA converts compounds **1a**, **1b**, **1c** and **1d**, but the kinetic parameters are lower as compared to DhaA31 and LinB. The same holds for DbjA, which only converts **1a**, **1c** and **1d** with a reasonable up to good activity. DmlA and DhlA both showed poor activity towards the tested substrates, only **1c** and **1d** were converted, with k_{cat}/K_M values between 0.015 and 0.34 and K_M values of >1 mM.

Exploring stereoselectivity

The enantioselectivity of the conversion of compounds **1** to haloalcohols **2** (Figure 1) was determined by measuring the enantiomeric excess of the haloalcohols **2** after a certain reaction time (Table 2 and Table 4). It should be taken into account that the determined enantiomeric excess of products **2** is depending on potential conversion towards the diol **3**, as described later.

Table 2: Enantiomeric excess of products **2** obtained in haloalkane dehalogenase catalysed conversion of substrates **1**.

enzyme	**2a***	**2b**	**2c**	**2d**	**2e**
DhaA	88%	18% (*R*)	42% (*R*)	41% (*R*)	N.D.
DbjA	85%	39% (*R*)	15% (*R*)	70% (*S*)	N.D.
LinB	4.4%	52% (*R*)	24% (*R*)	30% (*R*)	79% (*S*)
DhaA31	64%	17% (*R*)	6% (*S*)	19% (*R*)	57% (*S*)
DmlA	N.D.	6% (*S*)	18% (*R*)	39% (*R*)	N.D.
DhlA	N.D.	49% (*R*)	3% (*R*)	49% (*R*)	N.D.

N.D.: not determined, because of low activity. *absolute configuration was not determined for compound **2a**.

The enantiomeric excess of **2a** was high in the reactions catalysed by DbjA and DhaA. The value with LinB was very low, while with DmlA and DhlA the e.e. values could not be determined due to the low activity of the biocatalysts. For the dichloropropanol **2b**, moderate e.e. values were found and the highest enantiomeric excess was measured when LinB was used as the catalyst. The e.e. values for **2c** were low to moderate, with the highest value of 42% for DbjA. For **2d** the best result was obtained with DbjA. The enantiomeric excess of **2e** was only determined for LinB and DhaA31, which both gave values above 50%.

Tandem conversions for kinetic resolution of haloalcohols

Having assayed the catalytic properties and the enantioselectivity of haloalkane dehalogenases with compounds **1a-1e**, we proceeded to study the possibility of using these enzymes in a tandem desymmetrisation/kinetic resolution process (Scheme 1),

taking advantage of the fact that haloalkane dehalogenases have been described to convert haloalcohols to diols.[27]

Based on results presented in Table 2, we chose the most promising combinations of enzymes and substrates to perform a reaction in which the concentration of **1** and **2** and the enantiomeric excess of **2** were monitored over the course of the reaction.

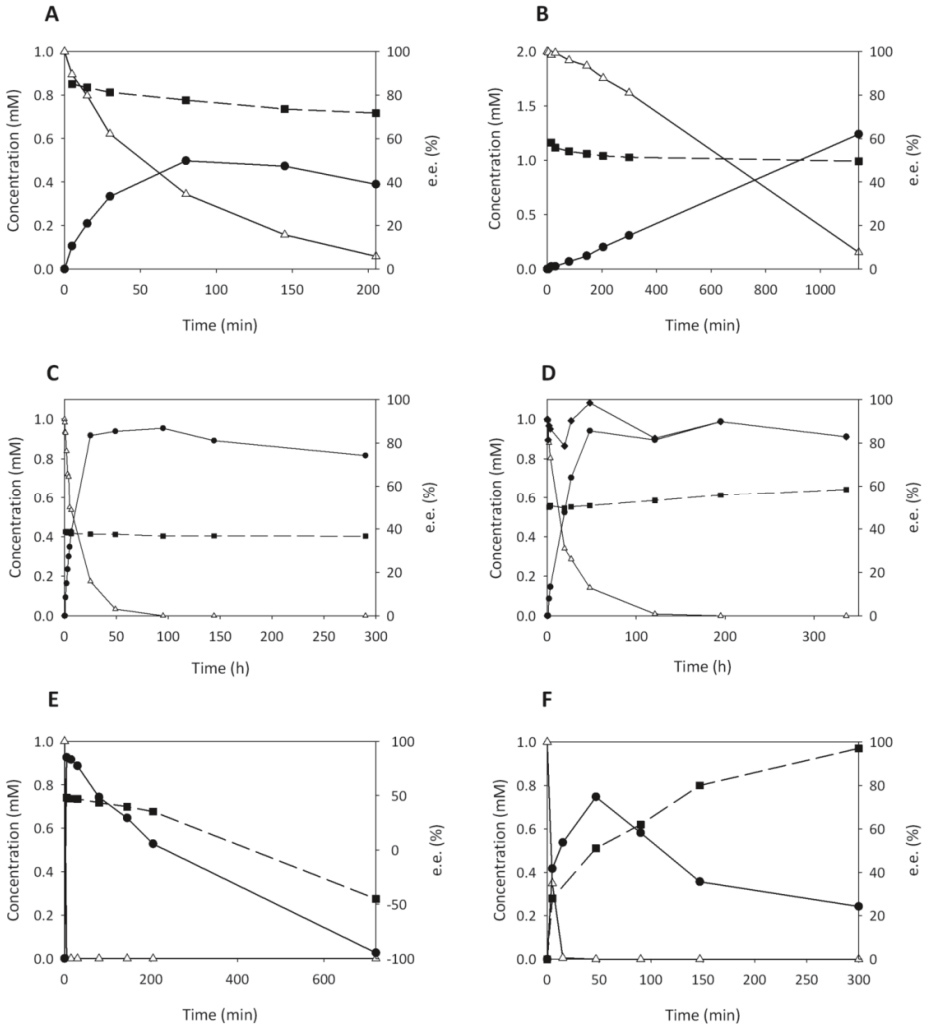

Figure 2: Tandem conversion of **1a**-**1d** followed in time. Concentrations of substrates **1** (Δ) and haloalcohols **b** (●) are depicted, together with the enantiomeric excess of haloalcohols **2** (■, broken line). (A) substrate **1a**, conversion with DbjA, (B) substrate **1b**, conversion with LinB, (C) substrate **1b**, conversion with DbjA, (D) substrate **1b**, conversion with DhlA, (E) substrate **1c**, conversion with DhaA, (F) substrate **1d**, conversion with DbjA.

Figure 2A shows the DbjA-catalysed conversion of **1a** to **2a**, which is converted further to the diol **3a**. The enantiomeric excess of **2a** starts at 85%, but this value decreases as the predominantly formed enantiomer of product **2a** is also the preferred substrate for the second reaction. This makes this process unattractive for the tandem desymmetisation and kinetic resolution of **2a**.

The graph in Figure 2B shows the conversion of **1b** by LinB, which was chosen because it provided the product **2b** with the highest enantiomeric excess (Table 2). The conversion of **1b** to **2b** is relatively slow (Table 1). The enantiomeric excess of **2b** is 58% at the beginning, and slightly decreases to 50% during the course of the reaction. Thus, enantiopure dichloropanol **2b** is not obtained, which makes LinB not suitable for its production. Next, the conversion of **1b** by DbjA (Figure 2C) and DhlA (Figure 2D) was attempted. The enantiomeric excess of **2b** when DbjA was used stayed the same over the whole reaction time, while the concentration of **2b** was decreasing. For DhlA, a small kinetic resolution effect was measured, as the e.e. of **2b** was slightly raised from 50 to 58%, but the enantioselectivity was too low and the reaction was very slow.

During the conversion of **1c** to **3c** by DhaA, the first reaction is very fast (Figure 2E). (*R*)-**2c** is the preferred product of the desymmetrisation step, but is also the preferred enantiomer for the second reaction leading to the diol **3c**. This second reaction even inverts the enantiomeric excess, as the conversion proceeds, since (*S*)-**2c** dominates at the end of the reaction. The unfavorable ratio of kinetic constants (Scheme 1) makes this reaction unsuitable for production of enantiopure **2c**.

Figure 2F shows the changes of concentrations of **1d** and **2d** during the course of conversion by DbjA. The desymmetrisation of tribromopropane **1d** is fast, but gives an enantiomeric excess of only 28% for (*S*)-**2d**. During the course of the second reaction, this value goes up slowly to 97% after 300 min, as the non-preferred enantiomer (*R*)-**2d** is the preferred substrate for the reaction to diol **3d** by DbjA. This confirms the beneficial effect of the enzyme-catalysed kinetic resolution for the e.e. of **2d**, even though the analytical yield at the e.e. of 97% is low, only 24%.

For 3-bromo-2-methylpropan-1-ol (**2d**), the commercially available enantiopure compounds were used to determine the catalytic efficiencies. The determined E-value with DbjA is 6 (Table 3), which in agreement with the time course experiment (Figure 2D) where (*R*)-**2d** is the preferred substrate for the formation of the diol **3d**.

Table 3: Kinetic parameters of conversion of 3-bromo-2-methylpropan-1-ol (**2d**) with DbjA

	k_{cat} (s^{-1})	K_m (mM)	k_{cat}/K_m (mM^{-1} s^{-1})	E-value
(*R*)-enantiomer	>0.7	>2.5	0.30	6
(*S*)-enantiomer	>0.11	>2.3	0.047	

The graph in Figure 3 shows the enantiomeric excess of **2e** and concentration of **1e** and **2e** during the course of the reaction catalysed by LinB. The first reaction of **1e** to **2e** is very fast and produces (*S*)-**2e** with an e.e. of 64%. In the course of the much slower second conversion of **2e** to the diol **3e** the e.e. of (*S*)-**2e** increases to 98% after 20 h, as (*R*)-**2e** is the preferred enantiomer for the second reaction, resulting in kinetic resolution of **2e**. The final analytical yield of the reaction is 52%. In the literature, various values were described for tandem desymmetrisation/kinetic resolution processes, ranging from 15% yield (95% e.e.)[14] to 51% yield (95% e.e.)[15] and 55% yield (99% e.e.).[28] Obviously, further improvements would require enzymes with higher complementary enantioselectivities. The engineering of enzymes with enhanced enantioselectivity has been explored in various studies [29,30] and include haloalkane dehalogenases.[18,25]

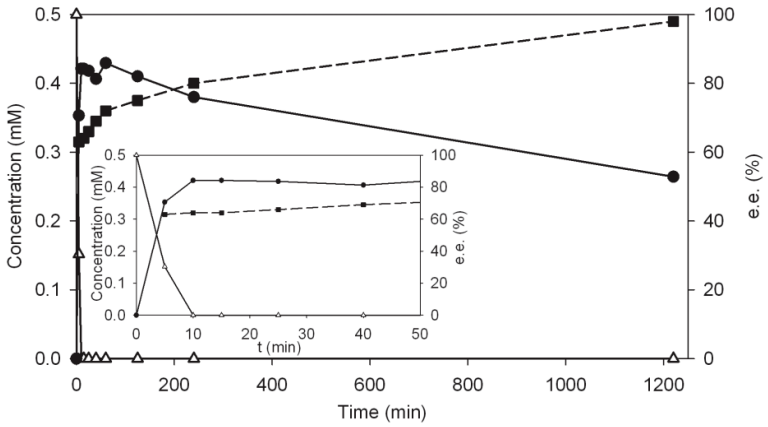

Figure 3: Tandem conversion of rac-1,3,-dibromo-2-phenylpropane (**1e**) by LinB followed over time. The concentration of **1e** (Δ) and **2e** (●) are depicted, together with the enantiomeric excess of **2e** (■, dotted line). The insert shows the first 50 min of the conversion.

CONCLUSIONS

In this chapter we report the activity of haloalkane dehalogenases towards prochiral and *meso* compounds **1a-1e.** The highest catalytic efficiencies were found for LinB and DhaA31. Enantiomeric excess values for products **2a**-**2e** were obtained in single time-point experiments. The occurrence of a tandem desymmetrisation and kinetic resolution in the most promising conversions was followed in time course experiments and showed that efficient tandem kinetic resolution of **2d** and **2e** could be performed. Although reported yields were only 24% and 52%, these results provide an interesting example of asymmetric transformation followed by kinetic resolution, catalysed by a single enzyme. This also comprises the first use of haloalkane dehalogenases for a tandem desymmetrisation-kinetic resolution process.

EXPERIMENTAL

^{1}H-NMR spectra were recorded at 300 or 400 MHz with $CDCl_3$ as solvent. ^{13}C-NMR spectra were obtained at 75.4 or 100.59 MHz in $CDCl_3$. Chemical shifts were determined relative to the residual solvent peaks ($CHCl_3$, δ = 7.26 ppm for ^{1}H, δ = 77.0 for ^{13}C). The following abbreviations are used to indicate signal multiplicity: s, singlet; d, doublet; t, triplet; q, quartet; m, multiplet; br, broad. Enantiomeric excess determinations were performed by capillary GC analysis or HPLC analysis using a flame ionisation detector or UV-detection, respectively (all in comparison with racemic products, column and conditions further specified in relevant experiment descriptions). Optical rotations were measured in $CHCl_3$ on a polarimeter with a 10 cm cell (*c* given in g/100 mL). Flash chromatography was performed on silica gel. Drying of solutions was performed with $MgSO_4$ or Na_2SO_4 and concentration steps were conducted with a rotary evaporator.

Compounds **1a**, **1c**, **3d** and **3e** were purchased at Sigma Aldrich, compounds **1b** and **2b** were purchased at TCI Europe, and compound **2c** was purchased at Acros Organics. Racemic compound **2a** was obtained following the literature procedure.[31]

General procedure 1: preparation of 1,3-dibromides from 1,3-diols.

N-Bromosuccinimide (2.2 mmol) was added at 0°C to the mixture of diol (1.0 mmol) and triphenylphosphine (2.2 mmol) in dichloromethane (10.0 mL). The cooling bath was removed and the reaction was stirred at room temperature for 30 min. The solvent was evaporated and the product was purified by column chromatography (Silicagel, 40-63 μm, pentane).

1d: 1,3-dibromo-2-methylpropane. Yield: 71%. Colorless oil. ^{1}H NMR (300 MHz, $CDCl_3$): *δ* 1.15 (d, 3H, ^{3}J = 7.2 Hz, C**H**$_3$), 2.22-2.44 (m, 1H, C**H**), 3.45 (dd, ^{2}J = 10.2 Hz ^{3}J = 6.0 Hz, 2H, 2 x C**H**$_2$Br), 3.53 (dd, ^{2}J = 10.2 Hz ^{3}J = 5.1 Hz, 2H, 2 x C**H**$_2$Br); ^{13}C NMR (50 MHz, $CDCl_3$): *δ* 18.1,37.2, 37.9; MS (EI+) *m/z* 216 (M^+, 15), 135 (70), 55 (100).

1e: 1,3-dibromo-2-phenylpropane. Yield: 66%. Colorless oil. ^{1}H NMR (400 MHz, $CDCl_3$): *δ* 3.34-3.41 (quintet, ^{3}J = 4.5 Hz, 1H, C**H**), 3.73 (dd, ^{2}J = 10.4 Hz ^{3}J = 6.4 Hz, 2H, 2 x C**H**$_2$Br), 3.80 (dd, ^{2}J = 10.4 Hz ^{3}J = 6.8 Hz, 2H, 2 x C**H**$_2$Br), 7.22-7.38 (m, 5H, Ar**H**); ^{13}C NMR (50 MHz, $CDCl_3$): *δ* 35.8, 49.2, 127.8, 128.2, 129.0, 139.8; MS (EI+) *m/z* 278 (M^+, 10), 197 (30), 183 (50), 117 (40), 104 (100), 91 (55).

Reference racemic compound ***rac*-2e** was obtained by performing general procedure 1 with 1 equivalent of both N-bromosuccinimide and triphenylphosphine. The compound was obtained as a colorless oil. ^{1}H NMR (400 MHz, $CDCl_3$): *δ* 3.18-3.25 (m, 1H, C**H**), 3.66 (dd, ^{2}J = 10.0 Hz ^{3}J = 6.4 Hz, 2H, 2 x C**H**$_2$Br), 3.95 (m, 2H, C**H**$_2$Br), 7.22-7.38 (m, 5H, Ar**H**), consistent with the literature.[32]

Determination of enantiomeric excess with single time point measurements

The enantiomeric excess values described in Table 1 were determined by adding enzyme (0.24-1.3 mg) to 10 ml of a solution of substrate (0.5 mM-2 mM) in 50 mM Tris, pH 8.2. The mixture was incubated at 30°C, for 3-90 min, depending on enzyme activity.

Table 4: incubation times, amount of enzyme and substrate concentrations used in incubations

Enzyme (amount)	**1a** (1mM)	**1b** (2mM)	**1c** (1mM)	**1d** (1mM)	**1e** (0.5mM)*
DhaA (0.64mg)	30 min	90 min	20 min	60 min	-
DbjA (0.56 mg)	5 min	90 min	20 min	60 min	-
LinB (0.48 mg)	30 min	90 min	20 min	60 min	60 min **
DhaA31 (0.64 mg)	30 min	20 min	3 min	60 min	60 min ***
DmlA (1.3 mg)	-	90 min	60 min	90 min	-
DhlA (0.62 mg)	-	90 min	60 min	90 min	-

* 20% DMSO was added to enhance the solubility
**divergent amount of LinB: 0.24 mg
***divergent amount of DhaA31: 0.32 mg

E.e. values of the haloalcohols **2** were determined by chiral chromatography analysis. For compound **2a**: Chiral GC analysis, Chiraldex G-TA (1 ml/min, isothermic, 42°C), retention times (min): 36.9 and 38.3. For compound **2b**: Chiral GC analysis, Hydrodex-β-TBDAc (1 ml/min, isothermic, 140°C), retention times (min): 8.2 (*S*) and 8.6 (*R*). For compound **2c**: Chiral GC analysis, Hydrodex-β-TBDAc (1 ml/min, isothermic, 140°C), retention times (min): 9.6 (*S*) and 9.9 (*R*). For compound **2d**: Chiral HPLC analysis, after transformation into *p*-nitrobenzoyl ester following literature procedure.[33] Chiralcel OJ-H, heptane/*i*-PrOH, 97/3, v/v, flow 0.5 mL/min, retention times (min): 36.3 (*R*) and 39.0 (*S*). For compound **2e**: Chiral HPLC analysis (Chiralcel OD-H, heptane/*i*-PrOH, 93/7, v/v, flow 0.5 mL/min), retention times (min): 19.4 (*R*) and 20.2 (*S*).

Determination of absolute configuration

For compound **2b** and **2c**, the absolute configuration was determined by transformation into the epihalohydrin[34] and comparison with a commercial sample. For compound **2d** by comparison with a commercial sample. The absolute configuration of compound **2e** was determined by isolation of the enzymatic reaction product and comparison of optical rotation with a literature value ($[\alpha]_D$ = +12.8 (c 0.67, $CHCl_3$ for 68% e.e.), lit.[32] $[\alpha]_D$ = -21.7 (c 1.8, $CHCl_3$ for the (*R*)-enantiomer).

General cloning strategy

For creation of the haloalkane dehalogenase gene constructs, the genes were cloned into a pBAD vector, including an *N*-terminal hexahistidine tag. The genes of interest from various sources, as described in chapter 3, were amplified by PCR from plasmid DNA (DhlA and DhaA) or from the original organisms (LinB, DbjA and DmlA). The gene for mutant DhaA31 was kindly supplied by J. Damborsky.

Protein expression, purification and analysis

Precultures were started by inoculating 5 mL of LB_{amp}-medium with *E. coli* TOP10 transformants from glycerol stocks and incubated overnight at 37°C, while shaking. The next day, 2L of LB_{amp}-medium was inoculated with 1% of an overnight culture and incubated at 37°C, while shaking. The enzyme expression was induced by adding 0.002% (w/v) L-arabinose at OD_{600} of 0.6. Cultures were incubated overnight while shaking at 30°C, except for the culture aimed for expression of LinB, which was incubated at 17°C. After growth, the cells were harvested, broken by sonication, ultracentrifuged and the supernatant with the haloalkane dehalogenases was used for purification using three in line his-trap Ni-NTA columns from GE healthcare attached to an AKTA purifier system. The purified enzymes were concentrated using an Amicon ultrafiltration cell and stored in TMG buffer (10 mM Tris.SO_4, 1 mM β-mercaptoethanol and 10% (v/v) glycerol, pH 7.5). Protein concentrations were determined by using Bradford reagent (Biorad) using bovine serum albumin as a standard. The purified enzyme was analysed using SDS-polyacrylamide gel electrophoresis.

Determination of kinetic parameters

Kinetic parameters were determined using a halide release assay. Assays were done in 200 µL incubations, in 50 mM Tris.SO_4, pH 8.2 at room temperature. For compound **1e**, 20% of DMSO was added to enhance the solubility up to 0.5 mM. Samples were taken at different time points and after adding mercuric thiocyanate and ferric ammonium sulfate the absorption was measured at 460 nm.[19,35] The initial rates of halide release at different substrate concentrations were plotted in a Michaelis-Menten graph in order to determine the kinetic parameters.

Tandem conversions for kinetic resolution of haloalcohols

To 10 mL of a solution of compound **1** in 50 mM Tris.SO_4, pH 8.2, enzyme was added and incubated at 30°C (for details, see Table 5). At various time points, 1 mL samples were taken and extracted with a solvent containing dodecane as internal standard. The samples were dried with $MgSO_4$. The enantiomeric excess values for haloalcohols **2a**-**2c** were determined by Chiral GC and for **2d** and **2c** by Chiral HPLC, as described before. For the reactions with compounds **1a**, **1b** and **1c**, the analysis was done with the same GC program, whereas for **1d** and **1e** an additional GC was used. For **1d**: GC (AT5 column: 80°C

→ 130°C (10°C /min), 130°C for 1 min, 130°C → 80°C (20°C /min); retention times: 3.8 min (**2d**); 4.4 min (**1d**)). For **1e**: GC (AT5 column: 80°C → 180°C (10°C /min), 180°C for 1 min, 180°C → 80°C (20°C/min); retention times: 10.9 min (**2e**); 11.9 min (**1e**)).

Table 5: Details of the tandem conversions starting from compound **1**

compound	**1a**	**1b**	**1b**	**1b**	**1c**	**1d**	**1e**
Enzyme (mg)	DbjA (0.56)	LinB (0.48)	DbjA (5.0)	DhlA (5.0)	DhaA (0.64)	DbjA (0.50)	LinB (0.24)
Solution (mL)	10	10	20	20	10	20	30
[substrate] (mM)	1	2	1	1	1	1	0.5
Substrate (mg)	2.2	2.9	2.9	2.9	2.8	4.3	4.2
Extraction solvent (mL)	chloro-form (0.5)	chloro-form (0.5)	chloro-form (0.5)	chloro-form (0.5)	chloro-form (0.5)	dichloro-methane (1.5)	diethyl-ether (2.0)
Sample volume (mL)	1	1	1	1	1	2	2

REFERENCES

[1] D. L. J. Clive and R. Subedi. *Chem. Commun*. **2000**, 237-238.
[2] Y. Igarashi, S. Otsutomo, M. Harada, and S. Nakano. *Tetrahedron Asymmetry*. **1997**, *8*, 2833-2837.
[3] W. Adam, L. Blancafort, and C. R. SahaMoller. *Tetrahedron Asymmetry*. **1997**, *8*, 3189-3192.
[4] F. Campos, M. P. Bosch, and A. Guerrero. *Tetrahedron Asymmetry*. **2000**, *11*, 2705-2717.
[5] N. Anand, M. Kapoor, S. Koul, S. C. Taneja, R. L. Sharma, and G. N. Qazi. *Tetrahedron Asymmetry*. **2004**, *15*, 3131-3138.
[6] J. D. White, J. Hong, and L. A. Robarge. *J. Org. Chem*. **1999**, *64*, 6206-6216.
[7] R. Rej, D. Nguyen, B. Go, S. Fortin, and J. F. Lavallee. *J. Org. Chem.* **1996**, *61*, 6289-6295.
[8] S. M. Lait, D. A. Rankic, and B. A. Keay. *Chem. Rev.* **2007**, *107*, 767-796.
[9] S. Tsuboi, N. Yamafuji, and M. Utaka. *Tetrahedron Asymmetry*. **1997**, *8*, 375-379.
[10] N. Itoh, A. K. Hasan, Y. Izumi, and H. Yamada. *Eur. J. Biochem.* **1988**, *172*, 477-484.
[11] T. Suzuki, N. Kasai, R. Yamamoto, and N. Minamiura. *Appl. Microbiol. Biotechnol*. **1993**, *40*, 273-278.
[12] M. Kapoor, N. Anand, K. Ahmad, S. Koul, S. S. Chimni, S. C. Taneja, and G. N. Qazi. *Tetrahedron Asymmetry*. **2005**, *16*, 717-725.
[13] R. Liu, P. Berglund, and H. E. Hogberg. *Tetrahedron Asymmetry*. **2005**, *16*, 2607-2611.
[14] Y. F. Wang, C. S. Chen, G. Girdaukas, and C. J. Sih. *J. Am. Chem. Soc*. **1984**, *106*, 3695-3696.
[15] K. J. Harris, Q. M. Gu, Y. E. Shih, G. Girdaukas, and C. J. Sih. *Tetrahedron Lett*. **1991**, *32*, 3941-3944.
[16] E. Vanttinen and L. T. Kanerva. *Tetrahedron Asymmetry*. **1992**, *3*, 1529-1532.

[17] R. J. Pieters, J. H. L. Spelberg, R. M. Kellogg, and D. B. Janssen. *Tetrahedron Lett*. **2001**, *42*, 469-471.
[18] Z. Prokop, Y. Sato, J. Brezovsky, T. Mozga, R. Chaloupkova, T. Koudelakova, P. Jerabek, V. Stepankova, R. Natsume, J. G. van Leeuwen, D. B. Janssen, J. Florian, Y. Nagata, T. Senda, and J. Damborsky. *Angew. Chem. Int. Ed Engl.* **2010**, *49*, 6111-6115.
[19] S. Keuning, D. B. Janssen, and B. Witholt. *J. Bact.* **1985**, *163*, 635-639.
[20] A. N. Kulakova, M. J. Larkin, and L. A. Kulakov. *Microbiology*. **1997**, *143*, 109-115.
[21] Y. Nagata, K. Miyauchi, J. Damborsky, K. Manova, A. Ansorgova, and M. Takagi. *Appl. Environ. Microbiol.* **1997**, *63*, 3707-3710.
[22] Y. Sato, M. Monincova, R. Chaloupkova, Z. Prokop, Y. Ohtsubo, K. Minamisawa, M. Tsuda, J. Damborsky, and Y. Nagata. *Appl. Environ. Microbiol.* **2005**, *71*, 4372-4379.
[23] M. Pavlova, M. Klvana, Z. Prokop, R. Chaloupkova, P. Banas, M. Otyepka, R. C. Wade, M. Tsuda, Y. Nagata, and J. Damborsky. *Nat. Chem. Biol*. **2009**, *5*, 727-733.
[24] P. Banas, M. Otyepka, P. Jerabek, M. Petrek, and J. Damborsky. *J. Comput. Aided Mol. Des*. **2006**, *20*, 375-383.
[25] J. G. van Leeuwen, H. J. Wijma, R. J. Floor, J.M. van der Laan, and D. B. Janssen. *ChemBioChem.* **2012**, *13*, 137-148.
[26] T. Bosma, J. Damborsky, G. Stucki, and D. B. Janssen. *Appl. Environ. Microbiol.* **2002**, *68*, 3582-3587.
[27] J. Damborsky, E. Rorije, A. Jesenska, Y. Nagata, G. Klopman, and W. J. Peijnenburg. *Environ. Toxicol. Chem.* **2001**, *20*, 2681-2689.
[28] R. Mitsui, S. Shinya, Y. Ichiyama, K. Kudo, T. Tsuno, and M. Tanaka. *Biosci. Biotechnol. Biochem*. **2007**, *71*, 1858-1864.
[29] M. T. Reetz and H. Zheng. *ChemBioChem*. **2011**, *12*, 1529-1535.
[30] S. Prasad, M. Bocola, and M. T. Reetz. *ChemPhysChem*. **2011**, *12*, 1550-1557.
[31] E. S. Huyser and R. H. C. Feng. *J. Org. Chem*. **1971**, *36*, 731-733.
[32] K. Sahasrabudhe, V. Gracias, K. Furness, B. T. Smith, C. E. Katz, D. S. Reddy, and J. Aube. *J. Am. Chem. Soc*. **2003**, *125*, 7914-7922.
[33] F. Rogel and J. D. Corbett. *J. Am. Chem. Soc*. **1990**, *112*, 8198-8200.
[34] N. Kasai and K. Sakaguchi. *Tetrahedron Lett*. **1992**, *33*, 1211-1212.
[35] J. P. Schanstra, J. Kingma, and D. B. Janssen. *J. Biol. Chem.* **1996**, *271*, 14747-14753.

CHAPTER 3

Kinetic resolution of α-bromoamides: experimental and theoretical investigation of highly enantioselective reactions catalysed by haloalkane dehalogenases

Alja Westerbeek, Wiktor Szymański, Hein J. Wijma, Siewert J. Marrink,
Ben L. Feringa, and Dick B. Janssen

Based on: Adv. Synth. Catal., 2011, 353, 931-944

ABSTRACT

Haloalkane dehalogenases from five sources were heterologously expressed in *Escherichia coli*, isolated, and tested for their ability to achieve kinetic resolution of racemic α-bromoamides, which are important intermediates used in the preparation of bioactive compounds. To explore the substrate scope, fourteen α-bromoamides, with different *C*-α- and *N*-substituents, were synthesised. Catalytic activity towards eight substrates was found, and for five of these compounds the conversion proceeded with a high enantioselectivity (E-value >200). In all cases, the (*R*)-α-bromoamide is the preferred substrate. Conversions on a preparative scale with a catalytic amount of enzyme (enzyme:substrate ratio less 1:50 w/w) were all completed within 17-46 h and optically pure α-bromoamides and α-hydroxyamides were isolated with good yields (31-50%). Substrate docking followed by molecular dynamics simulations indicated that the high enantioselectivity results from differences in the percentage of the time in which the substrate enantiomers are bound favorably for catalysis. For the preferred (*R*)-substrates, the angle between the attacking aspartate oxygen atom of the enzyme, the attacked carbon atom of the substrate, and the displaced halogen atom, is more often in the optimal range (>157°) for reactivity. This can explain the observed enantioselectivity of LinB dehalogenase in a kinetic resolution experiment.

INTRODUCTION

Enantiopure amides substituted at the α-position with a good leaving group are important precursors for the synthesis of non-natural peptides[1], diketopiperazines[2], α-alkylthioamides[3], and other compounds important in medicinal chemistry.[4] The use of haloalkane dehalogenases for the kinetic resolution of racemic α-bromoamides would present a biocatalytic route towards these valuable intermediates. Additional possibilities for the functionalisation of α-bromoamides are offered by the fact that subsequent reactions with nucleophiles may be carried out with either inversion or retention of configuration.[5] This results in the expansion of the stereochemical scope of possible derivatives and overcomes the limitations caused by the homochirality of the enzymes.

Haloalkane dehalogenases consist of an α/β-hydrolase domain and a cap domain, with the catalytic site located in between. The nucleophilic aspartate of the catalytic pentad catalyses the hydrolytic cleavage of halogenated alkanes, yielding the corresponding alcohols. Two other residues, a tryptophan and a tryptophan/asparagine, are involved in stabilising the halide. The remaining catalytic residues are a histidine and an aspartate/glutamate, which are activating a water molecule for hydrolysis of the alkyl-enzyme intermediate and stabilising the positive charge that develops on the histidine, respectively.[6] Various haloalkane dehalogenases were studied for biotechnological

applications.[7] Enantioselective conversions using haloalkane dehalogenases have been reported for esters and β-bromoalkanes.[8] We report here the enantioselectivity and diastereoselectivity of the dehalogenase catalysed conversion of α-bromoamides.

In the current study, we have screened the following six haloalkane dehalogenases for catalytic activity and enantioselectivity towards a series of α-bromoamides: DhlA, LinB, DbjA, DmlA, DhaA and its mutant DhaA31. Haloalkane dehalogenase from *Xanthobacter autotrophicus* (DhlA) is involved in growth on 1,2-dichloroethane as a sole carbon source.[9] DhaA was originally discovered in a *Rhodococcus rhodochrous* strain, growing on 1-chlorobutane.[10] LinB from *Sphingomonas paucimobilis* UT26 plays a role in the metabolism of hexachlorocyclohexane.[11] DbjA from *Bradyrhizobium japonicum* USDA110 and DmlA from *Mesorhizobium loti* MAFF303099 were discovered through genome mining.[12] DhaA31 is a DhaA mutant variant obtained by directed evolution towards enhanced catalytic activity for 1,2,3-trichloropropane.[13]

RESULTS AND DISCUSSION

Cloning and production of haloalkane dehalogenases

The haloalkane dehalogenase genes were expressed in *E. coli* (for further details, see Experimental Section). Typically, approximately 50 mg of enzyme was obtained per 1 L of overnight induced cultures after purification with Ni-NTA columns. The purity of the isolated enzymes was >95% as judged by SDS-polyacrylamide gel electrophoresis.

Catalytic activity and enantioselectivity/diastereoselectivity of haloalkane dehalogenases towards α-bromoamides

The obtained enzymes were screened for catalytic activity and enantio- or diastereoselectivity towards racemic α-bromoamides **1** (Scheme 1).

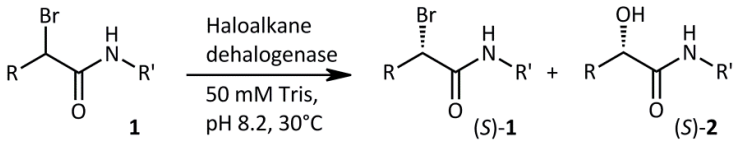

Scheme 1: Kinetic resolution of α-bromoamides.

In order to study the influence of different substituents in substrates **1**, we decided to independently change the *C*-α- and *N*-substituents (R and R' respectively, Scheme 1) and test for catalytic activity and selectivity for compounds **1a**-**1n** (Figure 1). Simple compounds (**1a**-**1d**) and *C*-protected dipeptide precursors (**1e-1j**, **1l**, **1m**) were chosen. Enantioselectivity or diastereoselectivity for these compounds is displayed in Table 1.

Compound **1a** (Figure 1, R = Me, R' = Bn) was converted by DbjA, LinB and DhaA31, with E-values of >200 for DbjA and DhaA31. Compound **1b** (R' = Ph) was converted by four enzymes, and enantioselectivities of >200 were found for DbjA, DhaA and DhaA31. Replacement of the aromatic group by an aliphatic chain (R' = *n*-Bu, compound **1c**), resulted in a loss of catalytic activity with almost all enzymes. Conversion of **1c** by DbjA and DmlA was measurable, yet low. LinB converted compound **1c** with an acceptable E-value of 74. When the R' substituent is a *t*-butyl group (compound **1d**), none of the studied haloalkane dehalogenases possesses detectable catalytic activity.

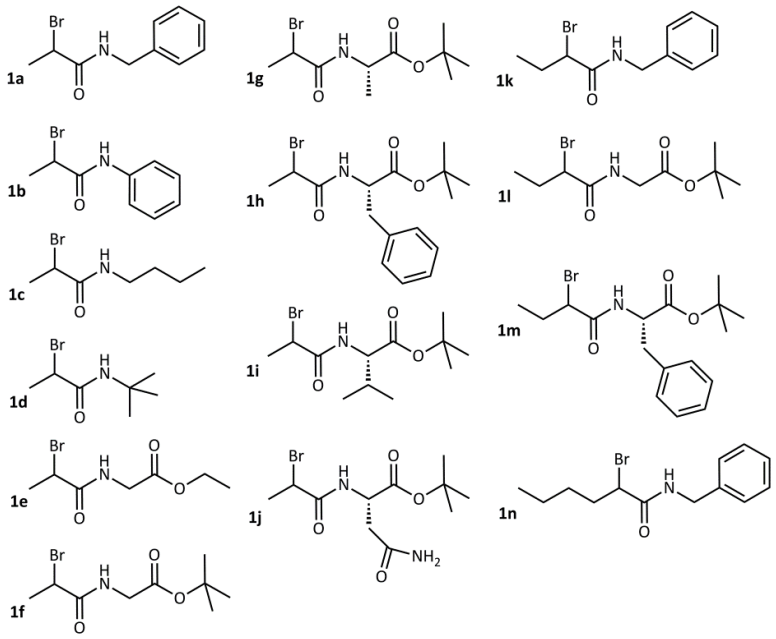

Figure 1: The α-bromoamides tested for dehalogenase reactions in this study.

Encouraged by the high enantioselectivities observed in the enzymatic conversions of compounds **1a**, **1b**, and **1c**, we decided to test the catalytic activity of haloalkane dehalogenases with ester derivatives that are potential dipeptide precursors. Catalytic activity towards a glycine ethyl ester derivative **1e** was observed with DbjA and LinB; albeit with low E-values (Table 1). However, changing the ethyl ester (**1e**) into a *t*-butyl ester (compound **1f**), enhances the enantioselectivity tremendously to an E-value of >200 with DbjA. For LinB, the E-value with **1f** did not improve when the ethylester was replaced by a *t*-butyl ester. The conversion rate for DmlA was low for both **1e** and **1f**.

Table 1: Enantioselectivity and diastereoselectivity (d.e.) of haloalkane dehalogenases[a)]

compound	DbjA	LinB	DhaA	DhaA31	DmlA
1a	>200 (15%)	67 (43%)	I [b)]	>200 (18%)	I
1b	>200 (50%)	28 (46%)	>200 (28%)	>200 (50%)	I
1c	ND [c)]	74 [d)] (53%)	I	ND	ND
1e	4 (57%)	10 (65%)	I	I	ND
1f	>200 (42%)	11 [e)] (67%)	I	I	ND
1g	I	d.e.Br > 99% [e)] d.e.OH > 99%[e)] (50%)	I	I	d.e.Br = 32% [e)] d.e.OH = 88% [e)] (27%)
1h	I	d.e.Br > 95% [d)] d.e.OH > 95% [d)] (50%)	I	I	I
1k	I	>200 [e)] (37%)	I	I	I

[a)] Reported are the E-values and for **1g** and **1h** the diasteriomeric excess (d.e.) of the remaining substrate (Br) or product (OH). Conversion is given in brackets. The E-values and conversions were calculated from the enantiomeric excess of substrate and product using the equations of Chen *et al.* [14]

[b)] I, Inactive, less than 10% conversion in 3 h. Compounds **1d**, **1i**, **1j**, **1l**, **1m** and **1n** are also not converted with detectable catalytic activity.

[c)] ND, not determined since conversion was too low to obtain a reliable E-value.

[d)] These values are taken from Table 2, as compounds were not detectable on small scale.

[e)] Incubations done overnight.

For further details see Experimental Section.

To determine the scope of possible amino acid substituents that can be incorporated into compound **1**, we tested an additional set of dipeptide precursors. For the L-alanine derivative **1g** a reasonable catalytic activity was observed only with LinB and DmlA. The diastereoselectivity with LinB was high, as the diastereomeric excess (d.e.) for both the bromoamide and the hydroxyamide product was over 99%. For DmlA the diastereoselectivity was not spectacular, as 32% d.e. and 88% d.e. was measured for the α-bromoamide and α-hydroxyamide, respectively. Catalytic activity with the L-phenylalanine derivative **1h** was only observed with LinB, where the diastereoselectivity was high, since a d.e. of over 95% was obtained for both the α-bromoamide and the α-hydroxyamide. For the compounds **1g** and **1h**, the (*R,S*)-α-bromoamide was preferred over the (*S,S*)-α-bromoamide. Of the other tested compounds, the L-valine derivative **1i** and L-asparagine derivative **1j** were not converted by any of the haloalkane dehalogenases.

Subsequently, we focused on the *C*-α-substituent (R, **Scheme 1**), which was altered from a methyl group in compound **1a** to an ethyl group (compound **1k**). Catalytic activity towards

compound **1k** was only found with LinB, with an excellent E-value of over 200. DbjA and DhaA31 show no catalytic activity when R is an ethyl group. Compound **1n**, where the *C*-α-substituent is changed into an *n*-butyl group, is not accepted as a substrate by any of the enzymes, which sets a limitation to the substituents at the *C*-α-position. Since LinB accepted both amino acid derived compounds (**1g** and **1h**) and an ethyl substituent at the *C*-α-position (compound **1k**), we have prepared additional compounds **1l** and **1m**, which combine these features. However, no detectable catalytic activity was found with any of the enzymes. This indicates that the *C*-α-substituent is at a sensitive position and a substituent larger than methyl is only accepted if the substituent at R' is small.

DhlA had no detectable catalytic activity for any of the compounds (**1a**-**n**). It has been reported that DhlA, the 1,2-dichloroethane dehalogenase from *X. autotrophicus*, only converts smaller substrates, mainly primary halides, which is in agreement with its smaller active site.[15]

In summary, LinB is the best enzyme in terms of catalytic activity, as it converts no less than eight of the fourteen tested compounds. This corresponds well to literature reports, where LinB was shown to have the largest active site cavity of all haloalkane dehalogenases of which the structure is solved.[16] It has the highest activity towards larger substrates, which is in agreement with its physiological function in tetrachlorocyclohexadiene degradation.[17] With respect to the enantioselectivity, DbjA is the best enzyme, as the E-value for three out of the four converted substrates is >200. This is in agreement with experimental data measured for conversion of α-bromoesters and β-bromoalkanes.[8b]

For all the compounds for which enzymatic activity and good selectivity were found, preparative kinetic resolution experiments were conducted with usually 80 mg of substrate. In a typical experiment, the substrate was incubated with a small amount of enzyme (enzyme:substrate ratio 1:21-1:124 w/w, Table 2). All conversions were complete within 17-46 h of incubation at 30°C. All products were obtained with high optical purity (95-99% e.e./d.e.), except for **1c**, for which an e.e. of 87% was found for the α-hydroxyamide. After the purification the yields for α-bromoamides as well as for α-hydroxyamide ranged from 31% to an excellent yield of 50% (Table 2).

The absolute configuration of the products of the kinetic resolutions was determined by comparison to literature data or by correlation synthesis of products **2** from commercially available enantiopure α-hydroxyacids. In all cases, the enzymes preferentially converted the (*R*)-enantiomer of the α-bromoamide with inversion of configuration to the (*S*)-enantiomer of the α-hydroxyamide.

Table 2: Results of the preparative scale experiments.

compound	enzyme	enzyme: substrate ratio (w:w)	time (h)	(*S*)-α-bromoamide		(*S*)-α-hydroxyamide		E-value
				yield	e.e./d.e.	yield	e.e./d.e.	
1a	DbjA	1:58	46	41%	>99%	50%	>99%	>200
1b	DbjA	1:124	17	44%	>99%	46%	>99%	>200
1c	LinB	1:110	20	47%	>99%	47%	87%	74
1f	DbjA	1:95	20	44%	98%	40%	>99%	>200
1g	LinB	1:67	43	48%	>99%	31%	97%	NA[a)]
1h	LinB	1:21	20	39%	>95%	39%	>95%	NA
1k	LinB	1:42	44	40%	>99%	31%	97%	>200

[a)] NA, Not applicable.

Preparative scale conversion

Since the preparative-scale conversions are limited by the low solubility of the substrates, we studied the possibility of increasing the solubility by the addition of the water-miscible cosolvent dimethylsulfoxide (DMSO). Substrate conversion, measured after 150 min, was compared to conversion in reactions without cosolvent (Figure 2). The relative conversion was still about 50% when up to 25% (v/v) DMSO was added to the substrate solution. Using these optimised conditions (25% DMSO), a larger preparative scale experiment was performed in which 250 mg of racemic **1a** was subjected to kinetic resolution by DbjA (2.8 wt% enzyme/ substrate), yielding after 44 h 44% of **1a** and 49% of **2a**, both with an e.e. of 99%.

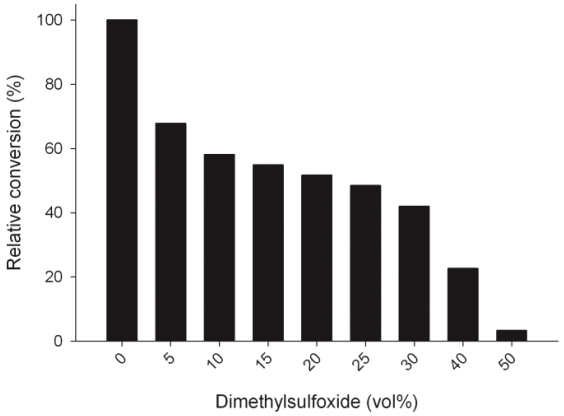

Figure 2: Conversion of **1a** by DbjA at various concentrations of dimethylsulfoxide.

Computational analysis of LinB stereoselectivity

To explain the origin of the enantioselective conversion of bromoamide **1f** by LinB, we carried out docking and MD simulations. A crystal structure of the enzyme is available.[18] Possible explanations for the observed (*R*)-selectivity with different substrates are (i) stronger binding of (*R*)-substrates, preventing the (*S*)-substrates from binding and conversion, or (ii) higher reactivity of the bound (*R*)-substrates, resulting in faster turnover than with the (*S*)-substrate. Two substrates, for which the enzyme differs in enantioselectivity, were selected: compound **1f** (E-value = 11) and **1k** (E-value >200). Both enantiomers of these compounds were docked into LinB.

The first possibility, preferential conversion of the (*R*)-substrate due to stronger binding as compared to the (*S*)-substrate, was evaluated by predicting the dissociation constants of the substrates to the enzyme by AutoDock4.[19] The program predicts the binding energy by calculating the difference in energy between a bound and unbound state based on separate potentials for H-bonding, desolvation, Van der Waals and electrostatic interactions, and for the entropy loss by the ligand upon binding, each with its own empirically determined weighing factor. The predicted binding energies [(*R*)-**1f**, ΔG = -24 kJ mol^{-1}; (*S*)-**1f**, ΔG = -25 kJ mol^{-1}; (*R*)-**1k**, ΔG = -26 kJ mol^{-1}; (*S*)-**1k**, ΔG = -29 kJ mol^{-1}] for the different substrates docked into LinB are within the reported error of the method (12 kJ mol^{-1})[19] identical to each other. Thus, there is no evidence that the enantioselective catalysis is due to preferential binding of the (*R*)-enantiomers by LinB.

The alternative explanation, that the observed enantioselectivity is due to the (*R*)-enantiomers binding in an orientation more suitable for catalysis, was evaluated by MD simulations of the enzyme-substrate complexes. Earlier work revealed that for poor substrates of a haloalkane dehalogenase the critical step in the catalytic cycle is the first step, in which an aspartate side-chain nucleophilically attacks the substrate with the halide as the leaving group.[20] Therefore, the relative reactivities for this nucleophilic attack were quantified as the percentage of the time during simulation that a near attack conformation (NAC) occurs. NACs are defined as having reacting atoms at Van der Waals distance and angles ± 15-20° of the angle of the forming bond in the TS.[21] NACs necessarily precede the transition state in the catalytic pathway[22], their presence corresponds to transition state stabilisation[23], and a higher percentage of NACs during simulations was found to correspond to a higher experimental catalytic rate.[21] The criteria to define a NAC for the initial nucleophilic attack were distances d_1 < 3.41 Å, d_2 < 3.50 Å, d_3 < 3.50 Å, angles θ_1 = 157-180°, θ_2 = 120-180°, θ_3 = 120-180° (Scheme 2); all criteria need to be met at the same time. The criteria for d_1 and θ_1 are from Hur *et al.*[24] while the criteria for d_2, d_3, θ_2, θ_3, which indicate whether there are H-bonds from the side-chains of Asn38 and Trp109 that stabilise the development of a negative charge on the bromide, were used additionally since these H-bonds enhance catalysis.[25]

The obtained percentage of the time that a NAC was present during the simulation were for (*R*)-**1f** 6.7±0.6%, for (*S*)-**1f** 0.41±0.09%, for (*R*)-**1k** 0.81±0.25%, and less than 0.001% for

(*S*)-**1k**. The ratio of these NAC percentages for (*R*/*S*)-**1f** was 16, in good agreement with the experimentally observed E-value. Furthermore, the ratio for (*R*/*S*)-**1k**, which is extremely high (> 800) since no NACs were observed for the (*S*)-enantiomer, is in excellent agreement with the experimentally observed E-value of >200. Thus, the MD simulations indicate that the enantioselectivity can indeed be due to differences in the reactivity of the bound substrate.

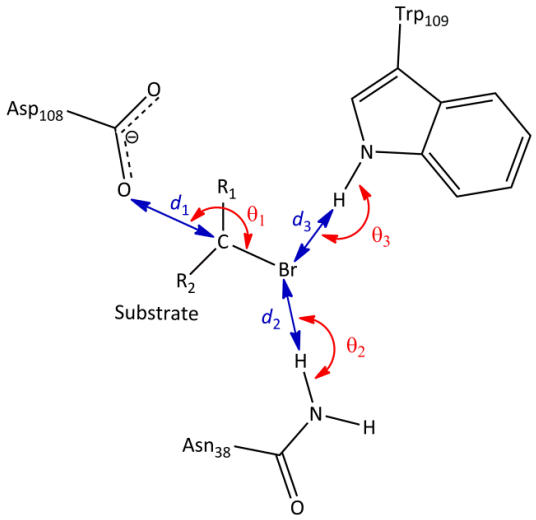

Scheme 2: Distances and angles relevant for nucleophilic attack and leaving group stabilisation in LinB-substrate complexes.

To explore the origin of the differences in reactivity of the bound substrates, the angles and distances that are important for a nucleophilic substitution reaction to occur were analysed (Scheme 2). The distribution of θ_1 in the (*R*)-**1f**-LinB complex has the highest overlap with the range of angles that are optimal for nucleophilic attack, more than with (*R*)-**1k** and (*S*)-**1f**, while for (*S*)-**1k** only a few excursions into the catalytically necessary range were observed (Figure 3). For all other catalytically relevant distances and angles, only minor differences in the overlap of the thermally accessible range with the catalytically relevant range were observed for the different enantiomers (data not shown). To verify that none of the other five criteria determined the reactivity of the substrates, the analysis was redone omitting the θ_1 criterion, indeed resulting in similar percentages of pseudo-reactive conformation [46.7±1.4% for (*R*)-**1f**), 75.2±0.7% for (*S*)-**1f**, 54±1% for (*R*)-**1k**, and 38.0±0.7% for (*S*)-**1k**], which cannot explain the observed enantioselectivities. This suggests that the main cause for differences in catalytic activity of bound substrate enantiomers is the frequency of occurrence of conformation with a suitable angle θ_1 for nucleophilic attack (Scheme 2).

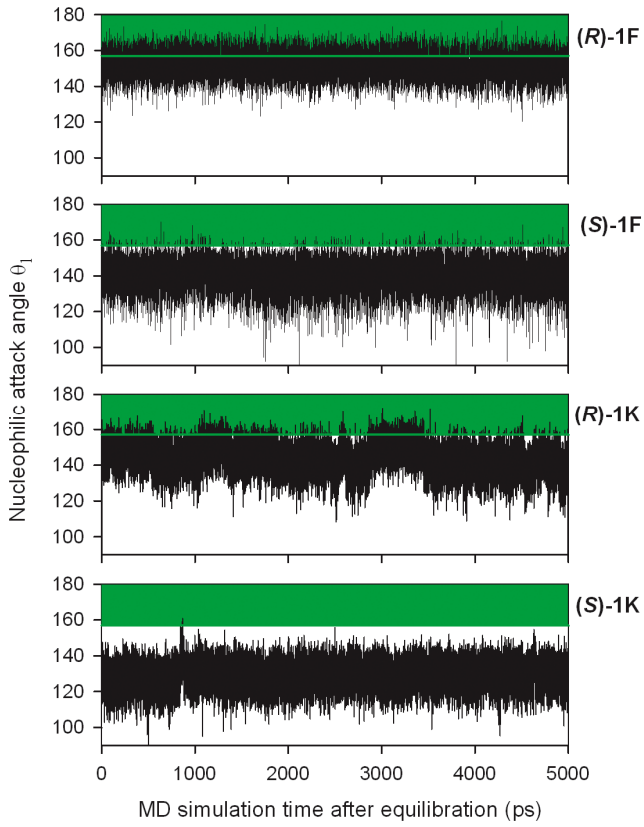

Figure 3: Nucleophilic attack angle θ_1 from an MD simulation of LinB-substrate complexes versus time. The black trace is the plot. Angles that fall within the range defined for the NAC are indicated with a green background and a green separation line. The displayed time range is 2000 to 7000 ps after start of the MD simulation. The labels on the right indicate the substrate.

To understand why the preferred (*R*)-substrates are bound with a distribution of the angle θ_1 that leads to a higher NAC percentage, the trajectories of the MD simulations were visually inspected. This revealed that the substrates are bound with a total of three H-bonds, similar to what was found earlier for the DbjA dehalogenase by modeling.[8b] The side-chain amide hydrogen of Asn38 and the indole hydrogen of Trp109 donate H-bonds to the halogen. Another H-bond is formed between the substrate amide hydrogen atom and a carboxylate oxygen of the catalytic Asp108 (Figure 4). The (*R*)- and (*S*)-substrates bind in similar, but mirrored, orientations in the active site ((*R*)- and (*S*)-substrates are shown superimposed). The R and R' substituents are bound in the same, mostly hydrophobic, substrate cavity. Most residues that line the active site and interact with the (*R*)-enantiomer also interact with the (*S*)-enantiomer (Figure 4).

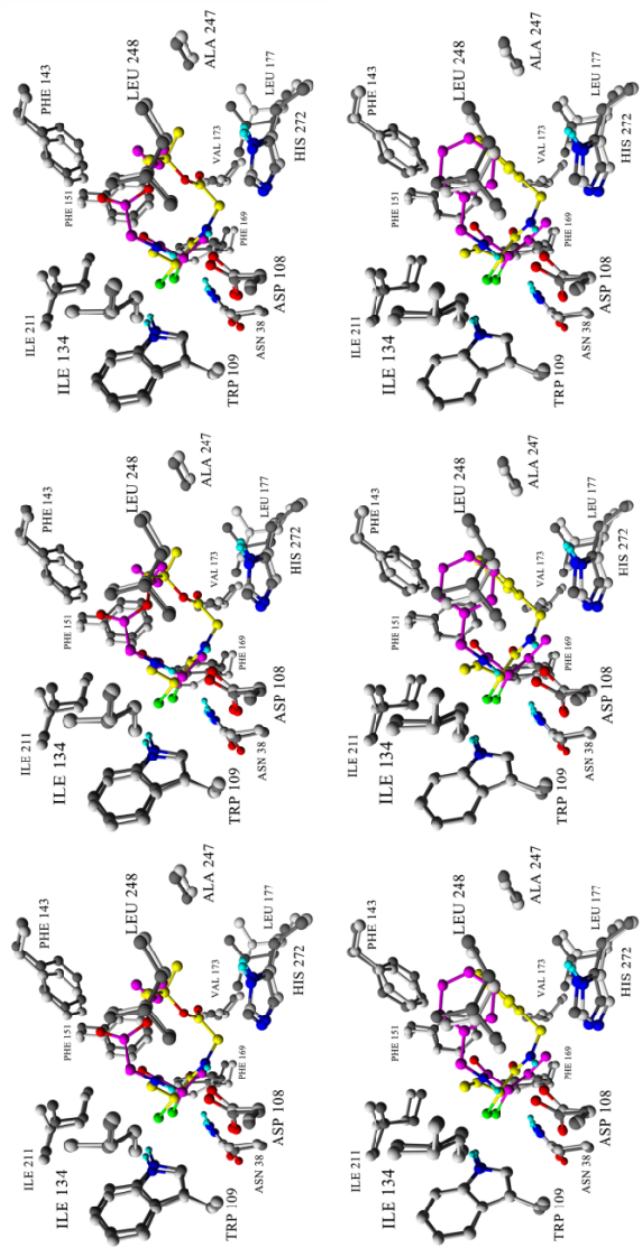

Figure 4: Stereo presentation of binding modes of **1f** (upper panels) and **1k** (lower panels) enantiomers in LinB during the MD simulations. Light gray, LinB carbon atoms that bind (*S*)-substrate; purple, carbon atoms of (*S*)-substrate; dark gray, LinB carbon atoms binding (*R*)-substrate; yellow, carbon atoms of (*R*)-substrate; blue, nitrogen atoms; green, bromide atoms; turquoise, hydrogen atoms involved in H-bonds. The atom positions are the average over all snapshots after equilibration. Pictures were created with Yasara (www.yasara.org) and Povray (www.povray.org).

Therefore, it was not possible to identify particular residues that are responsible for the observed enantioselectivity. Thus, the preferred (*R*)-substrates have a binding mode similar to that of (*S*)-substrates, but with a distribution of the θ_1 angle for nucleophilic attack that is better for reaching the transition state, and the decisive 10-25° difference is due to the way in which the R and R' substituents of the substrate fit in the irregularly shaped mostly hydrophobic substrate binding pocket

Kinetic characterisation of LinB enantioselectivity

Substrate **1f** was selected for further experimental characterisation of its steady-state kinetic preference for the (*R*)-enantiomer, since the lower E-value makes it possible to follow conversion of both enantiomers over time. Since the pure (*R*)-enantiomer of **1f** is not available, the kinetic parameters were determined from a time course depletion of racemic substrate by LinB (Figure 5A). In a plot of substrate concentration versus enzyme concentration × time (Selwyn's test of inactivation)[26], the points measured at high and low LinB concentrations superimpose (Figure 5B), which shows that no significant inactivation of LinB occurs during the 7 h assay. The E-value determined by fitting with numerical integration of the Michaelis-Menten equation was 24 ± 3, which is higher than found in a single timepoint measurement (Table 1). The obtained kinetic parameters were k_{cat}^S/K_m^S = 26 M^{-1} s^{-1}, $K_m^S \geq 1$ mM, the k_{cat}^R = 0.082 ± 0.04 s^{-1}, and the K_m^R = 0.13 ± 0.02 mM. For k_{cat}^S no unique value could be obtained since there was no saturation at the highest concentration tested (500 µM, maximum solubility), and for K_m^S only a lower limit (1 mM) could be obtained for the same reason.

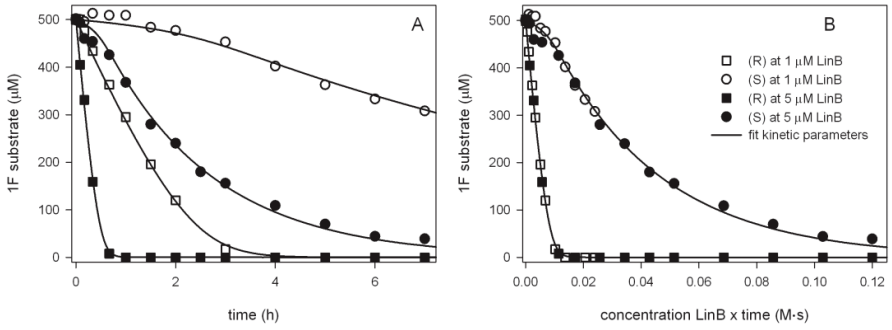

Figure 5: Time-course determination of kinetic parameters for the **1f** conversion by LinB. (A), Concentration of substrate enantiomers versus time at different LinB concentrations. See panel B for symbols. (B), Selwyn's plot to test for inactivation.

To investigate whether these kinetic parameters, which indicate a lower K_m for the preferred (*R*)-enantiomer, are compatible with a faster dehalogenation reaction of the preferred (*R*)-enantiomer without much stronger binding, as predicted by the docking energies and MD simulations, the steady-state kinetic parameters were fitted to the

minimal kinetic scheme[27] for LinB (Scheme 3). In this scheme, k_2 is the rate of carbon-halogen bond cleavage, and k_3 is the rate of hydrolysis of the covalent alkyl-enzyme intermediate.[6] In general, K_m can be larger than, equal to, or smaller than K_D (dissociation constant of the Michaelis complex) depending on the kinetic scheme and the constants.[28,29]

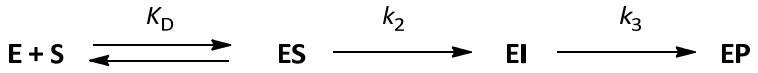

Scheme 3: Minimal kinetic scheme for a dehalogenase. ES, Michaelis complex; EI, covalent intermediate.

For the kinetic mechanism depicted in Scheme 3, equations 1 and 2 apply. We fitted the values of K_D^R, K_D^S, k_2^R, k_2^S, k_3^R, and k_3^S to reproduce all the measured values for **1f** conversion described in the previous paragraph, while constraining the ratio of k_2^R/k_2^S to the value of 16 that is predicted by the NAC analysis above. Under this constraint, it was still possible to obtain solutions that within 0.1% accuracy reproduced the steady-state kinetic values and kinetic resolution pattern (Fig. 5A). Inspection of equation 1 and 2 reveals that for the agreement it is required that the hydrolysis step (k_3) is slower than the dehalogenation step (k_2), which for LinB was indeed confirmed experimentally with different substrates.[27] In this situation, the higher k_2 for the preferred enantiomer does not result in a higher k_{cat} but in a lower K_m. Thus, the MD simulations that predict a faster k_2 for the best enantiomer are compatible with the measured steady state kinetics for the enantiomers of **1f** and the known kinetics of LinB, in which a faster k_2 lowers the K_m for the substrate. A difference in reaction rate causing enantioselectivity has also been observed in halohydrin dehalogenase, where unproductive binding of an epoxide substrate prevented conversion of (*S*)-halohydrins and unproductive binding also explains enantioselectivity of human AMP, dTMP and UMP-CMP kinases.[29]

$$k_{cat} = \frac{k_2 k_3}{k_2 + k_3} \quad (1)$$

$$K_m = K_D \frac{k_3}{k_2 + k_3} \quad (2)$$

CONCLUSIONS

In this paper we report highly enantioselective transformations of α-bromoamides using haloalkane dehalogenases. The kinetic resolution of α-bromoamides was shown to reach E-values of over 200. *C*-protected dipeptide precursors (**1f**-**1h**) are converted with high stereoselectivity by either DbjA or LinB, resulting in enantiopure (e.e. or d.e. > 95%)

precursors of peptidomimetics. In general, the enzymes show broader specificity with different *N*-substituents (R') (as smaller, aliphatic, hydrophilic groups are accepted) than with *C*α-substituents (R), where methyl is the universal group and only one compound with an ethyl group is converted (**1k**). Conversions on preparative scale with usually less than 2 wt% of enzyme over substrate gave high yields for both α-bromoamides and α-hydroxyamides, within 1-2 days. The results presented here add a new class of biocatalytic reactions to the repertoire of highly enantioselective biotransformations suitable for synthesis.

The molecular dynamics simulations of the LinB-substrate complexes indicate that differences in dynamic behavior of bound substrate, result in an unfavorable angle for nucleophilic attack by Asp108 in case of the non-preferred (*S*)-enantiomers of **1f** and **1k**. This influences the reaction rate of the bound substrates. The (*R*)- and (*S*)-substrates bind in conformations in which Asn38 and Trp109 make H-bonds to the halide leaving group, the substrate amide makes a H-bond to Asp108, and the remainder of the substrate binds in the mostly hydrophobic active site cavity of LinB. How the remainder of the substrate enantiomer fits into this asymmetric part of the substrate binding pocket appears to control the angle for nucleophilic attack, which ultimately determines enantioselectivity. The obtained steady state kinetic parameters for conversion of (*R*)-**1f** and (*S*)-**1f** were compatible with the data from MD simulations, and suggested that the effect of the faster dehalogenation step in the catalytic cycle is not that the k_{cat} increases for the preferred enantiomer but that its K_m is lowered, which ultimately leads to preferred conversion of the (*R*)-enantiomer.

EXPERIMENTAL

*General procedure for the synthesis of racemic α-bromoamides **1***

2-Bromoacyl bromide (2.0 mmol) and amine (2.0 mmol) were stirred in DCM (8 mL) at 5°C. Triethylamine (2.2 mmol or 5.0 mmol, when the amine hydrochloride was used as reactant) in DCM (2 mL) was added dropwise, and the cooling was stopped. After 2-4 hours the volatiles were evaporated and the product was purified by flash chromatography (Silicagel 40-63 μm, pentane/diethylether).

1a: *N*-Benzyl-2-bromopropionamide

Yield: 99%. White needles. R_f = 0.30 (pentane/diethylether, 1:1, v/v); mp. 94.1-94.3°C (lit.[30] 93.5-94.5°C); ^{1}H NMR (400 MHz, $CDCl_3$): δ 1.92 (d, ^3J = 6.8 Hz, 3H, C**H$_3$**), 4.54-4.82 (m, 3H, C**H**Br, C**H$_2$**Ph), 6.66 (br s, 1H, N**H**), 7.27-7.36 (m, 5H, Ar**H**). ^{1}H NMR consistent with literature data.[31] ^{13}C NMR (50 MHz, $CDCl_3$): δ 23.5, 44.4, 45.5, 127.9, 128.0, 129.1, 137.7, 169.4. Chiral HPLC analysis (Chiralcel AD, heptane/*i*-PrOH, 95/5, v/v), retention times (min): 11.3 (*R*) and 12.0 (*S*).

1b: *N*-Phenyl-2-bromopropionamide

Purchased from Sigma-Aldrich. Chiral HPLC analysis (Chiralcel ADH, heptane/*i*-PrOH, 95/5, v/v), retention times (min): 24.0 (*R*) and 31.1 (*S*).

1c: *N*-Butyl-2-bromopropionamide.

Yield: 96%. Colorless oil. R_f = 0.35 (pentane/diethylether. 1:1, v/v); ^{1}H NMR (300 MHz, $CDCl_3$): δ 0.95 (t, ^3J = 7.2 Hz, 3H, C**H$_3$**), 1.34-1.59 (m, 4H, C**H$_2$**), 1.90 (d, ^3J = 7.5 Hz, 3H, C**H$_3$**), 3.29 (m, 2H, C**H$_2$**), 4.43 (q, ^3J = 6.9 Hz, 2H, C**H$_2$**) 6.43 (br, s, 1H, N**H**). NMR consistent with literature data.[32] ^{13}C NMR ($CDCl_3$): δ 14.0, 20.2, 23.6, 31.6, 40.2, 46.0, 169.4. Chiral HPLC analysis (Chiralcel AD, heptane/*i*-PrOH, 98/2, v/v), retention times (min): 10.4 (*R*) and 11.5 (*S*).

1d: *N*-*t*-Butyl-2-bromopropionamide

Yield: 26%. White powder. R_f = 0.54 (pentane/diethylether. 1:1, v/v); mp. 119-120°C, (lit.[33] 119-121°C). ^{1}H NMR (400 MHz, $CDCl_3$): δ 1.36 (s, 9H, 3 C**H$_3$**), 1.83 (d, ^3J = 7.2 Hz, 3H, C**H$_3$**), 4.30 (q, ^3J = 7.2 Hz, 1H, C**H**Br), 6.16 (br, s, 1H, N**H**).

1e: Ethyl-2-(2-bromopropanamido)acetate

Yield: 71%. White crystals. R_f = 0.20 (pentane/diethylether. 1:1, v/v); mp. 54-55°C; ^{1}H NMR (400 MHz, $CDCl_3$): δ 1.30 (t, ^3J = 7.2 Hz, 3H, C**H$_3$**), 1.90 (d, ^3J = 7.2 Hz, 3H, C**H$_3$**), 4.05 (d, ^3J = 4.8 Hz, 2H, C**H$_2$**N), 4.24 (q, ^3J = 7.6 Hz, 2H, C**H$_2$**O), 4.45 (q, ^3J = 6.8 Hz, 1H, C**H**Br), 6.84 (br, s, 1H, N**H**). ^{13}C NMR ($CDCl_3$): δ 14.1, 23.0, 41.9, 44.3, 61.7, 169.3, 169.4. HRMS (ESI+) calc. for $C_7H_{12}NO_3Na$: 259.9893, found: 259.9892. HPLC (Chiralcel AD, heptane/*i*-PrOH, 9/1, v/v), retention times (min): 11.1 and 12.0 (absolute configuration not assigned).

1f: *t*-Butyl 2-(2-bromopropanamido)acetate

Yield: 91%. White powder. R_f = 0.40 (pentane/diethylether. 1:1, v/v); mp. 73-75°C. ^{1}H NMR (400 MHz, $CDCl_3$): δ 1.48 (s, 9H, 3 C**H$_3$**), 1.89 (d, ^3J = 7.2 Hz, 1H, C**H**Br), 3.95 (m, 2H, C**H$_2$**), 4.43 (q, ^3J = 6.8 Hz, 1H, C**H$_2$**), 6.85 (br, s, 1H, N**H**). ^{13}C NMR ($CDCl_3$): δ 23.3, 28.3, 42.8, 44.7, 83.0, 168.7, 169.5. HRMS (ESI+) calc. for $C_9H_{16}NO_3BrNa$: 288.0206, found: 288.0208. Chiral HPLC analysis (Chiralcel OD, heptane/*i*-PrOH, 95/5, v/v), retention times (min): 7.4 (*R*) and 9.2 (*S*).

1g: *t*-Butyl-2-[(2-bromopropanoyl)amino]-propanoate

Yield: 94%. White solid. D.r. = 1:1. Diastereoisomeric ratio was determined by ^{1}H NMR spectroscopy, by the comparison of CH(Br)C**H$_3$** signal (d, 1.87 ppm for (*S,S*), 1.89 ppm for (*R,S*)).

1h: *t*-Butyl-2-[(2-bromopropanoyl)amino]-3-phenylpropanoate

Yield: 85%. White solid. D.r. = 1:1. Diastereoisomeric ratio was determined by ^{1}H NMR spectroscopy, by the comparison of CH(Br)C**H$_3$** signal (d, 1.81 ppm for (*S,S*), 1.85 ppm for (*R,S*)).

1i: *t*-Butyl-2-[(2-bromopropanoyl)amino]-3-methyl-butanoate

Yield: 98%. Clear oil. D.r. = 1:1. Diastereoisomeric ratio was determined by ^{1}H NMR spectroscopy, by the comparison of CH(Br)C**H$_3$** signal (d, 1.87 ppm and 1.89 ppm, relative

configuration not determined). HRMS (ESI+) calc. for $C_{12}H_{22}NO_3BrNa$: 330.0681, found: 330.0664.

1j: *t*-Butyl-4-amino-2-[(2-bromopropanoyl)amino]-4-oxobutanoate

Yield: 71%. White solid. D.r. = 1:1. Diastereoisomeric ratio was determined by ^{1}H NMR spectroscopy, by the comparison of CH(Br)C**H$_3$** signal (d, 1.85 ppm and 1.87 ppm, relative configuration not determined).

1k: *N*-Benzyl-2-bromobutanamide

Yield: 99%. White powder. R_f = 0.25 (pentane/diethylether. 1:1, v/v). mp. 75-76°C. ^{1}H NMR (400 MHz, $CDCl_3$): δ 1.05 (t, ^3J = 7.2 Hz, 3H, C**H$_3$**), 2.06-2.21 (m, 2H, C**H$_2$**CHBr), 4.34 (dd, ^3J = 7.6 Hz, ^3J = 4.8 Hz, 1H, C**H**Br), 4.44-4.52 (m, 2H, C**H$_2$**NH), 6.77 (br, s, 1H, N**H**), 7.26-7.37 (m, 5H, Ar). ^{13}C NMR ($CDCl_3$, 50 MHz): δ 12.0, 29.6, 44.3, 53.9, 127.9, 127.9, 129.0, 137.8, 168.8. HRMS (ESI+) calc. for $C_{11}H_{14}NOBrNa$: 278.0151, found: 278.0141. Chiral HPLC analysis (Chiralcel OD, heptane/*i*-PrOH, 95/5, v/v), retention times (min): 13.8 (*R*) and 15.2 (*S*).

1l: *t*-Butyl-2-(2-bromobutananamido)acetate

Yield: 96%. White crystals. R_f = 0.54 (pentane/diethylether. 1:1, v/v); mp. 50-51°C; ^{1}H NMR (400 MHz, $CDCl_3$): δ 1.06 (t, ^3J = 7.2 Hz, 3H, C**H$_3$**), 1.48 (s, 9H, (C**H$_3$**)$_3$), 2.01-2.23 (m, 2H, CH_3C**H$_2$**), 3.95 (d, 2H, ^3J = 5.2 Hz, C**H$_2$**NH), 4.31 (dd, ^3J = 7.2 Hz, ^3J = 5.2 Hz, 1H, C**H**Br), 6.87 (br, s, 1H, N**H**). ^{13}C NMR ($CDCl_3$): δ 11.9, 28.3, 29.5, 42.8, 53.3, 82.9, 168.7, 168.9. HRMS (ESI+) calc. for $C_{10}H_{18}NO_3BrNa$: 302.0368, found: 302.0353.

1m: *t*-Butyl-2-[(2-bromobutanoyl)amino]-3-phenylpropanoate

Yield: 68%. Clear oil. D.r. = 1:1. Diastereoisomeric ratio was determined by ^{1}H NMR spectroscopy, by the comparison of CH_2C**H$_3$** signal (t, 0.98 ppm and 1.02 ppm, relative configuration not determined). HRMS (ESI+) calc. for $C_{17}H_{24}BrNO_3Na$: 392.0837, found: 392.0816.

1n: *N*-Benzyl-2-bromohexanamide

Yield: 93%. White solid. R_f = 0.57 (pentane/diethylether. 1:1, v/v). mp. 46-47°C. ^{1}H NMR (400 MHz, $CDCl_3$): δ 0.92 (t, ^3J = 6.8 Hz, 3H, C**H$_3$**), 1.32-1.56 (m, 4H, CH_3C**H$_2$**C**H$_2$**), 1.98-2.22 (m, 2H, C**H$_2$**CHBr), 4.36 (dd, ^3J = 8.0 Hz, ^3J = 4.8 Hz, 1H, C**H**Br), 4.42-4.53 (m, 2H, C**H$_2$**NH), 6.70 (br, s, 1H, N**H**), 7.26-7.38 (m, 5H, Ar). ^{13}C NMR ($CDCl_3$, 100 MHz): δ 14.1, 22.2, 29.6, 36.0, 44.4, 52.4, 127.9, 127.9, 129.0, 137.8, 168.9; HRMS (ESI+) calc. for $C_{13}H_{18}BrNONa$: 306.0469, found: 306.0454.

*Catalytic activity with compounds **1a**-**1n***

Catalytic activity was measured using a halide release assay in which the optical absorption was measured at 460 nm.[9] Assays were carried out in 200 µL incubations, with 1-1.5 mM substrate, in 50 mM Tris.SO_4, pH 8.2 at room temperature, using 15-35 µg enzyme.

*Stereoselectivity with compounds **1a**-**1n***

Typically 120-160 µg enzyme was added to a 5 mL solution of racemic α-bromoamide (1a-1n, 1-1.5 mM) in 50 mM Tris.SO4, pH 8.2, and incubated at 30°C.[20] Depending on catalytic activity, 2 mL sample was taken, after 1-16 h, extracted with 1.5 mL of diethylether or ethylacetate and dried. Solvents were evaporated and enantiomeric/diastereomeric excess of α-bromoamide and α-hydroxyamide were determined using Chiral HPLC (compound 1a-1c, 1e, 1f, 1k) or NMR (compound 1g and 1h). The E-values and conversions were calculated by substituting the enantiomeric excess of substrate and product in the equations for enantiomeric ratio.[14]

Preparative kinetic resolution experiments

Kinetic resolution of compound 1a

DbjA (1.4 mg) was added to a solution of *N*-Benzyl-2-bromopropionamide (**1a**, 0.34 mmol, 81 mg) in 250 mL of 50 mM Tris.SO_4 buffer, pH 8.2, and incubated at 30°C. After 46 h, the reaction mixture was extracted with diethylether (2 x 150 mL) and ethylacetate (1 x 150 ml), dried with $MgSO_4$ and solvent was evaporated. The products were purified by flash chromatography (Silicagel 40-63 µm).

(*S*)-1a: (*S*)-*N*-Benzyl-2-bromopropionamide: Eluted with pentane/diethylether, 6:4, v/v. Yield: 41% (33 mg, 0.14 mmol), white crystals. $[\alpha]_D^{20}$= -1.2 (c 1.0, $CHCl_3$), lit.[34] -1.2. Enantiomeric excess: >99% (HPLC).

(*S*)-2a: (*S*)-*N*-Benzyl-2-hydroxypropionamide: Eluted with pentane/ethylacetate, 3:7, v/v. Yield: 50% (30 mg, 0.17 mmol), colorless oil. R_f = 0.12 (pentane/ethylacetate, 4:6, v/v); $[\alpha]_D^{20}$= -10.0 (c 1.0, $CHCl_3$) lit.[35] -6.8 (c 0.69, $CHCl_3$); ^{1}H NMR (400 MHz, $CDCl_3$): δ 1.42 (d, ^3J = 6.8 Hz, 3H, C**H$_3$**), 3.25 (d, ^3J = 4.8 Hz, 1H, O**H**), 4.21-4.28 (m, 1H, C**H**OH), 4.42-4.44 (m, 2H, C**H$_2$**Ph), 6.97 (br s, 1H, N**H**), 7.24-7.37 (m, 5H, Ar**H**). ^{1}H NMR consistent with literature data.[35] Chiral HPLC analysis (Chiralcel AD, heptane/*i*-PrOH, 95/5, v/v), retention times (min): 11.3 (*R*) and 12.2 (*S*). Enantiomeric excess: > 99% (HPLC).

Kinetic resolution of compound 1b

DbjA (0.70 mg) was added to a solution of *N*-Phenyl-2-bromopropionamide (**1b**, 0.38 mmol, 87 mg) in 325 mL of 50 mM Tris.SO_4 buffer, pH 8.2, and incubated at 30°C. After 17 h, the reaction mixture was extracted with ethylacetate (3 x 150 mL), dried with $MgSO_4$ and the solvent was evaporated. The products were purified by flash chromatography (Silicagel 40-63 µm).

(*S*)-1b: (*S*)-*N*-Phenyl-2-bromopropionamide: Eluted with pentane/diethylether, 7:3, v/v. Yield: 45% (38 mg, 0.17 mmol), white crystals. $[\alpha]_D^{20}$= -29.0 (c 1.0, $CHCl_3$) lit.[36] -33.0. Enantiomeric excess: >99% (HPLC). R_f = 0.49 (pentane/diethylether, 1:1, v/v) ^{1}H NMR (300 MHz, $CDCl_3$): δ 1.98 (d, ^3J = 5.1 Hz, 3H, C**H$_3$**), δ 4.55 (q, ^3J = 5.7 Hz, 1H, C**H**Br), δ 7.16-7.55 (m, 5H, Ar**H**), δ 8.05 (br, 1H, CON**H**). ^{1}H NMR consistent with literature data.[37] Chiral HPLC

analysis (Chiralcel ADH, heptane/*i*-PrOH, 95/5, v/v), retention times (min): 24.0 (*R*) and 31.1 (*S*).

(*S*)-2b: (*S*)-*N*-Phenyl-2-hydroxypropionamide: Eluted with pentane/ diethylether, 4:6, v/v. Yield: 46% (29 mg, 0.18 mmol), colorless oil. $[\alpha]_D^{20}$= -14.2 (c 1.0, $CHCl_3$) lit.[38] -15.6. Enantiomeric excess: >99% (HPLC). R_f = 0.12 (pentane/diethylether, 1:1, v/v); ^{1}H NMR (400 MHz, $CDCl_3$): δ 1.52 (d, ^3J = 6.4 Hz, 3H, C**H$_3$**), 3.22 (br s, 1H, O**H**), 4.35 (q, ^3J = 6.4 Hz, 1H, C**H**OH), 7.12 (t, ^3J = 8.0 Hz, 1H, Ar**H**), 7.32 (app t, ^3J = 8.0 Hz, 2H, Ar**H**) 7.55 (d, ^3J = 8.0 Hz, 2H, Ar**H**), 8.51 (br s, 1H, N**H**). ^{13}C NMR ($CDCl_3$): δ 21.4, 69.1, 120.0, 124.8, 129.3, 137.4, 172.8. NMR is consistent with literature data.[39] Chiral HPLC analysis (Chiralcel ADH, heptane/*i*-PrOH, 95/5, v/v), retention times (min): 27.7 (*R*) and 35.5 (*S*).

Kinetic resolution of compound 1c

LinB (0.72 mg) was added to a solution of *N*-Butyl-2-bromopropionamide (**1c**, 0.38 mmol, 79 mg) in 250 mL of 50mM Tris.SO_4 buffer, pH 8.2, and incubated at 30°C. After 20 h, the reaction mixture was extracted with ethylacetate (3 x 150 mL), dried with $MgSO_4$ and the solvent was evaporated. The products were purified by flash chromatography (Silicagel 40-63 μm).

(*S*)-1c: (*S*)-*N*-Butyl-2-bromopropionamide: Eluted with pentane/diethylether, 1:1, v/v. Yield: 47% (37 mg, 0.18 mmol), colorless oil. $[\alpha]_D^{20}$= -16.4 (c 1.0, $CHCl_3$) lit.[32] -10.2 (c 0.8, $CHCl_3$, for e.e. = 90%) . Enantiomeric excess: >99% (HPLC).

(*S*)-2c: (*S*)-*N*-Butyl-2-hydroxypropionamide: Eluted with ethylacetate. Yield: 47% (26 mg, 0.18 mmol), colorless oil. $[\alpha]_D^{20}$= -14.2 (c 1.0, $CHCl_3$) lit. -16.2.[40] Enantiomeric excess: 87% (HPLC). R_f = 0.18 (pentane/ethylacetate, 4:6, v/v); ^{1}H NMR (300 MHz, $CDCl_3$): δ 0.93 (t, ^3J = 7.2 Hz, 3H, C**H$_3$**CH_2), 1.30-1.56 (m, 4H, C**H$_2$C H$_2$**), 1.43 (d, ^3J = 6.6 Hz, 3H, C**H$_3$**), 2.94 (d, ^3J = 4.2 Hz, 1H, O**H**), 3.25-3.32 (m, 2H, C**H$_2$**NH_2), 4.20-4.24 (m, 1H, C**H**OH), 6.55 (br s, 1H, N**H**). ^{13}C NMR (50 MHz, $CDCl_3$): δ 14.0, 20.3, 21.6, 31.8, 39.1, 68.6, 174.5. HRMS (ESI+) calc. for $C_7H_{15}NO_2Na$: 168.0995, found: 168.0991. Chiral HPLC analysis (Chiralcel AD, heptane/*i*-PrOH, 98/2, v/v), retention times (min): 25.0 (*R*) and 27.9 (*S*).

Kinetic resolution of compound 1f

DbjA (0.84 mg) was added to a solution of *t*-Butyl-2-(2-bromopropionamido)acetate (**1f**, 0.30 mmol, 80 mg) in 200 mL of 50mM Tris.SO_4 buffer, pH 8.2, and incubated at 30°C. After 20 h, the reaction mixture was extracted with ethylacetate (3 x 150 mL), dried with $MgSO_4$ and solvent was evaporated. The products were purified by flash chromatography (Silicagel 40-63 μm).

(*S*)-1f: (*S*)-*t*-Butyl-2-(2-bromopropanamido)acetate: Eluted with pentane/diethylether, 6:4, v/v. Yield: 44% (35 mg, 0.13 mmol). $[\alpha]_D^{20}$= -12.2 (c 1.0, $CHCl_3$). Enantiomeric excess: 98% (HPLC).

(*S*)-2f: (*S*)-*t*-Butyl-2-(2-hydroxypropanamido)acetate: Eluted with ethylacetate. Yield: 40% (24 mg, 0.12 mmol), colorless oil. $[\alpha]_D^{20}$= -21.0 (c 1.0, $CHCl_3$). Enantiomeric excess: >99.5% (HPLC). R_f = 0.15 (pentane/ethylacetate, 4:6, v/v); ^{1}H NMR (400 MHz, $CDCl_3$): δ 1.42 (d, ^3J = 6.8 Hz, 3H, C**H**$_3$), 1.46 (s, 9H, (C**H**$_3$)$_3$) 3.87-4.01 (m, 3H, C**H**$_2$NH$_2$**,** O**H**), 4.27 (q, ^3J = 6.8 Hz, 1H, C**H**OH), 7.14 (br s, 1H, N**H**). ^{13}C NMR (100 MHz, $CDCl_3$): 21.2, 28.2, 41.8, 68.6, 82.7, 169.3, 175.4; HRMS (ESI+) calc. for $C_9H_{17}NO_4Na$: 226.1050, found: 226.1053. Chiral HPLC analysis (Chiralcel OD, heptane/*i*-PrOH, 95/5, v/v), retention times (min): 11.3 (*S*) and 12.6 (*R*). The configuration was determined by comparison with HPLC retention time obtained for reference compound, which was synthesised from L-lactic acid and alanine tert-butyl ester hydrochloride by EDC/HOBt mediated coupling.

Kinetic resolution of compound 1g

LinB (1.2 mg) was added to a solution of *t*-Butyl-2-[(2-bromopropanoyl)amino]-propanoate (**1g**, 0.29 mmol, 80 mg) in 250 ml of 50mM Tris.SO_4 buffer, pH 8.2, and incubated at 30°C. After 43 h, the reaction mixture was extracted with ethylacetate (3 x 150 mL), dried with $MgSO_4$ and solvent was evaporated.

(*S,S*)-1g: (*S,S*)-*t*-Butyl-2-[(2-bromopropanoyl)amino]-propanoate. Eluted with pentane/diethylether, 8:2, v/v. Yield: 38% (30 mg, 0.11 mmol), white solid. Diastereoisomeric excess: >95% (NMR). $[\alpha]_D^{20}$= -1.0 (c 1.0, $CHCl_3$); ^{1}H NMR (400 MHz, $CDCl_3$): δ 1.39 (d, ^3J = 6.8 Hz, 3H, C**H**$_3$), 1.47 (s, 9H, C(C**H**$_3$)$_3$, 1.86 (d, ^3J = 6.8 Hz, 3H, C**H**$_3$), 4.36-4.50 (m, 2H, C**H**Br, C**H**NH), 6.91 (br s N**H**); ^{13}C NMR ($CDCl_3$): δ 18.5, 23.2, 28.2, 44.8, 49.5, 82.6, 168.9, 172.0; HRMS (ESI+) calc. for $C_{10}H_{18}NO_3BrNa$: 302.0367, found: 302.0380.

(*S,S*)-2g: (*S,S*)-*t*-Butyl-2-[(2-hydroxypropanoyl)amino]-propanoate. Eluted with diethylether. Yield: 32% (20 mg, 0.09 mmol), clear oil. Diastereoisomeric excess: >95% (NMR). R_f = 0.51 (pentane/ethylacetate. 4:6, v/v); $[\alpha]_D^{20}$= -25.8 (c 1.0, $CHCl_3$); mp 137-138°C. ^{1}H NMR (400 MHz, $CDCl_3$): δ 1.39 (d, ^3J = 6.8 Hz, 3H, C**H**$_3$), 1.43 (d, ^3J = 6.8 Hz, 3H, C**H**$_3$), 1.47 (s, 9H, C(C**H**$_3$)$_3$, 2.75 (d, ^3J = 4.4 Hz, 1H, O**H**), 4.20-4.27 (m, 1H, C**H**NH), 4.43-4.50 (m, 1H, C**H**OH), 6.94 (br s, 1H, NH); ^{13}C NMR ($CDCl_3$): δ 18.8, 21.3, 28.2, 48.5, 68.5, 82.4, 172.5, 174.4; HRMS (ESI+) calc. for $C_{10}H_{19}NO_4Na$: 240.1212, found: 240.1198. Diastereoisomeric excess was determined using ^{1}H NMR spectroscopy, by the comparison of CH(OH)C**H**$_3$ signal (d, 1.39 ppm for (*S,S*), 1.41 ppm for (*R,S*)). The configuration was determined by comparison of NMR data to the spectrum obtained for reference compound, which was synthesised from L-lactic acid and alanine *tert*-butyl ester hydrochloride by EDC/HOBt mediated coupling.

Kinetic resolution of compound 1h

LinB (0.72 mg) was added to a solution of *t*-Butyl-2-[(2-bromopropanoyl)amino]-3-phenylpropanoate (**1h**, 0.043 mmol, 15 mg) in 50 ml of 50mM Tris.SO_4 buffer, pH 8.2, and

incubated at 30°C. After 20 h, the reaction mixture was extracted with ethylacetate (3 x 25 mL), dried with $MgSO_4$ and solvent was evaporated.

(*S,S*)-1h: (*S,S*)-*t*-Butyl-2-[(2-bromopropanoyl)amino]-3-phenylpropanoate. Eluted with pentane/diethylether, 8:2, v/v. Yield: 39% (6 mg, 0.017 mmol), white solid. Diastereoisomeric excess: >95% (NMR). $[\alpha]_D^{20}$ = +39.5 (c 0.4, $CHCl_3$); mp 66-67°C. ^{1}H NMR (400 MHz, $CDCl_3$): δ 1.43 (s, 9H, C(C**H$_3$**)$_3$, 1.81 (d, ^3J = 6.8 Hz, 3H, C**H$_3$**), 3.07-3.18 (m, 2H, C**H$_2$**Ar), 4.36 (q, ^3J = 6.4 Hz, 1H, C**H**Br), 4.65-4.75 (m, C**H**NH), 6.77 (br s N**H**), 7.17-7.31 (m, 5H, Ar**H**); ^{13}C NMR ($CDCl_3$): δ 22.9, 28.0, 37.8, 44.5, 53.9, 82.8, 127.1, 128.4, 129.6, 135.7, 168.6, 170.1; HRMS (ESI+) calc. for $C_{16}H_{22}NO_3BrNa$: 378.0681, found: 378.0658.

(*S,S*)-2h: (*S,S*)-*t*-Butyl-2-[(2-hydroxypropanoyl)amino]-3-phenylpropanoate. Eluted with diethylether. Yield: 39% (5 mg, 0.017 mmol), white powder. Diastereoisomeric excess: >95% (NMR). R_f = 0.49 (pentane/ethylacetate. 4:6, v/v); $[\alpha]_D^{20}$= +36.8 (c 1.0, $CHCl_3$); mp 66-67ºC. ^{1}H NMR (400 MHz, $CDCl_3$): δ 1.33 (d, ^3J = 6.8 Hz, 3H, C**H$_3$**), 1.40 (s, 9H, C(C**H$_3$**)$_3$, 3.05-3.15 (m, 2H, C**H$_2$**Ar), 4.20 (q, ^3J = 6.4 Hz, 1H, C**H**OH), 4.47 (br s, 1H, OH), 4.73 (m, C**H**NH), 7.08 (d, ^3J = 8.0 Hz, 1H, NH); ^{13}C NMR ($CDCl_3$): δ 21.3, 28.2, 38.3, 53.3, 68.5, 82.8, 127.2, 128.6, 129.7, 136.1, 170.8, 174.6; HRMS (ESI+) calc. for $C_{16}H_{24}NO_4$: 294.1700, found: 294.1687. Diastereoisomeric excess was determined by the comparison of CH(OH)C**H$_3$** ^{1}H NMR signal (d, 1.34 ppm for (*S,S*), 1.37 ppm for (*R,S*)). The configuration was determined by comparison of NMR data to the spectrum obtained for reference compound, which was synthesised from L-lactic acid and phenylalanine *t*-butyl ester hydrochloride by EDC/HOBt mediated coupling.

Kinetic resolution of compound 1k

LinB (1.9 mg) was added to a solution of *N*-benyl-2-bromobutanamide (**1k**, 0.31 mmol, 80 mg) in 350 ml of 50mM Tris.SO_4 buffer, pH 8.2, and incubated at 30°C. After 44 h, the reaction mixture was extracted with ethylacetate (3 x 200 mL), dried with $MgSO_4$, and solvent was evaporated.

(*S*)-1k: (*S*)-*N*-Benzyl-2-bromobutanamide. Eluted with pentane/diethylether, 8:2, v/v. Yield: 40% (33 mg, 0.13 mmol), white solid. $[\alpha]_D^{20}$= -21.0 (c 1.0, $CHCl_3$). Enantiomeric excess: >99% (HPLC).

(*S*)-2k: (*S*)-*N*-Benzyl-2-hydroxybutanamide. Eluted with diethylether. Yield: 31% (20 mg, 0.10 mmol), white powder. R_f = 0.50 (pentane/ethylacetate, 4:6, v/v); $[\alpha]_D^{20}$= -43.8 (c 1.0, $CHCl_3$) lit.[41] -42.0 (c 5.0, MeOH); ^{1}H NMR (400 MHz, $CDCl_3$): δ 0.98 (t, ^3J = 7.6 Hz, 3H, C**H$_3$**), 1.62-1.92 (m, 2H, CH_3C**H$_2$**), 2.90 (s, 1H, O**H**), 4.08-4.14 (m, 1H, C**H**OH), 4.44-4.46 (m, 2H, C**H$_2$**Ph), 6.88 (br s, 1H, N**H**), 7.28-7.36 (m, 5H, Ar**H**). ^{13}C NMR ($CDCl_3$): δ 9.4, 28.2, 43.4, 73.3, 127.8, 128.0, 129.0, 138.2, 173.8; Chiral HPLC analysis (Chiralcel AD, heptane/*i*-PrOH, 95/5, v/v), retention times (min): 14.4 (*R*) and 19.2 (*S*). Enantiomeric excess: 97% (HPLC).

Racemic samples of products (2) were obtained in EDC/HOBt mediated coupling of α-hydroxy-acids with amines. Analytical data for compound **2**, of which the respective α-bromoamides were not converted by the enzymes with sufficient selectivity, are presented below.

2e: Ethyl-2-(2-hydroxypropanamido)acetate. Colorless oil. R_f = 0.23 (pentane/ethylacetate; 4:6, v/v); ^{1}H NMR (300 MHz, $CDCl_3$): δ 1.29 (t, ^3J = 7.5 Hz, 3H, C**H$_3$**), δ 1.46 (d, ^3J = 7.2 Hz, 3H, C**H$_3$**), δ 2.36 (br, N**H**), δ 4.06 (t, ^3J = 4.8 Hz, 2H, C**H$_2$**), δ 4.23 (q, ^3J = 7.5 Hz, 2H, C**H$_2$**), δ 4.31 (q, ^3J = 6.9 Hz 1H, C**H**OH), δ 7.02 (br, O**H**). ^{13}C NMR: δ 14.4, 21.3, 41.2, 61.9, 68.7, 170.2, 175.3. HRMS (ESI+) calc. for $C_7H_{13}NO_4Na$: 198.0737, found: 198.0733. HPLC (Chiralcel AD, heptane/*i*-PrOH, 95/5, v/v), retention times (min): 16.6, 18.0 (absolute configuration not assigned).

*Conversion of N-Benzyl-2-bromopropionamide (**1a**) with dimethyl sulfoxide*

Activity of DbjA in a solvent mixture of buffer and dimethyl sulfoxide

DbjA (160 µg) was added to 5 mL of 1.3 mM solution of **1a** in a mixture of 50 mM Tris.SO_4, and DMSO (0-50% v/v), pH 8.2. After 150 min of incubation at 30°C, a sample of 2 ml was extracted with 1.5 ml diethylether, dried, evaporated and analysed by Chiral HPLC, as described before. Conversions were calculated from the enantiomeric excess of both substrate and product.[14]

Preparative scale experiment in 25 vol% dimethyl sulfoxide

DbjA (7 mg) was added to a solution of *N*-Benzyl-2-bromopropionamide (**1a**, 0.97 mmol, 250 mg) in 240 ml of 50 mM Tris.SO_4, pH 8.2 and 25 % (v/v) dimethyl sulfoxide. The mixture was incubated at 30°C for 44h and extracted with 2 x 150 ml diethyl ether and 2 x 150 ml ethyl acetate. The products were purified by flash chromatography as described above.

*Time course experiment for (S)-t-butyl-2-(2-bromopropanamido)acetate (**1f**)*

To 30 ml solution of (*S*)-*t*-butyl-2-(2-bromopropanamido)acetate (**1f**, 0.030 mmol, 8.0 mg) LinB (1 or 5 mg) was added. At various times samples were taken. A sample of 200 µL was mixed with 50 µL 250 mM potassium phosphate buffer, pH 2 and analysed by reverse-phase HPLC (Nucleosil 100 (C18) column, 50% acetonitrile and 50% 50 mM potassium phosphate buffer, pH 2, flow 1 ml/min (retention times (min): 8.5 (**2f**); 29.5 (**1f**)). Enantiomeric excess of **1f** and **2f** was determined by Chiral HPLC as described above. The obtained time-course (Figure 5B) was fitted to $d[R]/dt = - k_{cat}^R[LinB][R] / (((1 + [S]/K_m^S)\times K_M^R) + [R])$, $d[S]/dt = - k_{cat}^S[LinB][S] / (((1 + [R]/K_m^R)\times K_M^S) + [S])$,[42] and the E-value = $(k_{cat}^R/K_m^R)/(k_{cat}^S/K_m^S)$ using Scientist 2.0 (Micromath). The reported errors are the standard deviations.

General cloning strategy

For the creation of the haloalkane dehalogenase constructs, the genes were cloned into a modified pBADmycHISA vector, which included an N-terminal hexahistidine tag. In this vector, the histidine-tag was cloned between *Nco*I and *Nde*I, resulting in the following sequence: 5'-CCATGGGCAGCAGCCATCATCATCATCACAGCAGCGGCCTGGTGCCGCGCGG CAGCCATATG-3'. The genes of interest, from various sources, as described in the introduction, were amplified by PCR, from plasmid DNA (*dhlA* and *dhaA*) or from the original organisms (*linB*, *dbjA* and *dmlA*) and cloned via *Nde*I restriction site. The mutant *dhaA31* gene was supplied by J. Damborsky.

Protein expression, purification and analysis

Precultures were started by inoculating 5 ml of LB_{amp}-medium with *E. coli* TOP10 transformants from 10% v/v glycerol stocks and incubated overnight at 37°C, while shaking. The next day, 2 L of LB, supplemented with 50 µg/ml ampicillin, was inoculated with 1% of an overnight culture and incubated at 37°C under vigorous aeration. The enzyme expression was induced by adding 0.002% w/v L-arabinose at OD_{600} ~ 0.6. Cultures were incubated overnight at 30°C, except for LinB which was incubated at 17°C. Then, the cells were harvested, lysed by sonication, and subsequently the haloalkane dehalogenases were purified using three in line his-trap Ni-NTA columns from GE healthcare attached to an ÄKTA purifier system. The purified enzymes were concentrated using an Amicon ultrafiltration cell and stored in TMG buffer (10 mM Tris.SO_4, 1 mM β-mercaptoethanol, 10% v/v glycerol, and pH 7.5). Protein concentrations were determined by Bradford reagent (Biorad) using bovine serum albumin as a standard. The purified enzyme was analysed using SDS-polyacrylamide gel electrophoresis.

Docking

Three-dimensional structures of the substrates (*R*/*S*)-**1f** and (*R*/*S*)-**1k** were created with Chem3D (CambridgeSoft) and subsequently geometry-optimised with Yasara (www.yasara.org) by AM1 quantum mechanics[43] in combination with the implicit solvent model COSMO.[44] Substrate partial charges for docking and MD simulation were calculated with the AM1-BCC method[45], which gives accuracy similar to that of RESP[46], at a much lower computational cost. Prior to docking the substrates into LinB (PDB file 1MJ5[18]), the most likely protonation states (at pH 8.5) of the different side-chains were predicted.[47] Of the predicted side-chain protonation states, only one seemed in disagreement with the surrounding H-bonding pattern; this His107 was manually corrected to be singly protonated at its N_ε. The catalytically important residue His272 was singly protonated at its N_δ, as found earlier to be the relevant protonation state for catalysis.[18] In the active site, two crystallographic waters (HOH 3508 and HOH 3050, these water molecules are not part of the substrate binding site, both are important for

their H-bonds to active site residues) were preserved while the halide and other waters in the active site were manually removed. To minimise the chance of missing the catalytically most relevant binding mode of the substrate, 800 separate docking runs were carried out for every substrate enantiomer with AutoDock 4.[48] This docking was carried out with the maximum number of energy evaluations set to 2,500,000. The starting structures for the MD simulations were chosen based on a geometric ranking criterion that approximately describes the suitability of its binding orientation for catalysis. For all docked substrate orientations the distances d_1, d_2, and d_3 (Scheme 2) were measured and the sum S = (2 × d_1) + d_2 + d_3 was calculated for each orientation. The single orientation selected for each enantiomer had the lowest S of all. Dissociation constants were predicted by AutoDock 4.[19]

MD simulations

The docked enzyme-substrate complexes were placed in a rectangular simulation cell with periodic boundary conditions and distances between protein and wall of at least 10 Å. Water (TIP3P) and 13 sodium ions to neutralise the simulation cell were positioned in the box by Yasara[47c]; this software was also used for the MD simulations, with the leap-frog integration scheme. Since the goal of the simulations was to reliably predict the angles and distances in the active site of the enzyme, the Yamber3 force-field was used; Yamber3 is an Amber99-derived force-field that was specifically parameterised to more accurately reproduce the three-dimensional structure of proteins.[47a,49] Long-range (> 7.86 Å) Coulomb interactions were calculated with a particle mesh Ewald algorithm[50] with 4th degree B-spline functions. No constraints on bond-lengths involving hydrogen atoms were applied. Prior to the MD simulation, an energy minimisation was carried out to remove clashes and relieve conformational stress. This energy minimisation was ended when the total energy improved by less than 0.05 kJ mol^{-1} per atom during 400 fs. During the simulations, the time step was 1.25 fs, with the non-bonded interactions updated once every two time steps.

The production phase simulation of 5000 ps was preceded by a slow warming (in steps of 5 K from 5 to 298 K in 30 ps) and an equilibration phase (1970 ps). The temperature was controlled by a Berendsen thermostat.[51] During the entire simulation, snapshots were saved every 5 ps to analyse Root Mean Square Deviation (RMSD) and energy; only those snapshots obtained after equilibration were used for calculation of the Root Mean Square Fluctuations (RMSF) of the protein. The RMSF of the crystal structure was calculated from its B-factors via RMSF = √ (¾B-factor / π2) [please note that this equation is an approximation, B-factors are not fully equivalent to RMSF]. To more densely sample the catalytically important distances and angles during the simulation, these were recorded every 100 fs during the production phase (in total 50000 times). The commonly used alternative would be to obtain them from the 1000 snapshots. For every recorded set of

distances and angles it was determined whether they met all criteria for a NAC. The reported errors were obtained by block averaging.[52]

ACKNOWLEDGEMENTS

We thank Jiri Damborsky (University of Brno, Czech Republic) for supplying the mutant gene DhaA31, Philip Poole (University of Reading, United Kingdom) for supplying bacterial strain Mesorhizobium loti MAFF303099 and Mark O'Brian (University of New York at Buffalo, USA) for supplying bacterial strain Bradyrhizobium japonicum USDA110. We thank T. Tiemersma-Wegman for technical assistance with HPLC and HRMS. This project is financially supported by the B-Basic partner organisations (www.b-basic.nl) through B-Basic, a public-private NWO-ACTS program. Part of this research was funded by an NWO ECHO grant.

REFERENCES

[1] W. Szymański, M. Zwolinska, and R. Ostaszewski. *Tetrahedron*. **2007**, *63*, 7647-7653.
[2] P. Marchetti. *Tetrahedron Lett.* **2003**, *44*, 4121-4123.
[3] M. Murphy, D. Lynch, M. Schaeffer, M. Kissane, J. Chopra, E. O'brien, A. Ford, G. Ferguson, and A. R. Maguire. *Org. Biomol. Chem.* **2007**, *5*, 1228-1241.
[4] W. M. Kazmierski, E. Furfine, A. Spaltenstein, and L. L. Wright. *Bioorg. Med. Chem. Lett.* **2006**, *16*, 5226-5230.
[5] F. Dangeli, P. Marchetti, and V. Bertolasi. *J. Org. Chem.* **1995**, *60*, 4013-4016.
[6] D. B. Janssen. *Curr. Opin. Chem. Biol.* **2004**, *8*, 150-159.
[7] a) G. Stucki and M. Thuer. *Environ. Sci. Technol.* **1995**, *29*, 2339-2345; b) G. V. Los, L. P. Encell, M. G. McDougall, D. D. Hartzell, N. Karassina, C. Zimprich, M. G. Wood, R. Learish, R. F. Ohana, M. Urh, D. Simpson, J. Mendez, K. Zimmerman, P. Otto, G. Vidugiris, J. Zhu, A. Darzins, D. H. Klaubert, R. F. Bulleit, and K. V. Wood. *ACS Chem. Biol.* **2008**, *3*, 373-382.
[8] a) R. J. Pieters, J. H. Lutje Spelberg, R. M. Kellogg, and D. B. Janssen. *Tetrahedron Lett.* **2001**, *42*, 469-471; b) Z. Prokop, Y. Sato, R. Brezovsky, T. Mozga, R. Chaloupkova, T. Koudelakova, P. Jerabek, V. Stepankova, R. Natsume, J. G. E. van Leeuwen, D. B. Janssen, J. Florian, Y. Nagata, T. Senda, and J. Damborsky. *Angew. Chem.* **2010**, *49*, 6111-6115.
[9] S. Keuning, D. B. Janssen, and B. Witholt. *J. Bacteriol.* **1985**, *163*, 635-639.
[10] A. N. Kulakova, M. J. Larkin, and L. A. Kulakov. *Microbiology*. **1997**, *143*, 109-115.
[11] Y. Nagata, K. Miyauchi, J. Damborsky, K. Manova, A. Ansorgova, and M. Takagi. *Appl. Environ. Microbiol.* **1997**, *63*, 3707-3710.
[12] Y. Sato, M. Monincova, R. Chaloupkova, Z. Prokop, Y. Ohtsubo, K. Minamisawa, M. Tsuda, J. Damborsky, and Y. Nagata. *Appl. Environ. Microbiol.* **2005**, *71*, 4372-4379.
[13] M. Pavlova, M. Klvana, Z. Prokop, R. Chaloupkova, P. Banas, M. Otyepka, R. C. Wade, M. Tsuda, Y. Nagata, and J. Damborsky. *Nat. Chem. Biol.* **2009**, *5*, 727-733.
[14] C. S. Chen, Y. Fujimoto, G. Girdaukas, and C. J. Sih. *J. Am. Chem. Soc.* **1982**, *104*, 7294-7299.
[15] K. H. Verschueren, F. Seljee, H. J. Rozeboom, K. H. Kalk, and B. W. Dijkstra. *Nature*. **1993**, *363*, 693-698.
[16] J. Marek, J. Vevodova, I. K. Smatanova, Y. Nagata, L. A. Svensson, J. Newman, M. Takagi, and J. Damborsky. *Biochemistry*. **2000**, *39*, 14082-14086.

[17] Y. Nagata, T. Nariya, R. Ohtomo, M. Fukuda, K. Yano, and M. Takagi. *J. Bacteriol.* **1993**, *175*, 6403-6410.

[18] A. J. Oakley, M. Klvana, M. Otyepka, Y. Nagata, M. C. Wilce, and J. Damborsky. *Biochemistry*. **2004**, *43*, 870-878.

[19] R. Huey, G. M. Morris, A. J. Olson, and D. S. Goodsell. *J. Comp. Chem.* **2007**, *28*, 1145-1152.

[20] J. P. Schanstra, J. Kingma, and D. B. Janssen. *J. Biol. Chem.* **1996**, *271*, 14747-14753.

[21] T. C. Bruice. *Chem. Rev.* **2006**, *106*, 3119-3139.

[22] a) T. C. Bruice. *Acc. Chem. Res.* **2002**, *35*, 139-148; b) T. C. Bruice and S. J. Benkovic. *Biochemistry*. **2000**, *39*, 6267-6274.

[23] A. Warshel, P. K. Sharma, M. Kato, Y. Xiang, H. B. Liu, and M. H. M. Olsson. *Chem. Rev.* **2006**, *106*, 3210-3235.

[24] S. Hur, K. Kahn, and T. C. Bruice. *Proc. Natl. Acad. Sci. USA*. **2003**, *100*, 2215-2219.

[25] a) M. Bohac, Y. Nagata, Z. Prokop, M. Prokop, M. Monincova, M. Tsuda, J. Koca, and J. Damborsky. *Biochemistry*. **2002**, *41*, 14272-14280; b) C. Kennes, F. Pries, G. H. Krooshof, E. Bokma, J. Kingma, and D. B. Janssen. *Eur. J. Biochem.* **1995**, *228*, 403-407; c) G. H. Krooshof, I. S. Ridder, A. W. J. W. Tepper, G. J. Vos, H. J. Rozeboom, K. H. Kalk, B. W. Dijkstra, and D. B. Janssen. *Biochemistry*. **1998**, *37*, 15013-15023; d) K. Kahn and T. C. Bruice. *J. Phys. Chem. B*. **2003**, *107*, 6876-6885; e) E. Y. Lau, K. Kahn, P. A. Bash, and T. C. Bruice. *Proc. Natl. Acad. Sci. USA*. **2000**, *97*, 9937-9942; f) F. C. Lightstone, Y. J. Zheng, and T. C. Bruice. *J. Am. Chem. Soc.* **1998**, *120*, 5611-5621; g) J. Damborsky, M. Kuty, M. Nemec, and J. Koca. *J. Chem. Inf. Comp. Sci.* **1997**, *37*, 562-568.

[26] A. Cornish-Bowden, *Fundamentals of Enzyme Kinetics*, Butterworths, London-Boston, **1979**, pp. 49-51.

[27] Z. Prokop, M. Monincova, R. Chaloupkova, M. Kivana, Y. Nagata, D.B. Janssen and J. Damborsky. *J. Biol. Chem*. **2003**, *278*, 45094-45100.

[28] a) B.F. Cook, W.W. Cleland, *Enzyme Kinetics and Mechanism*, Garland Science, London, New York, **2007**, pp. 15. A. Fersht, *Enzyme Structure and Mechanism*, 2nd ed, W.H. Freeman and Co, New York, 1985, pp. 102.

[29] a) R.M. de Jong, J.J. Tiesinga, A. Villa, L. Tang, D.B. Janssen, and B.W. Dijkstra. *J. Am. Chem. Soc.* **2005**, *127*, 13338-13343. b) J.A. Alexandre, B. Roy, D. Topalis, S. Pochet, C. Périgaud, D. Deville-Bonne. *Nucleic Acids Res.* **2007**, *35*, 4895-4904.

[30] S. Kushner, R. I. Cassell, J. Morton, and J. H. Williams. *J. Org. Chem.* **1951**, *16*, 1283-1288.

[31] G. Zanotti, F. Filira, A. Delpra, G. Cavicchioni, A. C. Veronese, and F. Dangeli. *J. Chem. Soc.Perkin Trans. 1*. **1980**, 2249-2253.

[32] M. Quiros, V. M. Sanchez, R. Brieva, F. Rebolledo, and V. Gotor. *Tetrahedron Asymm*. **1993**, *4*, 1105-1112.

[33] S. R. Safir, H. Dalalian, W. Fanshawe, K. Cyr, R. Lopresti, R. Williams, S. Upham, L. Goldman, and S. Kushner. *J. Am. Chem. Soc.* **1955**, *77*, 4840-4844.

[34] F. Dangeli, P. Marchetti, G. Cavicchioni, G. Catelani, and F. M. K. Nejad. *Tetrahedron Asymm*. **1990**, *1*, 155-158.

[35] S. N. Savinov and D. J. Austin. *Org. Lett.* **2002**, *4*, 1415-1418.

[36] F. Dangeli, P. Marchetti, R. Rondanin, and V. Bertolasi. *J. Org. Chem.* **1996**, *61*, 1252-1255.

[37] G. Cavicchioni, P. Scrimin, A. C. Veronese, G. Balboni, and F. Dangeli. *J. Chem. Soc. , Perkin Trans. 1*. **1982**, 2969-2972.

[38] F. Maran. *J. Am. Chem. Soc.* **1993**, *115*, 6557-6563.

[39] G. Z. Wang, T. Mallat, and A. Baiker. *Tetrahedron Asymm*. **1997**, *8*, 2133-2140.

[40] S. V. Rogozhin and Y. A. Davidovich. *Bull. Acad. Sci. USSR Div. Chem. Sci.* **1970**, *19*, 2041.

[41] L. Gajewczyk and A. Zejc. *Pol. J. Chem.* **1990**, *64*, 567-571.

[42] J.H. Lutje Spelberg, R. Rink, R.M. Kellogg and D.B. Janssen. *Tetrahedron Asymm*. **1998**, *9*, 459-466.

[43] a) M. J. S. Dewar, E. G. Zoebisch, E. F. Healy, and J. J. P. Stewart. *J. Am. Chem. Soc.* **1985**, *107*, 3902-3909; b) M. J. S. Dewar and E. G. Zoebisch. *Theochem-J. Mol. Struc.* **1988**, *49*, 1-21; c) J. J. P. Stewart. *J. Comp. -Aid. Mol. Des.* **1990**, *4*, 1-45.

[44] A. Klamt. *J. Phys. Chem.* **1995**, *99*, 2224-2235.
[45] A. Jakalian, D. B. Jack, and C. I. Bayly. *J. Comput. Chem.* **2002**, *23*, 1623-1641.
[46] C. I. Bayly, P. Cieplak, W. D. Cornell, and P. A. Kollman. *J. Phys. Chem.* **1993**, *97*, 10269-10280.
[47] a) E. Krieger, T. Darden, S. B. Nabuurs, A. Finkelstein, and G. Vriend. *Proteins*. **2004**, *57*, 678-683; b) E. Krieger, G. Koraimann, and G. Vriend. *Proteins*. **2002**, *47*, 393-402; c) E. Krieger, J. E. Nielsen, C. A. E. M. Spronk, and G. Vriend. *J. Mol. Graph. Model.* **2006**, *25*, 481-486.
[48] G. M. Morris, R. Huey, W. Lindstrom, M. F. Sanner, R. K. Belew, D. S. Goodsell, and A. J. Olson. *J. Comp. Chem.* **2009**, *30*, 2785-2791.
[49] J. M. Wang, P. Cieplak, and P. A. Kollman. *J. Comp. Chem.* **2000**, *21*, 1049-1074.
[50] U. Essmann, L. Perera, M. L. Berkowitz, T. Darden, H. Lee, and L. G. Pedersen. *J. Chem. Phys.* **1995**, *103*, 8577-8593.
[51] H. J. C. Berendsen, J. P. M. Postma, W. F. Van Gunsteren, A. Dinola, and J. R. Haak. *J. Chem. Phys.* **1984**, *81*, 3684-3690.
[52] H. Flyvberg, H.G. Petersen, *J. Chem. Phys.*, **1989**, *91*, 461-466.

CHAPTER 4

A dynamic kinetic resolution process employing a haloalkane dehalogenase

Alja Westerbeek, Wiktor Szymański, Ben L. Feringa, and Dick B. Janssen

Based on: ACS Catal., 2011, *1*, 1654-1660

ABSTRACT

The first dynamic kinetic resolution process with a haloalkane dehalogenase is described, allowing the efficient preparation of enantiopure α-hydroxyamides from racemic α-bromoamides. A simple membrane reactor is used to separate the enzyme from the non-soluble, polymer-based and metal-free racemising agent. A model substrate, *N*-phenyl-2-bromopropionamide, was converted to (*S*)-*N*-phenyl-2-hydroxypropionamide either with 63% yield and 95% e.e or with 78% yield and 88% e.e..

INTRODUCTION

The use of green, chemoenzymatic processes for the preparation of valuable, enantiopure building blocks is gathering increasing attention in recent years due to the high activity and selectivity offered by enzymes, in combination with the simple way of catalyst production and the use of environmentally benign process conditions.[1-3] The majority of the enzyme-catalysed conversions that are used for the preparation of enantiopure α-substituted esters and amides employ hydrolytic enzymes in an enantioselective kinetic resolution. In these processes one enantiomer of the substrate is hydrolysed by an amidase, esterase or lipase, while the other enantiomer remains unconverted by the enzyme.

The intrinsic limitation of kinetic resolution processes stems from the fact that in a perfectly enantioselective reaction the enantiopure product still can be obtained with a yield of only 50%. One of the most widely applied methods to overcome this limitation is the use of dynamic kinetic resolution (DKR) processes, in which the enantioselective kinetic resolution is combined with a fast *in situ* racemisation of the substrate (Scheme 1).[4,5] In an optimal situation a yield of 100% of optically pure product can be obtained in a DKR, as the non-preferred enantiomer of the substrate is constantly converted to the preferred one. The *in situ* racemisation of the substrate is performed either in a chemical way[6] or by using an additional enzyme (racemase).[7] A chemoenzymatic DKR can be achieved with a base-catalysed or transition metal-catalysed racemisation, or through racemisation involving a nucleophilic displacement.[8]

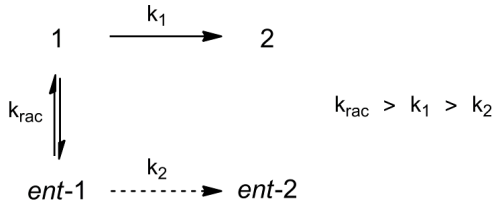

Scheme 1: Schematic overview of a dynamic kinetic resolution.

The α-hydroxyamide scaffold is present in a variety of compounds with confirmed biological activity, such as pantothenic acid (vitamin B5, **A**, Figure 1),[9] the cholesterol-lowering drug bestatin (**B**, Figure 1)[10] and the antibiotics amikacin (**C**, Figure 1)[11] and cefamandole (**D**, Figure 1).[12] Furthermore, chiral α-hydroxyamides are precursors of α-hydroxy-lactams,[13] α-amino acids,[14] and small, non-natural peptides.[15] Chemical routes for the preparation of enantiopure hydroxyamides are mainly based upon asymmetric hydrogenation with rhodium[16] or ruthenium[17] complexes and enantioselective ene-reactions.[18] The main biocatalytic routes to enantiopure α-hydroxyamides rely on the kinetic resolution of racemic α-acyloxamides[19] and α-bromoamides.[20] Chemoenzymatic DKR processes aiming at chiral alcohols rely on (i) enzymatic enantioselective alcohol acylation combined with *in situ* substrate racemisation by ruthenium complexes[21-23] or (ii) enzymatic enantioselective hydrolysis of the allylic alcohol esters combined with *in situ* racemisation of substrate via π-allyl–palladium complexes.[24] In these processes, transition metal complexes are used, which limits their potential application because of environmental and economic reasons.

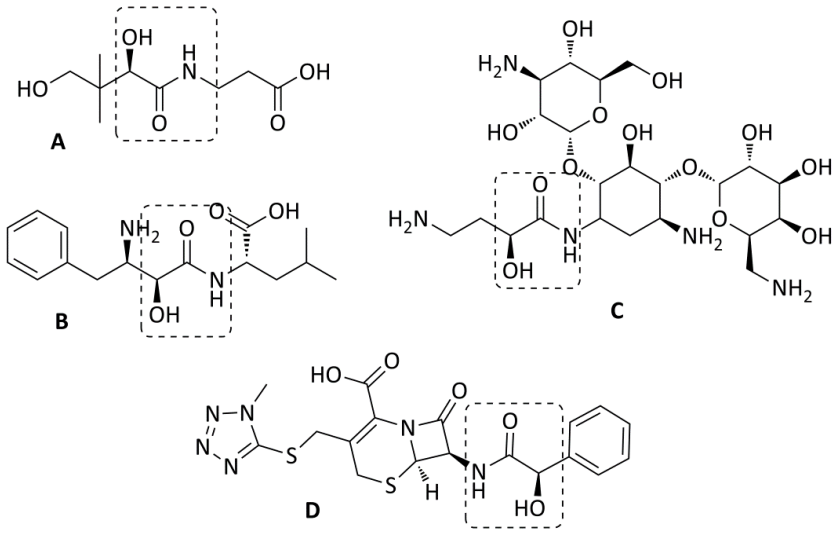

Figure 1: Bioactive compounds bearing an α-hydroxyamide scaffold.

Recently, it was described that haloalkane dehalogenases can perform kinetic resolution of α-haloesters[25] and α-haloamides,[20] with E-values of up to >200. In preparative conversions, yields of up to 50% and e.e. values of up to 99% in the conversions catalysed by haloalkane dehalogenases DbjA and LinB were reported. Here we describe our efforts towards increasing the efficiency of a haloalkane dehalogenase-catalysed process by designing a reaction setup for the dynamic kinetic resolution, using racemic α-bromoesters and α-bromoamides as substrates. To obtain a suitable system, key

parameters were optimised, including the enzyme type, the racemisation agent, and reaction conditions.

RESULTS AND DISCUSSION

Haloalkane dehalogenase-catalysed kinetic resolution of model compounds

For the current study, we used the α-haloesters (**1a** and **1b**), and α-haloamide **1c** shown in Figure 2. This choice was inspired by the high enantioselectivity observed in haloalkane dehalogenase-catalysed conversions of compounds **1a**-**1c**. A high enantioselectivity (E>200) was reported previously by Prokop *et al.*[25] for the conversion of **1a** catalysed by the bacterial haloalkane dehalogenases DbjA and DhaA. We observed that the same level of selectivity is obtained in DbjA-catalysed conversions of compounds **1b**, **1c**[20] and **1d**.

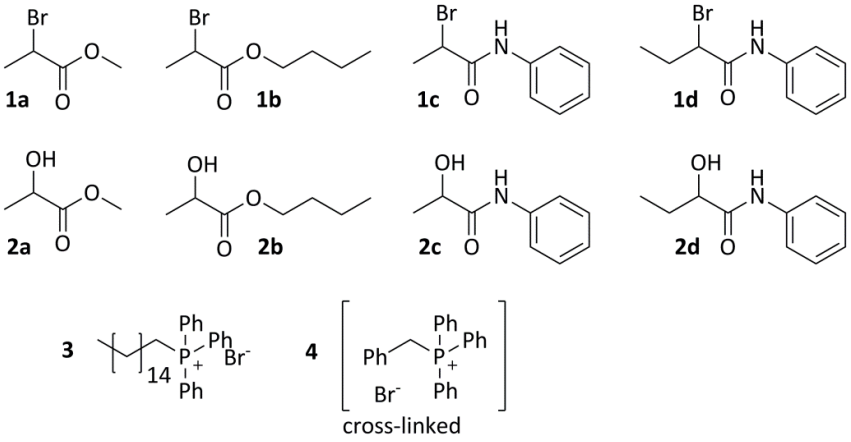

Figure 2: Compounds used in this research: substrates for the enzyme-catalysed reactions **1**, products of these reactions **2** and racemisation agents **3** and **4**.

Selection of the racemising agent

Compound (*S*)-**1a**, obtained by kinetic resolution of *rac*-**1a**, was used as a model substrate in studies aimed at optimising the racemisation process. Inspired by a literature report[26] on the racemisation of α-haloesters in lipase-catalysed dynamic kinetic resolution, we envisioned the use of bromide ions as racemising agents, expecting the S_N2 reaction-based shuffling of the bromide group. In our initial attempt, sodium bromide was used as the most simple source of bromide ions (Table 1, entries 2-5).

Under the tested reaction conditions bromoester (*S*)-**1a** does not racemise spontaneously (Table 1, entry 1), but racemisation occurred when NaBr was added. The degree of racemisation depended on the concentration of sodium bromide, which supports the assumption that bromide salts can be used for racemisation of compound **1a** and act

through nucleophilic displacement (Table 1, entries 2-5). However, we did not observe full racemisation, even when 800 mM salt was used (Table 1, entry 5).

Table 1: Influence of the concentration of racemising agents on the decrease of the enantiomeric excess of an initially enantiopure sample of compound **1a**

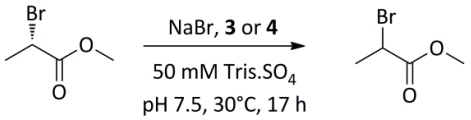

(*S*)-**1a** >99% e.e. **1a**

Entry	Racemisation agent	[Br] (mM)	Br^- equivalents per mol of (*S*)-**1a**	e.e. of **1a** (%)
1	none	-	-	>99%
2	NaBr	200	20	85
3	NaBr	400	40	73
4	NaBr	600	60	64
5	NaBr	800	80	59
6	**3**	0.15	0.05	98
7	**3**	0.45	0.15	92
8	**3**	1.5	0.5	59
9	**3**	3	1	19
10	**4**	2.6	0.65	28
11	**4**	10	2.5	0
12	**4**	53	13	0

Subsequently, the activity of DbjA was tested in the presence of 400 mM NaBr, but no conversion of substrate was observed. Since a bromide ion is a product of the enzymatic reaction, this lack of activity could be caused by product inhibition. To test this, the binding affinity for bromide ions to DbjA was determined by fluorescence quenching experiments. Such measurements, based on the fluorescent tryptophan(s) in the active site that bind(s) the halide during the dehalogenase reaction, have been used before to assay the binding of the halide for other haloalkane dehalogenases.[27] DbjA has one tryptophan residue at position 104,[28] which flanks the active site and is involved in bromide binding during catalysis,[25] and accordingly the protein was susceptible to fluorescence quenching, in agreement with the product inhibition. From the titration curve, a dissociation constant (K_D) of $(1.9\pm0.2)\times10^2$ mM was found. Since bromide ions at high concentrations apparently block the activity of the enzyme, NaBr cannot be used as

an effective racemisation agent in a dynamic resolution. Therefore, an additional activation of substrate towards nucleophilic attack of Br^- is needed to enable the lowering of salt concentration.

The report from Jones and Williams[26] suggests the use of two systems for the efficient racemisation of the substrate: a lipophilic phosphonium bromide (compound **3** in Figure 2) and a polymer-based phosphonium bromide (compound **4** in Figure 2). Therefore, we tested the racemisation of (*S*)-**1a** with compounds **3** and **4** as racemisation agents. The reaction with one equivalent of **3** yielded (*S*)-**1a** with an enantiomeric excess that has dropped from 99% to 19% (Table 1, entry 9). When the amount of racemising agent is lowered (Table 1, entries 6-8) the racemisation proceeds slower, and at 0.05 equivalents (Table 1, entry 6), the effect is negligible. However, when we tested the activity of the enzyme in the presence of one equivalent of compound **3**, no conversion of substrate **1a** with DbjA or DhaA was detected. In conclusion, compound **3** cannot be used as a racemisation agent in a dynamic kinetic resolution process with the studied dehalogenases.

Therefore, we continued to test the racemisation efficiency of polymer **4** as a Br^- source, in the form of a finely powdered, water-insoluble solid, which forms a suspension upon agitation in buffer. We expected that due to its insolubility it might have a smaller negative effect on enzymatic activity as compared to compound **3**.

Efficient racemisation of (*S*)-**1a** was achieved already at low amounts of **4**. When 0.65 equivalents of bromide ions (per mol of **1a**) were added in the form of salt **4**, a drop in e.e. from >99 to 28% was observed (Table 1, entry 12). The use of 2.5 equivalents of **4** (Table 1, entry 11) results in complete racemisation of **1a**. Upon comparison to the data collected in Table 1, entries 2-5, we conclude that Br anions alone cannot cause the racemisation, as much higher concentrations of NaBr are needed to obtain results comparable to the ones using compound **4**. No explanation is provided in the literature for the fact that compound **4** dramatically increases the racemisation rate as compared to free bromide.[26] We suggest that the polymer acts as a Lewis acid that polarises the carbon-bromide bond in the substrate, resulting in higher rate of an S_N2-type attack of the free bromide ions. Alternatively, the interaction of the polymer with the substrate can be based around the carbonyl group of the ester moiety, which would also result in the substrate activation towards an S_N2 process.

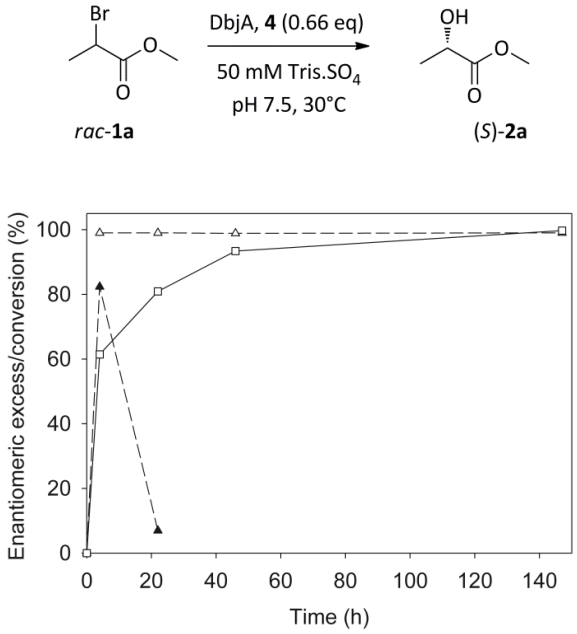

Figure 3: Dynamic kinetic resolution with **1a**. Symbols: (▲) enantiomeric excess of **1a**; (Δ) enantiomeric excess of **2a**; (□) conversion. Concentrations and e.e. values were determined using chiral GC. During later stages of the reaction (>30 h) the e.e. of remaining **2a** could not be reliably determined due to its low concentration.

Subsequently, the activity of the enzyme in the presence of compound **4** was tested in a dynamic kinetic resolution process (Figure 3). In this process the product was formed with high e.e. (99% during the whole course of the experiment), showing that the enzyme was still active in the presence of polymer **4** and that its enantioselectivity was not affected. In the beginning of the process the enzymatic conversion of (*R*)-**1a** was faster than the racemisation, resulting in high enantiomeric excess of the remaining (*S*)**-1a** at the first measured time (Figure 3). In later stages the e.e. of (*S*)**-1a** dropped due to its racemisation, which was accompanied by further conversion of the substrate. However, we suspected that the conversion of the substrate might also be caused by spontaneous hydrolysis of the ester bond in the substrate. To test this, the kinetic resolution of **1a** with DbjA was followed in a time course experiment. The concentration of the non-preferred substrate decreased, while the e.e. of product **2a** stayed >99%, which supported the assumption that **1a** was susceptible to non-enzyme catalysed ester hydrolysis (Figure 4).

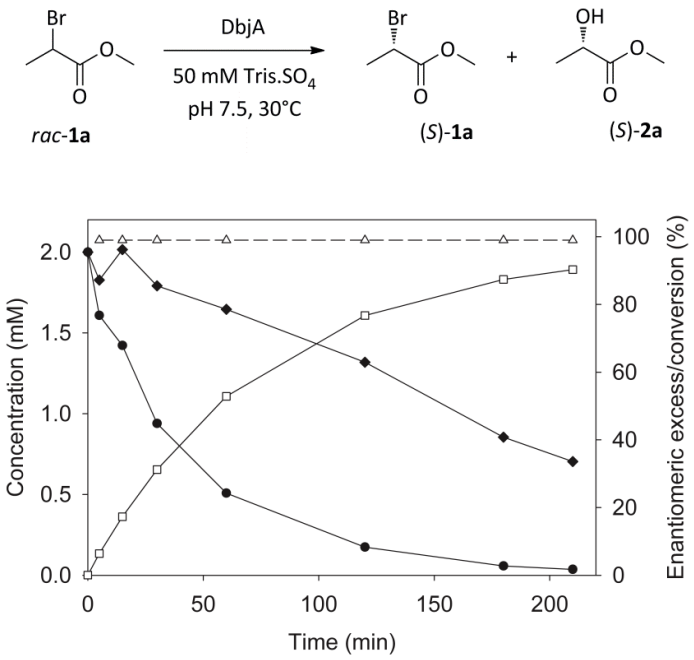

Figure 4: Kinetic resolution of **1a**. Symbols: (●) concentration of (*R*)-**1a**; (♦) concentration of (*S*)-**1a**; (Δ) enantiomeric excess of **2a**; (□) conversion. Concentrations and e.e. values were determined using chiral GC.

On the basis of these results, we chose compound **4** as an efficient racemising agent that did not abolish the enzymatic activity and did not affect the enantioselectivity of the biotransformation. We also selected the stable substrates butyl 2-bromopropionate (**1b**) and *N*-phenyl-2-bromopropionamide (**1c**) for further optimisation experiments.

Optimisation of the reaction conditions

Subsequently, the ability to achieve dynamic kinetic resolution using substrate **1b** and racemising agent **4** was tested (Figure 5). Conversion of **1b** in the presence of **4** was observed and enantiopure **2b** was formed. Furthermore, racemisation by **4** occurred, as the e.e. of **1b** decreased over time. We concluded that a dynamic kinetic resolution was achieved, albeit with low efficiency. The rate of non-enzyme catalysed hydrolysis was found to be much smaller than in the case of compound **1a**, as the slow drop in the concentration of (*S*)-**1b** (Figure 5) was accompanied by an increase of (*R*)-**1b** (Figure 5).

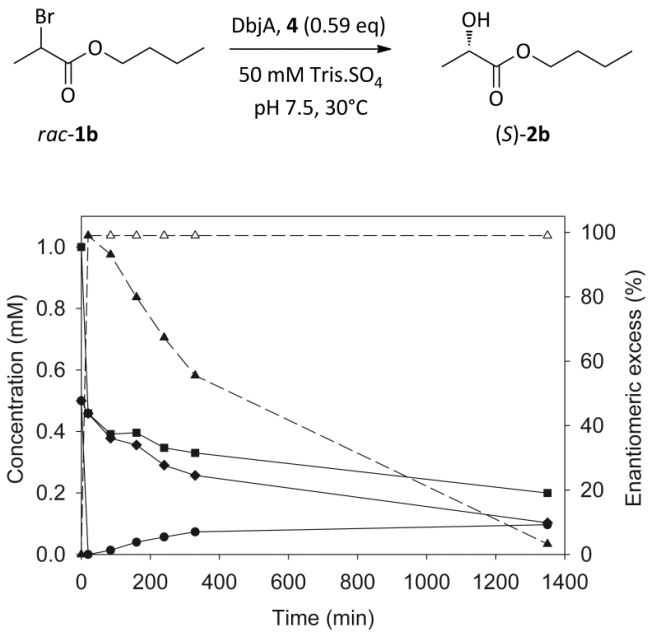

Figure 5: Dynamic kinetic resolution with **1b**. Symbols: (●) concentration of (*R*)-**1b**; (♦) concentration of (*S*)-**1b**; (■) total concentration of **1b**; (▲) enantiomeric excess of **1b**; (Δ) enantiomeric excess of **2b**. Concentrations and e.e. values were determined using chiral GC.

We suspected that either a too low concentration of compound **4** or inactivation of the enzyme could result in the observed slow reaction. Increasing the concentration of **4** led to faster racemisation, but the activity of the enzyme was reduced. Addition of an extra amount of the enzyme still failed to bring the reaction to full conversion. These results suggested that compound **4** might inactivate the enzyme during the course of the reaction. To test whether this was a reversible phenomenon, we conducted an experiment in which compound **4** was removed from the reaction mixture by centrifugation. No further conversion of (*R*)**-1a** was observed. However, the addition of a new amount of enzyme to this reaction mixture resulted in full conversion of (*R*)**-1a**, showing that the polymer inactivates the enzyme in a non-reversible manner.

As the enzymatic activity was reduced by the presence of compound **4**, we decided to further optimise the reaction setup by taking advantage of the insolubility of polymer **4** and separating the enzyme and **4** using a membrane reaction system. Two variants of such processes can be performed in which either the polymer, which has the particle size of 37-74 microns (reaction setup A), or the enzyme (reaction setup B) are enclosed in a membrane container of which the pore size excludes the possibility of protein or polymer leakage, but allows for the substrate/product transport across the membrane.

In reaction setup A, the membrane bag was filled with the suspension of racemisation polymer **4** and was placed into a solution containing the substrate and the enzyme. In

reaction setup B, the membrane compartment was filled with enzyme, placed in a solution containing substrate and compound **4** and attached to the cap of the reaction container. Both reaction setups were tested in the DKR of compound **1c** (Figure 6A and 6B). The agitation of the heterogeneous reaction system, which was found to be required for the efficient mass transfer to and from the non-soluble racemisation agent, was achieved either with 'head over tail' rotation (reaction setup A) or stirring with a magnetic stirrer (reaction setup B).

The reaction in setup A (Figure 6A) was fast in the beginning. However, after 20 h, it seems that the racemisation is the limiting factor, as the concentration of the preferred substrate is very low and the conversion is slow (Figure 6A). To confirm this, extra enzyme was added after 27 h, which did not significantly increase the reaction rate. To test whether a different mode of agitation could result in a more efficient racemisation process, the reaction mixture was shaken after 49 h. Indeed, a drop in e.e. of the substrate was observed, which confirmed that the agitation of **4** plays a crucial role in the DKR process. On the other hand, when the system was shaken, no more product was formed between 49 and 66 h, which observation hints at the possibility of enzyme inactivation during the shaking process. In conclusion, the rate of mass transfer to catalytic racemisation site is too low if the racemisation catalyst is in the membrane compartment.

Since the ratio of racemisation should be higher than the resolution, mass transfer limitation should be prevented. This was efficiently achieved in the alternative experimental setup B, in which compound **4** is stirred with the substrate without affecting the enzyme separated by the membrane (Figure 6B). The use of this setup indeed improves the rate of racemisation, as the enantiomeric excess of **1c** is kept below 40% during the whole reaction time. In this preparative scale experiment the product was isolated after 7 days with a yield of 61% and an e.e. value of 95%.

We observed that the total concentration of substrate and product (Figure 6B) decreases in the first 17 h, limiting the yield of the reaction. Incubating the substrate or product with either compound **4** or the membrane revealed that this drop in concentration is caused by the binding of **1a** by the racemisation catalyst **4**. Inspired by these results we reduced the amount of **4** four times to increase the yield of a preparative scale reaction. To avoid the further loss of product, which might happen during the extraction of the reaction mixture with an organic solvent, the whole reaction mixture was lyophilised prior to flash chromatography purification. The isolated yield indeed increased to 78%, but the e.e. of (*S*)-**2c** dropped to 88%, which is most likely caused by a limiting racemisation rate. Unconverted substrate **1c** was also recovered (22%) with an e.e. of 55%.

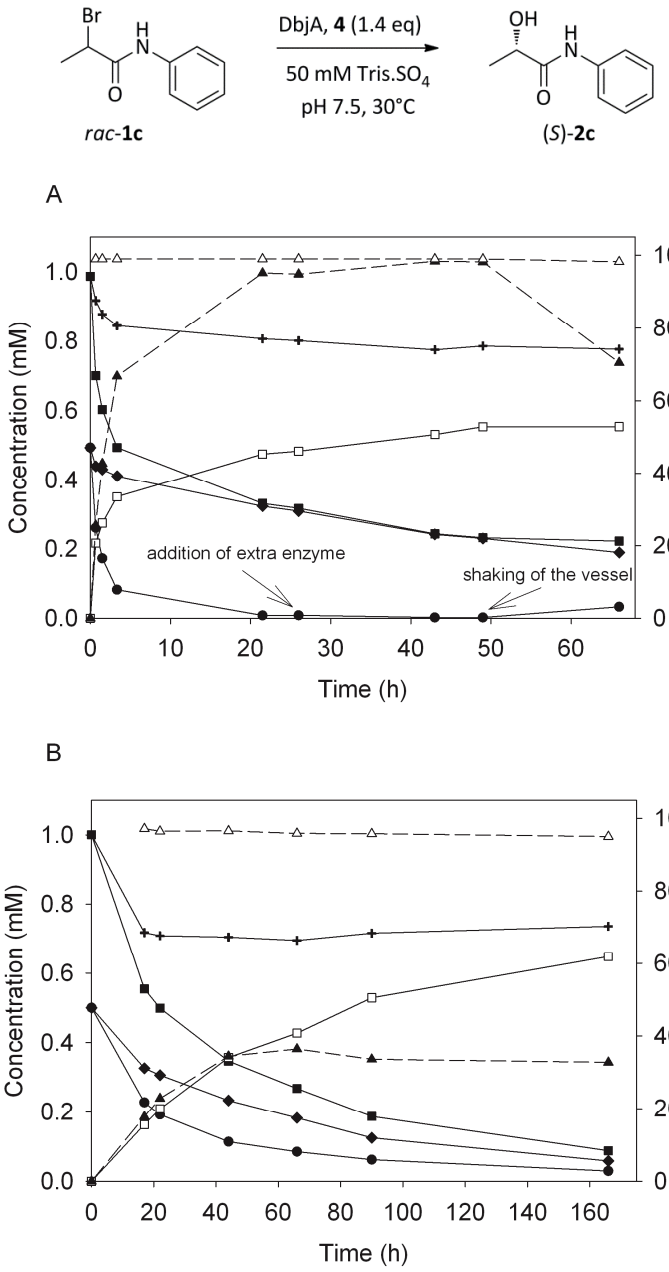

Figure 6: Dynamic kinetic resolution with **1c** using different reaction setups, see text for reaction setup A and B. Symbols: (●) concentration of (*R*)-**1c**; (♦) concentration of (*S*)-**1c**; (■) total concentration of **1c**; (▲) enantiomeric excess of **1c**; (□) concentration of **2c**; (Δ) enantiomeric excess of **2c**; (+) total concentration of **1c** and **2c**. Concentrations were determined by reverse-phase HPLC and e.e. values were determined using chiral HPLC.

A DKR was also observed with compound **1d**. After 7 days of incubation with 25 wt%, a conversion of 33% was observed and the e.e. of (*S*)-**2d** was 91% while the e.e. of the remaining **1d** was 14%. In conclusion, the polymer was active in the racemisation of compound **1d** and the enzymatic reaction was proceeding. However, the activity of the biocatalyst was not sufficient to obtain a complete conversion. The results suggest that expanding the substrate range of haloalkane dehalogenase may contribute to broaden the scope of this dynamic kinetic resolution.

CONCLUSIONS

In this chapter we present the first successful dynamic kinetic resolution process employing haloalkane dehalogenases, aimed at the preparation of enantiopure α-hydroxyamides, important precursors in medicinal chemistry. We have optimised the system to produce alcohols from bromoalkanes using a haloalkane dehalogenase (DbjA) and racemising agents. Because the enzyme is susceptible to interfacial inactivation, we used a semi-permeable membrane for the physical separation of the enzyme and the suspended racemising agent. In this final setup bromoamide (*S*)-**2c** could be produced with 63% isolated yield and 95% e.e. or with 78% yield and a lower e.e. of 88%. Together with the dynamic kinetic resolution of haloalcohols described by Haak *et al,*[29] this work lays the foundation for the use of a new chemoenzymatic DKR process aimed at chiral alcohols which does not employ expensive and environmentally hazardous heavy metal complexes.

EXPERIMENTAL

General

Production and purification of the haloalkane dehalogenases was performed as described before.[20]

Methyl *rac*-2-bromopropionate, methyl *rac*-lactate, methyl (*S*)-lactate, butyl *rac*-lactate, butyl (*S*)-lactate, *N*-phenyl-2-bromopropionamide and triphenylphosphine, polymer-bound, 200-400 mesh (2% cross-linked phosphine polymer) were purchased from Sigma-Aldrich. (1-Hexadecyl)triphenylphosphonium bromide was purchased from Alfa Aesar. Butyl *rac*-2-bromopropionate was purchased from TCI. *N*-phenyl-2-hydroxypropionamide was synthesised as described before.[20] The membrane bag used was purchased from Spectrumlabs and had a cut off of 3.5 kD (vol/length: 1.1 ml/cm).

*Preparation of N-phenyl-2-bromobutanamide (**1d**)*

2-Bromobutyric acid (2.0 mmol) and aniline (2.0 mmol) were stirred in DCM (8 mL) at 5 °C. Triethylamine (2.2 mmol) in DCM (2 mL) was added dropwise, and the cooling was removed. After 2-4 h the volatiles were evaporated. Solvents were evaporated and the product was purified by precipitation from AcOEt/pentane. Yield 91%. White powder. R_f = 0.82 (pentane/AcOEt. 1:1, v/v). mp. 99-100°C (lit.[30] 98-99). ^{1}H NMR (400 MHz, $CDCl_3$): δ 1.11 (t, ^3J = 7.6 Hz, 3H, C**H$_3$**), 2.11-2.30 (m, 2H, CH_3C**H$_2$**), 4.27 (dd, ^3J = 7.6 Hz, ^3J = 5.2 Hz, 1H, C**H**Br), 7.15 (t, ^3J = 7.6 Hz, 1H, Ar**H** *para*), 7.35 (app t, ^3J = 7.6 Hz, 2H, Ar**H** *meta*), 7.35 (d, ^3J = 7.6 Hz, 2H, Ar**H** *ortho*), 8.09 (br, s, 1H, N**H**). ^{13}C NMR ($CDCl_3$, 100 MHz): δ 11.8, 29.4, 54.1, 120.0, 125.0, 129.1, 137.1, 166.5; HRMS (ESI+) calc. for $C_{10}H_{13}BrNO$: 242.0175, found: 242.0166. Chiral HPLC analysis (Chiralcel AD, heptane/*i*-PrOH, 95/5, v/v), retention times (min): 9.9 (*R*) and 11.3 (*S*).

*Preparation of N-phenyl-2-hydroxybutanamide (**2d**), using a modified literature[31] procedure*

A solution of ***N*-**phenyl-2-bromobutanamide (1.00 mmol, 242 mg), formic acid (4.00 mmol, 151 µL), NaOH (4.00 mmol, 160 mg) and tetrabutylammonium bromide (31 mg) in 4 mL of a 1:1 (v/v) mixture of toluene and water was stirred and refluxed for 1 h. The reaction mixture was cooled, diluted with AcOEt (30 mL) and washed with water (2 x 20 mL). The organic phase was dried ($MgSO_4$) and the solvent was evaporated. The residue was dissolved in methanol (10 mL) and NaOH (100 mg) was added in one portion. After 10 min of stirring, the volatiles were evaporated and the residue was dissolved in AcOEt (30 mL) and washed with 1N aq. HCl (20 mL). The organic phase was dried and the product was purified by flash chromatography (Silicagel 40-63 µm, pentane/AcOEt) and subsequent precipitation from Et_2O / pentane. Yield: 22%. White powder. R_f = 0.66 (pentane/AcOEt. 1:1, v/v). mp. 89-90 °C (lit.[32] 88-89). ^{1}H NMR (400 MHz, $CDCl_3$): δ 1.02 (t, ^3J = 7.6 Hz, 3H, C**H$_3$**), 1.74-1.99 (m, 2H, CH_3C**H$_2$**), 3.04 (d, ^2J = 4.8 Hz, 1H, O**H**), 4.17-4.21 (m, 1H, C**H**OH), 7.12 (t, ^3J = 7.6 Hz, 1H, Ar**H** *para*), 7.32 (app t, ^3J = 7.6 Hz, 2H, Ar**H** *meta*), 7.55 (d, ^3J = 7.6 Hz, 2H, Ar**H** *ortho*), 8.46 (br, s, 1H, N**H**). ^{13}C NMR ($CDCl_3$, 100 MHz): δ 9.16, 27.8, 73.5, 119.8, 124.6, 129.0, 137.2, 171.9; HRMS (ESI+) calc. for $C_{10}H_{14}NO_2$: 180.1019, found: 180.1010. Chiral HPLC analysis (Chiralcel AD, heptane/*i*-PrOH, 95/5, v/v), retention times (min): 18.3 (*R*) and 22.3 (*S*). The absolute configuration was determined by comparison with the retention time of pure (*S*)-enantiomer, obtained by reacting (*S*)-2-hydroxybutyric acid with *N*-sulfinylaniline, according to a published procedure.[32]

*Determination of concentration and enantiomeric excess of compound **1a**-**c** and **2a**-**c***

1a/2a: Chiral GC, Chiraldex B-PM (0.9 ml/min, 5°C/min from 50°C to 100°C, 10°C/min from 100°C to 150°C, 10°C/min from 150°C to 50°C), retention times (min): 12.0 (*R*) and 12.7 (*S*) (**2a**); 13.2 (*S*) and 14.5 (*R*) (**1a**).

1b/2b: Chiral GC, CP chiralsil (0.7 ml/min, 50°C (40 min), 3°C/min from 50°C to 150°C, 10°C/min from 150°C to 50°C), retention times (min): 59.3 (*R*) and 59.5(*S*) (**2b**); 61.1 (*S*) and 61.5 (*R*) (**1b**).
1c/2c: Chiral HPLC, Chiralpak ASH, heptane/*i*-PrOH, 97/3, v/v. Compound **1c**: retention times (min): 22.1 (*S*) and 26.7 (*R*). Compound **2c**: retention times (min): 37.2 (*R*) and 43.9 (*S*). Quantification of **1c**/**2c** was performed by reverse-phase HPLC, using a calibration curve (Nucleosil 100 (C18) column, 50% acetonitrile and 50% 50 mM potassium phosphate buffer, pH 2.0, flow 1 mL/min (retention times (min) : 8.5 (**2c**); 29.5 (**1c**)).
1d/2d: Chiral HPLC, Chiralpak ADH, heptane/*i*-PrOH, 95/5, v/v. Compound **1d**: retention times (min): 17.8 (*R*) and 20.8 (*S*). Compound **2d**: retention times (min): 28.8 (*R*) and 48.5 (*S*).

*Preparation of enantiopure (S)-**1a** for the racemisation studies*
Enantiopure (*S*)**-1a** was prepared via kinetic resolution by haloalkane dehalogenase DbjA. DbjA (400 µg) was added to a solution of **1a** (1.20 mmol, 200 mg) in 120 ml of 50 mM Tris.SO_4 (pH 8.2) and incubated at 30°C. After 17 h, the reaction mixture was extracted with diethyl ether (3 x 75 mL), the organic phases were dried with $MgSO_4$ and evaporated. The enantiomeric excess was determined by Chiral GC, as described before and was >99% for (*S*)-**1a**.

*Racemisation of (S)-**1a** by sodium bromide*
To enantiopure (S)-**1a** (~10 mM) in 7.5 ml 50 mM Tris.SO_4 pH 7.5, different amounts of NaBr (200-800 mM) were added. After 17 h at 30°C, the reaction mixture was extracted with 5 ml diethyl ether, the organic phases were dried, evaporated and enantiomeric excess was determined by chiral GC as described before.

Fluorescence quenching experiment for K_D determination
Tryptophan fluorescence was measured using a Spex Fluorlog 322 fluorescence spectrophotometer (Jobin Yvon) in a stirred quartz cuvette, at 25°C. The excitation wavelength used was 280 nm and the emission wavelength was 350 nm. To 800 µl of 0.7 µM DbjA in 50 mM Tris.SO_4, pH 8.2, NaBr solution (6 M in 50 mM Tris.SO_4), pH 8.2) was titrated in steps of 10 µl to a final concentration of 2 M. Data for fluorescence quenching were corrected for the dilution and curves were fitted using Sigmaplot.

*Racemisation of (S)-**1a** by racemising agent **3***
To a 10 ml samples of 3.0 mM solution of (*S*)-**1a** in 50 mM Tris.SO_4 (pH 7.5), different amounts of **3** were added and the mixtures were incubated at 30°C. After 17 h, the reaction mixtures were extracted with 10 ml diethyl ether, dried, evaporated and enantiomeric excess was determined by chiral GC as described before.

*Synthesis of polymer-based phosphonium bromide (compound **4**)*[33]

Benzyl bromide (700 µl, 6.0 mmol) was added to 1.0 g of 2% cross-linked phosphine polymer in 10 ml of DMF and the mixture was stirred for 48 h at 70°C. The mixture was cooled, the solid was filtered, washed with toluene (2 x 10 ml), dichloromethane (2 x 10 ml) and diethylether (2 x 10 ml), and subsequently dried under vacuum (at 60°C), yielding 1.4 g of phosphonium salt. The bromide content was determined by elemental analysis as 17% Br, corresponding to a bromide loading of 0.0021 mol per gram of the prepared polymer.

*Racemisation of (S)-**1a** by racemising agent **4***

To 4.0 ml of 4 mM solution of (*S*)**-1a** in 50 mM Tris.SO_4 (pH 7.5), 0.65, 2.5 or 13 equivalents of **4** were added and the suspensions incubated at 30°C. After 17 h, the reaction mixtures were extracted with 10 ml diethyl ether, dried, and the enantiomeric excess was determined by chiral GC as described before.

Enzymatic reactions

Test experiment for DKR with 1a and compound 3

To a 30 ml of 0.3 or 3 mM solution of 1a in 50 mM Tris.SO4, pH 7.5, 1 equivalent of **3** and 400 µg DbjA/320 µg DhaA was added and incubated at 30°C. After 16 h, the reaction mixtures were extracted with 10 ml diethyl ether, the organic phases were dried, and the enantiomeric excess was determined by chiral GC.

DKR with 1a and compound 4

To 25 ml of 3 mM solution of **1a** in 50 mM Tris.SO_4, pH 7.5, compound **4** (0.66 equivalents) and 1.4 mg DbjA was added and the bottle was agitated at 30°C. At various times, samples of 5 ml were taken and extracted with 5 ml of diethyl ether (with 3 mM dodecane as an internal standard), the organic phases were dried, and the enantiomeric excess was determined by chiral GC.

Kinetic resolution of 1a

To 45 ml of 4 mM solution of **1a** in 50 mM Tris.SO_4, pH 7.5, 100 µg DbjA was added and incubated at 30°C. At various timepoints, samples of 5 ml were taken and extracted with 5 ml of diethyl ether (with 1 mM dodecane as internal standard), the organic phases were dried, and the enantiomeric excess was determined by chiral GC.

DKR with 1b and compound 4

To 45 ml of 1 mM solution of **1b** in 50 mM Tris.SO_4, pH 7.5, 0.59 equivalents of **4** and 100 µg DbjA was added and agitated at 30°C. At various time points, samples of 5 ml were taken and extracted with 5 ml of diethyl ether (with 1 mM dodecane as internal standard), the organic phases were dried, and the enantiomeric excess was determined by chiral GC.

DKR with 1c and compound 4 in a membrane bag

To 100 ml of 1 mM solution of **1c** in 50 mM Tris.SO_4, pH 7.5, a membrane bag filled with 67 mg of compound **4** in 5 ml of 50 mM Tris.SO_4, pH 7.5 (1.4 equivalents) and 500 µg DbjA was added and the bottle was rotated head over tail at 30°C. An extra portion of 500 µg DbjA was added after 27 h and after 49 h the system was shaken at 140 rpm. At various time points, samples of 2 ml were taken and extracted with 2 ml of ethyl acetate, the organic phases were dried, evaporated, and enantiomeric excess and the concentration was determined by chiral HPLC.

DKR with 1c and compound 4, with DbjA in a membrane bag

To 100 ml of 1 mM solution of **1c** in 50 mM Tris.SO_4, pH 7.5, with 67 mg (1.4 equivalents) of compound **4**, a membrane bag filled with 500 µg DbjA in 4 ml of 50 mM Tris.SO_4, pH 7.5 was added. The membrane was attached to the cap of the bottle; the racemising agent **4** was added to the solution, which was stirred and incubated at 30°C. Samples were analysed by chiral HPLC and reverse-phase HPLC, as described before. After 7 d the reaction mixture was filtered over a Schott funnel and the residue was washed with ethyl acetate. Subsequently the reaction mixture was extracted with 5 x 50 ml ethyl acetate. The collected organic phases were dried and the volatiles were evaporated. Product **2c** was purified by flash chromatography (Silicagel, 40-63 µm, eluents: **1c:** pentane/diethyl ether (6:4); **2c**: pentane/ethyl acetate (3:7). The yield of (*S*)-**2c** was 61% with an enantiomeric excess of 95%.

The same conversion was done with 17 mg (0.35 equivalents) of compound **4** and 1.2 mg DbjA. After 14 d the reaction mixture was lyophilised. Products **1c** and **2c** were purified by flash chromatography. The yield of (*S*)-**2c** was 78% with an enantiomeric excess of 88%, 22% of **1c** was recovered (e.e. 55%).

DKR with 1d and compound 4, with DbjA in a membrane bag

To 100 ml of 0.75 mM solution of **1c** in 50 mM Tris.SO_4, pH 7.5, with 50 mg (1.4 equivalents) of compound **4**, a membrane bag filled with 4.5 mg DbjA in 4 ml of 50 mM Tris.SO_4, pH 7.5 was added. The membrane was attached to the cap of the bottle; the racemising agent **4** was added to the solution, which was stirred and incubated at 30°C. After 7 d the reaction mixture was filtered over a Schott funnel and the residue was washed with ethyl acetate. Subsequently the reaction mixture was extracted with 4 x 50 ml ethyl acetate and 2 x 50 ml chloroform. The collected organic phases were dried and the volatiles were evaporated. The conversion was 33%, e.e of (*S*)-**2d** was 91% and the e.e. of recovered **2c** was 14%.

ACKNOWLEDGEMENTS

We thank Prof. Kurt Faber (University of Graz) and Ana Toplak (University of Groningen) for useful discussions. We thank Theodora Tiemersma-Wegman, Monique Smith and Piet Wietzes for their technical assistance with HPLC and GC.

REFERENCES

[1] D. Monti, G. Ottolina, G. Carrea, S. Riva. *Chem. Rev.* **2011**, *111*, 4111-4140.
[2] E. Brenna, C. Fuganti, F. G. Gatti, S. Serra. *Chem. Rev.* **2011**, *111*, 4036-4072.
[3] E. Garcia-Urdiales, I. Alfonso, V. Gotor. *Chem. Rev.* **2011**, *111*, PR110-PR180.
[4] H. Pellissier. *Tetrahedron* **2008**, *64*, 1563-1601.
[5] H. Pellissier. *Tetrahedron* **2011**, *67*, 3769-3802.
[6] N. J. Turner. *Curr. Opin. Chem. Biol.* **2004**, *8*, 114-119.
[7] B. Schnell, K. Faber, W. Kroutil. *Adv. Synth. Catal.* **2003**, *345*, 653-666.
[8] O. Pamies, J. E. Backvall. *Trends Biotechnol.* **2004**, *22*, 130-135.
[9] M. Kondo, L. L. Zhang, H. P. Ji, Y. Kou, B. X. Ou. *J .Agri .Food Chem.* **2009**, *57*, 8788-8792.
[10] J. F. Evans, S. Kargman. *FEBS Letters* **1992**, *297*, 139-142.
[11] R.S. Edson, C. L. Terrell. *Mayo Clin. Proc.* **1999**, *74*, 519-528.
[12] L. V. Tremblay, H. Xu, J. S. Blanchard. *Biochemistry* **2010**, *49*, 9685-9687.
[13] S. Sebti, A. Foucaud. *Synthesis* **1983**, 546-549.
[14] W. Szymanski, R. Ostaszewski. *Tetrahedron Asymmetry* **2006**, *17*, 2667-2671.
[15] W. Szymanski, R. Ostaszewski. *Tetrahedron* **2008**, *64*, 3197-3203.
[16] K. Tani, K. Suwa, E. Tanigawa, T.Ise, T. Yamagata, Y. Tatsuno, S. Otsuka. *J. Organomet. Chem.* **1989**, *370*, 203-221.
[17] F. Hapiot, F. Agbossou, A. Mortreux. *Tetrahedron Asymmetry* **1997**, *8*, 2881-2884.
[18] D. A. Evans, J. Wu. *J. Am. Chem. Soc.* **2005**, *127*, 8006-8007.
[19] W. Szymanski, R. Ostaszewski. *J. Mol. Catal. B: Enzym.* **2007**, *47*, 125-128.
[20] Chapter 3 of this thesis.
[21] A. L. E. Larsson, B. A. Persson, J. E. Backvall. *Angew. Chem.,Int. Ed.* **1997**, *36*, 1211-1212.
[22] B. A. Persson, A. L. E. Larsson, M. Le Ray, J. E. Backvall. *J. Am. Chem. Soc.* **1999**, *121*, 1645-1650.
[23] J. H. Choi, Y. H. Kim, S. H. Nam, S.T. Shin, M. J. Kim, J. Park. *Angew. Chem.,Int. Ed.* **2002**, *41*, 2373-2376.
[24] J. V. Allen, J. M. J. Williams. *Tetrahedron Lett.* **1996**, *37*, 1859-1862.
[25] Z. Prokop, Y. Sato, J. Brezovsky, T. Mozga, R. Chaloupkova, T. Koudelakova, P. Jerabek, V. Stepankova, R. Natsume, J. G. E. van Leeuwen, D. B. Janssen, J. Florian, Y. Nagata, T. Senda, J. Damborsky. *Angew.Chem.,Int. Ed.* **2010**, *49*, 6111-6115.
[26] M. M. Jones, J. M. J. Williams. *Chem .Commun.* **1998**, 2519-2520.
[27] F. Pries, J. Kingma, M. Pentenga, G. van Pouderoyen, C. M. Jeronimus-Stratingh, A.P. Bruins, D. B. Janssen. *Biochemistry* **1994**, *33*, 1242-1247.
[28] Y. Sato, M. Monincova, R. Chaloupkova, Z. Prokop, Y. Ohtsubo, K. Minamisawa, M. Tsuda, J. Damborsky, Y. Nagata. *Appl. Environ. Microbiol.* **2005**, *71*, 4372-4379.
[29] R. M. Haak, F. Berthiol, T. Jerphagnon, A. J. Gayet, C. Tarabiono, C .P. Postema, V. Ritleng, M. Pfeffer, D. B. Janssen, A. J. Minnaard, B. L. Feringa, J. G. J. de Vries. *J. Am. Chem. Soc.* **2008**, *130*, 13508-13509.
[30] E. Schroepl, R. Pohloudek-Fabini. *Pharmazie,* **1968**, *23*, 638-641.
[31] R. A. Felix, E. G. Teach. US 4650512 A1 Patent
[32] J. M. Shin, Y. H. Kim. *Tetrahedron Lett.,* **1986**, *27*, 1921-1924.
[33] M. Bernard, W. T. Ford. *J. Org. Chem.* **1983**, *48*, 326-332.

CHAPTER 5

A simple, enantioconvergent, chemoenzymatic synthesis of optically active α-substituted amides

Wiktor Szymański, Alja Westerbeek, Dick B. Janssen, and Ben L. Feringa

Based on: Angew. Chem. Int. Ed., 2011, *50*, 10712-10715

ABSTRACT

A chemoenzymatic enantioconvergent process for the preparation of α-substituted amides is described. It employs a haloalkane dehalogenase catalysed enantioinverting transformation of α-bromoamides and two subsequent reactions. Various *N*-, *O*- and *S*-substituted amides were synthesised and yields up to 96% and e.e.'s up to 98% were reported.

INTRODUCTION

Enantiopure amides **1**, substituted in the Cα-position with an azide or a simple *N*-, *O*- or *S*-substituent (Figure 1) form an important class of compounds and are key intermediates in medicinal chemistry. The α-azidoamide **1** (Nu = N_3) motif is found in bioactive molecules, such as the antibiotic azidocillin (Figure 1). The azide group is considered to be an isostere of an amino group, which has increased bulkiness and does not get positively charged at physiological pH.[1] The introduction of an azide function into the Cα-position of peptides is also aimed at the synthesis of enzyme inhibitors that, after binding to their targets and subsequent Staudinger type ligation with biotin-phosphine, are subjected to streptavidin pulldown.[2] Furthermore, enantiopure α-azidoamides are important reagents for 'click' chemistry[3] and valuable precursors in the synthesis of amino acids[4] and peptides.[5,6]

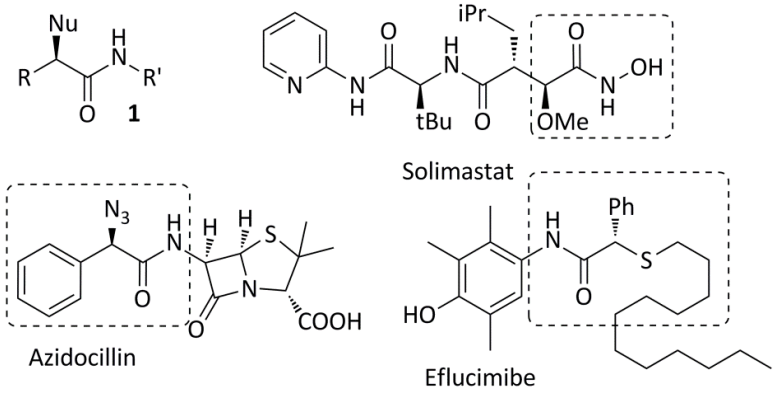

Figure 1: General structure **1** and examples of bioactive compounds derived from **1**.

The chiral scaffold of an amide with a simple *O*-substituent (**1**, Nu = OR) in the α position can be found in numerous bioactive compounds, such as Solimastat (Figure 1) - an inhibitor of matrix metalloproteinase[7] and other anti-cancer[8] and anti-convulsant[9] agents. Bioactive molecules that incorporate a chiral amide motif with an *S*-substituent (**1**, Nu = SR), include lipid-lowering agent Eflucimibe,[10] TNFα convertase inhibitors[11] and renin inhibitors.[12]

Considering the importance of the broad family of enantiopure α-hetero-substituted amides **1**, we decided to investigate the possibility of designing an enantioconvergent, chemoenzymatic process for their preparation. We present here a time- and cost-efficient synthetic route, characterised by high enantioselectivity and product versatility, for the first time taking the advantage of intrinsic, compatible reactivity of the products of haloalkane dehalogenase-catalysed reactions.

Enantioconvergent processes are transformations in which both enantiomers of a chiral substrate are converted into the same enantiomer of the product via different pathways.[13] Such processes allow for the highly efficient transformation of cheap, racemic starting materials into valuable, enantiopure products, by increasing the yield beyond the theoretical value of 50% that can be obtained from the common transformation of only one enantiomer, i.e. via kinetic resolution. Chemoenzymatic, enantioconvergent syntheses can be carried out in three general ways (Figure 2).

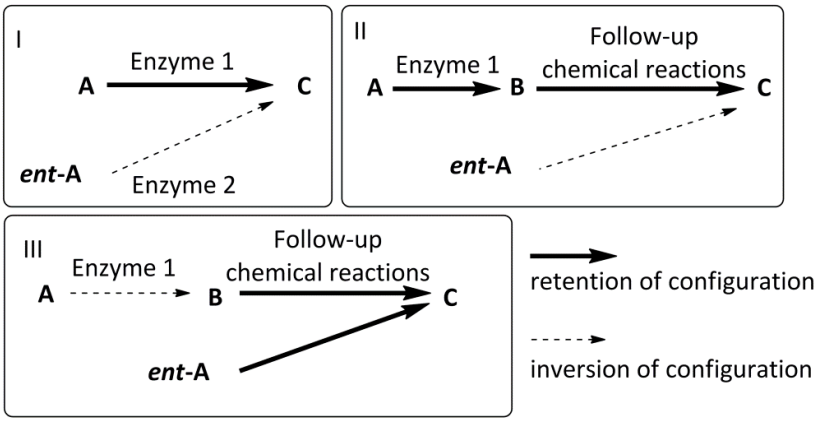

Figure 2: Strategies used in chemoenzymatic, enantioconvergent processes. Reactions represented by bold arrows proceed with retention of configuration. Reactions represented by dashed arrows proceed with inversion of configuration.

The first approach (Figure 2.I) employs two enzymes that express opposite enantiopreference. One of them catalyses the transformation of substrate **A** to product **C** with retention of configuration, while the other one inverts the stereochemistry in the conversion of ***ent*-A** to **C**, usually via an S_N2-type of process. This approach has been applied mainly for the hydrolysis of epoxides, using two epoxide hydrolases[14,15] or one enzyme which catalyses the convergent transformations of both enantiomers with distinct regioselectivity.[16-18]

The second approach (Figure 2.II) uses one enzyme to perform a kinetic resolution of racemic substrate **A**. In a subsequent set of reactions enantioenriched compounds ***ent*-A** and **B** are transformed into a single product **C**, while one of these transformations proceeds with retention and the other with inversion of configuration. Such

deracemisations can be, for example, performed by combining the lipase-catalysed kinetic resolution of racemic esters with a subsequent stereoinversion of the obtained enantioenriched alcohols via sulfonyl esters,[4,19,20] nitrate esters[19] or a Mitsunobu protocol.[21]

The third approach (Figure 2.III) relies on the use of a single, enantioinverting enzyme for the conversion of one of the enantiomers of substrate **A** into product **B**. In the follow-up reaction this product and, optionally, the unreacted ***ent*-A,** are transformed into the final compound **C** with retention of configuration. Most recent examples of such syntheses include the use of inverting alkyl sulfatases for enantioselective sulfate ester hydrolysis, which yields an alcohol and an unreacted enantiomer of the sulfate ester, both with the same absolute configuration.[22-24] Follow up chemical hydrolysis of the enantioenriched sulfate ester, which proceeds with retention of configuration, yields the same enantiomer of the alcohol as the one produced in the enzymatic, inverting step.

The use of the first approach (Figure 2.I) is severely limited, despite its apparent efficiency and elegance, by low availability of enzyme pairs that show complementary enantioselectivity. The efficiency of the latter approaches (Figures 2.II and 2.III) strongly depends on the high enantioselectivity of the enzymatic reaction and high atom economy of the chemical steps (which is especially low in case of the Mitsunobu protocol).[21] Furthermore, it is advantageous if no separation of intermediates is needed and the purification steps are reduced to a minimum.[22]

Haloalkane dehalogenases are enzymes that catalyse the hydrolytic cleavage of carbon-halide bonds, employing a catalytic aspartate for the nucleophilic displacement of the halide in a S_N2 type of reaction.[25] This process yields a covalent intermediate in which the product is bound to the enzyme by an ester bond. This bond is subsequently hydrolysed to form the product and to recover the nucleophilic aspartate. Overall, the reaction proceeds with inversion of configuration, therefore the enzyme can be efficiently used in the process described in Figure 2.III.

Additional possibilities stem from the fact that this reaction yields two enantiopure compounds, a haloalkane and an alcohol, that possess high intrinsic reactivity and outstanding potential for functionalisation. In particular, both the halide (directly) and the hydroxide (upon simple activation) can be regarded as efficient leaving groups, which sets the stage for a number of nucleophilic displacements leading to diverse classes of products.

RESULTS AND DISCUSSION

We designed a chemoenzymatic, enantioconvergent process (Scheme 1) for the synthesis of enantiopure amides **1** (Figure 1), using the general approach described in Figure 2.III.

This process uses haloalkane dehalogenases as the inverting enzymes in the biocatalytic step and sulfonyl esters for the follow-up, chemical transformations.

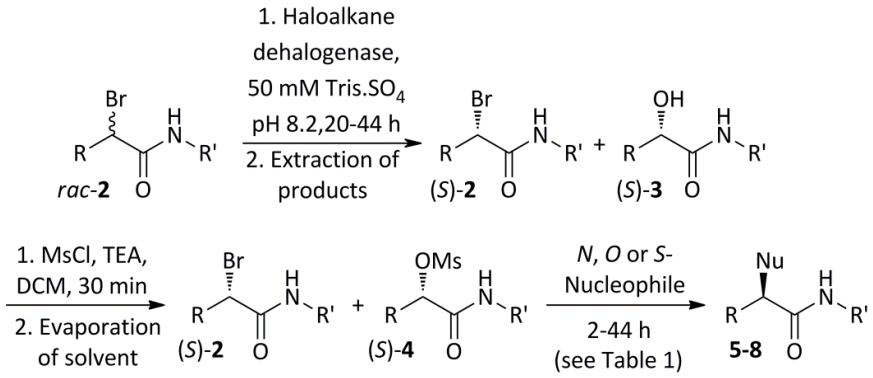

Scheme 1: Chemoenzymatic, enantioconvergent preparation of compounds **5**-**8**.

We have established that easily prepared, racemic α-bromoamides (*rac*-**2**) can be converted by haloalkane dehalogenases with high enantioselectivity (E values up to >200).[26] Upon extraction of aqueous enzymatic reaction mixture, both products (*S*)-**2** and (*S*)-**3** can be obtained with high overall yields (>80%). We expected that no separation of intermediates would be needed prior to the conversion of alcohols (*S*)-**3** into methanesulfonyl esters (*S*)-**4** and that this reaction mixture also would not have to be processed before the final step (Scheme 1). These simplifications to the procedure would fulfill the requirements of limiting the intermediate separations and purification steps in the processes described in Figure 2.III. In the last reaction, in which the α-bromoamide (*S*)-**2** and the α-mesyloxyamide (*S*)-**4** are both converted in a S_N2 type of process into final products (*R*)-**1**, we employed azide and benzylamine as *N*-nucleophiles, ethanethiol as a *S*-nucleophile and phenol as an *O*-nucleophile.

Racemic α-bromoamide **2a** (Figure 3), a precursor of compound **4a** (Scheme 2), undergoes kinetic resolution catalysed by haloalkane DbjA with excellent enantioselectivity (E>200).[26]

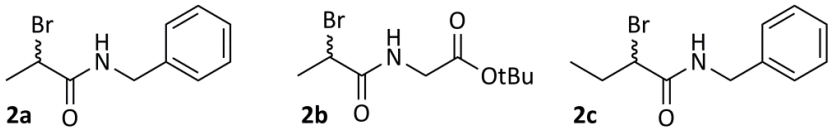

Figure 3: Racemic α-bromoamides **2**, which were used as substrates in this study.

To establish the best conditions for the reactions of mixtures of α-bromoamides (*S*)-**2** and α-methanesulfonyloxyamides (*S*)-**4** with the model nucleophiles, we performed a study in which the racemic model compound **4a** was reacted under various conditions towards racemic products **5a-8a** (Scheme 2). The results obtained for the reactions of **4a** with the model nucleophiles are presented in Table 1.

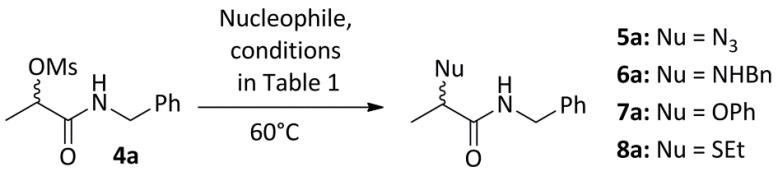

Scheme 2: Model reactions of racemic compound **4a** with representative nucleophiles. For conditions see Table 1.

Table 1: Results of the model transformations of compound **4a**.

Entry	Nucleophile	Solvent	K_2CO_3	Time	Product	Yield[a]
1	NaN_3 (5 eq.)	DMF	-	2 h	**5a**	96%
2	$BnNH_2$ (2 eq.)	DMF	2 eq.	46 h	**6a**	<50%
3	$BnNH_2$ (2 eq.)	MeCN	2 eq.	46 h	**6a**	71%
4	PhOH (2 eq.)	MeCN	2 eq.	20 h	**7a**	73%
5	EtSH (2 eq.)	MeCN	2 eq.	46 h	**8a**	71%
6	EtSH (2 eq.)	DMF	2 eq.	20 h	**8a**	70%

[a] Isolated yield.

The reaction of compound **4a** with sodium azide in DMF as a solvent resulted in full conversion of the substrate in 2 h, and product **5a** was isolated in almost quantitive yield (Table 1, entry 1). When similar conditions were employed for the introduction of another *N*-nucleophile, benzylamine, in the presence of potassium carbonate as a base, the reaction took 46 h to reach full conversion and the product was isolated with low yield due to the formation of side-products (Table 1, entry 2). The use of acetonitrile as a solvent, instead of DMF (Table 1, entry 3), resulted in a much cleaner reaction and product **6a** was isolated after 46 h with good yield. When these conditions were used for the reaction of compound **4a** with phenol (Table 1, entry 4), full conversion of substrate was achieved already after 20 h. Under the same conditions, **4a** could be converted to the α-ethylthioamide **8a** in 46 h with 71% yield (Table 1, entry 5). Virtually the same yield was obtained with DMF as a solvent, but the reaction time was shorter (Table 1, entry 6). On the basis of these results, the latter conditions were chosen for the planned enantioconvergent chemoenzymatic synthesis of compound **8a** and its analogs.

To study the feasibility of the transformations presented in Scheme 1, we focused on three model substrates (Figure 3). Racemic compounds **2** are readily accessible in >90% yield in one step from simple starting materials.[26] Furthermore, compound **2b**, which includes a moiety derived from the most simple amino acid, glycine, was chosen to show

that our methodology has prospects in the context of peptide preparation. Compound **2c**, on the other hand, features an ethyl substituent on the Cα position, which enabled us to assay the influence of steric hindrance on the efficiency of the final step of the transformation presented in Scheme 1.

Subsequently, we conducted a series of reactions aiming at the enantioconvergent, chemoenzymatic preparation of compounds **5-8** (Scheme 1, Table 2).

Table 2: Results obtained for the enantioconvergent, chemoenzymatic preparation of compound **5-8**.

Substrate	***rac*-2a**[a]	***rac*-2b**[b]	***rac*-2c**[c]
Nucleophile	(*R*)-Product (isolated yield from ***rac*-2**, *ee*)		
NaN_3	**5a:** 81%, 98% *ee*	**5b:** 73%, 97% *ee*	**5c:** 80%, 95% *ee*
$BnNH_2$	**6a:** 81%, 97% *ee*	**6b:** 96%, 91% *ee*	**6c:** 85%, 90% *ee*
PhOH	**7a:** 70%, 95% *ee*	**7b:** 57%, 93% *ee*	**7c:** 66%, 96% *ee*
EtSH	**8a:** 82%, 28% *ee*	**8b:** 76%, 92% *ee*	**8c:** 63%, 73% *ee*

Conditions of enzymatic reaction: [a] DbjA (1.7 wt%, 42 h); [b] DbjA (1.1 wt%, 20 h); [c] LinB (2.3 wt%, 44 h).

The racemic precursors *rac*-**2** were initially subjected to a haloalkane dehalogenase mediated kinetic resolution (Scheme 1), providing a selective transformation to α-hydroxyamides (*S*)-**3** using DbjA and haloalkane dehalogenase from *Sphingomonas paucimobilis* UT26 (LinB). In the enzymatic reactions, after 20-44 h conversions of 50% were observed, which is crucial for the efficient enantioconvergent process.[27,28] The enantiomeric excess of the products was found to be >97% in all of the cases. Noteworthy, only a small amount of enzyme was used for these conversions (Table 2), which typically corresponds to 0.01 mol% of biocatalyst.

The reaction mixtures obtained from the biotransformations were extracted with ethyl acetate and no further product separation or purification was required. After evaporation of the solvent, the crude mixtures of enantiomerically enriched α-bromoamides (*S*)-**2** and α-hydroxyamides (*S*)-**3** were subjected to the reactions in which compounds (*S*)-**3** were mesylated to give intermediates (*S*)-**4** (Scheme 1). We observed that this reaction proceeds cleanly and did not affect the α-bromoamides (*S*)-**2**.

Crude reaction mixtures obtained in the second step were concentrated *in vacuo*, and no purification or separation of intermediates (*S*)-**2** and (*S*)-**4** was required. This step was followed by the introduction of nucleophiles, using the optimised conditions for S_N2-reactions (Table 1, entries 1, 3, 4 and 6).

The reactions leading to α-azidoamides (*R*)-**5a-c** gave the products in 73-81% yield (based on rac-**2a**), providing the proof of principle for the proposed, enantioconvergent synthetic route by showing that both products of the enzymatic reaction can be efficiently transformed into a single product (Table 2). The high enantiomeric excess (e.e.>95%) of

the obtained products renders our methodology suitable for the preparation of chiral α-azidoamides, important precursors for peptide synthesis.

Transformations in which benzylamine was used as a nucleophile led to α-(benzylamino)amides (*R*)-**6a**-**c** (Table 2) with even better yields than in the case of azide. High enantiomeric excess of the products (up to 97% for product (*R*)-**6a**) further confirms the potential of the presented methodology for the preparation of peptide analogs.

The yields obtained in the syntheses of α-phenoxyamides (*R*)-**7a**-**c** were generally lower (Table 2) than for the reactions with sodium azide and benzylamine, yet still significantly superior to the maximum theoretical yield of 50% that could be obtained if only one product of the enzyme-catalysed kinetic resolution was used for further transformations. Considering the high enantiomeric excess of the products (93-96% e.e., Table 3), we conclude that the presented methodology can efficiently be used for the stereoselective preparation of chiral amides substituted with *O*-nucleophiles.

In the transformations aimed at α-ethylthioamides (*R*)-**8** good yields were obtained for the products (Table 2), albeit the e.e. values were lower. In the least satisfying case of compound (*R*)-**8a** only 28% e.e. was found. We suspect that this enhanced racemisation may result from the increased acidity of the proton attached to the Cα position of compounds **8**, is due to the presence of the ethylthio substituent that stabilises the intermediate carbanion.[29,30] The deprotonation and subsequent reprotonation (enolisation) of compound **8** under the basic conditions of the reaction in which it is prepared (2 eq. of potassium carbonate) would lead to its racemisation. To confirm this hypothesis we checked the e.e. of compound **8c** after 2 weeks of storage at 4°C and we found that it decreased from the initial value of 73% to 69%. Subsequently, we incubated the compound under the nucleophilic displacement reaction conditions (2 eq. of potassium carbonate, DMF) for 5 h and found that its e.e. dropped again to the value of 65%. These data support our notion on the enhanced tendency for the racemisation of products **8**.

CONCLUSIONS

We have designed an efficient, enantioconvergent process for the synthesis of various enantiopure α-substituted amides, which form an important class of chiral building blocks in medicinal chemistry. The process combines the high enantioselectivity of haloalkane dehalogenase-catalysed resolution with the efficient and convergent transformation of both the starting material and the biocatalysis product into a single enantiomer of the final compounds **1**. The products are obtained in high yield (up to 96% after 3 steps) and with high enantiomeric excess (up to 98%) in the case of configurationally stable compounds **5**-**7**. In the whole process the purification/separation steps are eliminated, rendering it a practical and time-efficient methodology. At this moment we are directing

our efforts towards using directed evolution methodologies for the broadening of the substrate scope of haloalkane dehalogenases, and as a consequence fully enhancing the versatility of the new process.

EXPERIMENTAL

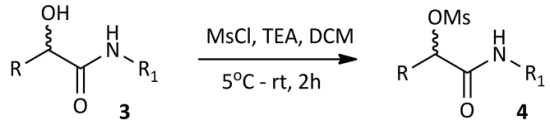

*General procedure A: Synthesis of racemic α-methanesulfonyloxy-amides **4***

A stirred solution of α-hydroxyamide **3** (1.10 mmol) and triethylamine (2.0 mmol, 280 µL) in DCM (5 mL) was cooled in an ice-water bath. A solution of methanesulfonyl chloride (1.40 mmol, 108 µL) in DCM (1 mL) was added over 5 min. The cooling bath was removed and the reaction mixture was left stirring at room temperature for 2 h. The volatiles were evaporated and the product was purified by flash chromatography (Silicagel, 40-63 µm, pentane/AcOEt, 1:1, v/v).

4a: 1-(Benzylamino)-1-oxopropan-2-yl methanesulfonate

Yield: 91%. White crystals. R_f = 0.54 (pentane/AcOEt. 1:1, v/v); mp. 92-93.5°C; ^{1}H NMR (400 MHz, $CDCl_3$): δ 1.64 (d, ^3J = 6.8 Hz, 3H, C**H$_3$**CH), 3.05 (s, 3H, C**H$_3$**SO$_2$), 4.41-4.53 (m, 2H, PhC**H$_2$**), 5.11 (q, ^3J = 6.8 Hz, 1H, C**H**OMs), 6.67 (br s, 1H, N**H**), 7.25-7.37 (m, 5H, Ar**H**); ^{13}C NMR (75 MHz, $CDCl_3$): δ 19.2, 39.0, 43.7, 116.0, 127.9, 128.0, 129.0, 137.6, 168.8; HRMS (ESI+) calc. for $C_{11}H_{16}NO_4S$: 258.0795, found: 258.0802.

4b: *tert*-Butyl 2-(2-((methylsulfonyl)oxy)propanamido)acetate

Yield: 87%. White crystals. R_f = 0.57 (pentane/AcOEt. 1:1, v/v); mp. 101-102°C; ^{1}H NMR (400 MHz, $CDCl_3$): δ 1.48 (s, 9H, (C**H$_3$**)$_3$), 1.64 (d, ^3J = 6.8 Hz, 3H, C**H$_3$**CH), 3.15 (s, 3H, C**H$_3$**SO$_2$), 3.95 (d, ^3J = 5.2 Hz, 2H, NHC**H$_2$**), 5.11 (q, ^3J = 6.8 Hz, 1H, C**H**OMs), 6.88 (br s, 1H, N**H**); ^{13}C NMR (75 MHz, $CDCl_3$): δ 19.0, 28.0, 38.7, 41.8, 76.3, 82.6, 168.3, 168.8; HRMS (ESI+) calc. for $C_{10}H_{19}NO_6SNa$: 304.0825, found: 304.0831.

4c: 1-(Benzylamino)-1-oxobutan-2-yl methanesulfonate

Yield: 86%. White crystals. R_f = 0.57 (pentane/AcOEt. 1:1, v/v); mp. 79-80°C; ^{1}H NMR (400 MHz, $CDCl_3$): δ 1.02 (t, ^3J = 7.2 Hz, 3H, C**H$_3$**CH$_2$), 1.93-2.12 (m, 2H, C**H$_2$**CH) 3.05 (s, 3H, C**H$_3$**SO$_2$), 4.41-4.53 (m, 2H, PhC**H$_2$**), 4.99 (dd, ^3J = 6.4 Hz, ^3J = 4.8 Hz, 1H, C**H**OMs), 6.64 (br s, 1H, N**H**), 7.25-7.36 (m, 5H, Ar**H**); ^{13}C NMR (75 MHz, $CDCl_3$): δ 9.1, 26.1, 38.8, 43.7, 81.6, 127.9, 128, 129.0, 137.7, 168.2; HRMS (ESI+) calc. for $C_{12}H_{17}NO_4SNa$: 294.0770, found: 294.0754.

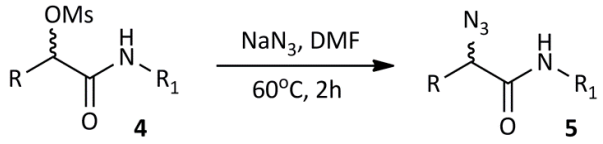

*General procedure B: Synthesis of racemic α-azidoamides **5***

To a solution of α-methanesulfonyloxy-amide **4** (0.10 mmol) in DMF (0.5 mL) was added sodium azide (0.50 mmol, 33 mg) and the resultant suspension was stirred at 60°C. After 2 h the volatiles were evaporated and the product was purified by flash chromatography (Silicagel, 40-63 μm, pentane/AcOEt, 9:1 to 4:1, v/v).

5a: 2-Azido-*N*-benzylpropanamide

Yield: 96%. Clear oil. R_f = 0.64 (pentane/AcOEt. 1:1, v/v); ^{1}H NMR (400 MHz, $CDCl_3$): δ 1.57 (d, ^3J = 7.2 Hz, 3H, C**H$_3$**CH), 4.12 (q, ^3J = 7.2 Hz, 1H, C**H**N$_3$), 4.44 (d, ^3J = 6.0 Hz, 2H, NHC**H$_2$**), 6.67 (br s, 1H, N**H**), 7.27-7.37 (m, 5H, Ar**H**); ^{13}C NMR (75 MHz, $CDCl_3$):δ 17.4, 43.7, 59.5, 127.9, 128.0, 129.0, 137.8, 169.9; HRMS (ESI+) calc. for $C_{10}H_{13}N_4O$: 205.1084, found: 205.1083. HPLC (Chiralcel AD, heptane/*i*-PrOH, 95/5, v/v, 1 mL/min), Rt (min): 9.6 (*R*), 11.3 (*S*).

5b: *tert*-Butyl 2-(2-azidopropanamido)acetate

Yield: 99%. Clear oil. R_f = 0.74 (pentane/AcOEt. 1:1, v/v); ^{1}H NMR (400 MHz, $CDCl_3$): δ 1.47 (s, 9H, (C**H$_3$**)$_3$), 1.55 (d, ^3J = 7.2 Hz, 3H, C**H$_3$**CH), 3.91-3.93 (m, 2H, NHC**H$_2$**), 4.10 (q, ^3J = 7.2 Hz, 1H, C**H**N$_3$), 6.80 (br s, 1H, N**H**); ^{13}C NMR (75 MHz, $CDCl_3$): δ 17.3, 28.2, 42.1, 59.3, 82.8, 168.8, 170.1; HRMS (ESI+) calc. for $C_9H_{16}N_4O_3Na$: 251.1115, found: 251.1115. HPLC (Chiralcel OJ, heptane/*i*-PrOH, 95/5, v/v, 1 mL/min), Rt (min): 7.4 (*S*), 7.8 (*R*).

5c: 2-Azido-*N*-benzylbutanamide

Yield: 96%. Clear oil. R_f = 0.80 (pentane/AcOEt. 1:1, v/v); ^{1}H NMR (400 MHz, $CDCl_3$): δ 1.01 (t, ^3J = 7.2 Hz, 3H, C**H$_3$**CH$_2$), 1.85-2.06 (m, 2H, C**H$_2$**CH) 3.99 (dd, ^3J = 6.4 Hz, ^3J = 4.4 Hz, 1H, C**H**N$_3$), 4.38-4.50 (m, 2H, NHC**H$_2$**), 6.70 (br s, 1H, N**H**), 7.25-7.37 (m, 5H, Ar**H**); ^{13}C NMR (75 MHz, $CDCl_3$): δ 9.8, 25.7, 43.7, 65.7, 127.9, 128.0, 129.0, 137.9, 169.2; HRMS (ESI+) calc. for $C_{11}H_{14}N_4ONa$: 241.1065, found: 241.1043. HPLC (Chiralcel AD, heptane/*i*-PrOH, 95/5, v/v, 1 mL/min), Rt (min): 8.6 (*R*), 10.2 (*S*).

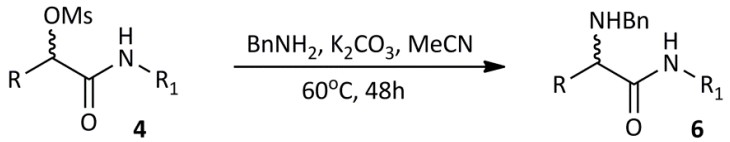

*General procedure C: Synthesis of racemic α-benzylamino-amides **6***

To a solution of α-methanesulfonyloxy-amide **4** (0.20 mmol) and benzylamine (0.40 mmol, 44 μL) in MeCN (1.5 mL) was added potassium carbonate (0.40 mmol, 55 mg) and the resultant suspension was stirred at 60°C overnight. Another portion of benzylamine (1.0 mmol, 110 μL) was added and the stirring at 60°C continued for next 24 h. The volatiles

were evaporated and the product was purified by flash chromatography (Silicagel, 40-63 μm, pentane/AcOEt, 9:1 to 1:3, v/v).

6a: N-benzyl-2-(phenoxy)propanamide

Yield: 71%. Clear oil. R_f = 0.25 (pentane/AcOEt. 1:1, v/v); ^{1}H NMR (400 MHz, $CDCl_3$): δ1.35 (d, ^3J = 6.9 Hz, 3H, C**H$_3$**CH), 1.56 (br s, 1H, N**H**), 3.31 (q, ^3J = 6.9 Hz, 1H, C**H**NH), 3.73 (s, 2H, CHNHC**H$_2$**), 4.45 (d, ^3J = 6.0 Hz, 2H, CONHC**H$_2$**), 7.20-7.37 (m, 10H, Ar**H**), 7.61 (br s, 1H, N**H**); ^{13}C NMR (75 MHz, $CDCl_3$): δ 20.1, 43.2, 52.9, 58.2, 127.5, 127.6, 127.8, 128.2, 128.8, 128,9, 138.8, 139.7, 175.0; HRMS (ESI+) calc. for $C_{17}H_{21}N_2O$: 269.1648, found: 269.1646. HPLC (Chiralcel OJ, heptane/*i*-PrOH, 95/5, v/v, 1 mL/min), Rt (min): 23.9 (*S*), 28.5 (*R*).

6b: *tert*-butyl 2-(2-phenoxypropanamido)acetate

Yield: 83%. Clear oil. R_f = 0.30 (pentane/AcOEt. 1:1, v/v); ^{1}H NMR (400 MHz, $CDCl_3$): δ 1.33 (d, ^3J = 6.8 Hz, 3H, C**H$_3$**CH), 1.47 (s, 9H, (C**H$_3$**)$_3$), 1.58 (br s, 1H, N**H**Bn), 3.27 (q, ^3J = 6.8 Hz, 1H, C**H**NH), 3.72 (d, ^2J = 12.8 Hz, 1H, COC**H$_2$**), 3.84 (d, ^2J = 12.8 Hz, 1H, COC**H$_2$**), 3.86-4.00 (m, 2H, PhC**H$_2$**), 7.24-7.33 (m, 5H, Ar**H**), 7.68 (br s, 1H, CON**H**); ^{13}C NMR (50 MHz, $CDCl_3$): δ 19.9, 28.3, 41.8, 52.8, 57.9, 82.8, 127.4, 128.4, 128.7, 139.8, 169.2, 175.2; HRMS (ESI+) calc. for $C_{16}H_{25}N_2O_3$: 293.1860, found: 293.1856. HPLC (Chiralcel OD, heptane/*i*-PrOH, 9/1, v/v, 1 mL/min), Rt (min): 6.7 (*R*), 7.4 (*S*).

6c: *N*-benzyl-2-(phenoxy)butanamide

Yield: 23%. Clear oil. R_f = 0.40 (pentane/AcOEt. 1:1, v/v); ^{1}H NMR (400 MHz, $CDCl_3$): δ 0.95 (t, ^3J = 7.6 Hz, 3H, C**H$_3$**CH$_2$), 1.60-1.86 (m, 3H, CH$_3$C**H$_2$**, N**H**), 3.15 (dd, ^3J = 7.2 Hz, ^3J = 5.2 Hz, 1H, C**H**NH), 3.66-3.76 (m, 2H, CHNHC**H$_2$**), 4.46 (d, ^3J = 6.0 Hz, 2H, CONHC**H$_2$**), 7.20-7.35 (m, 10H, Ar**H**), 7.56 (br s, 1H, N**H**); ^{13}C NMR (75 MHz, $CDCl_3$):δ 10.4, 26.9, 43.2, 53.2, 64.0, 127.5, 127.6, 127.9, 128.3, 128.8, 128.9, 138.8, 139.7, 174.2; HRMS (ESI+) calc. for $C_{18}H_{23}N_2O$: 283.1805, found: 283.1797. HPLC (Chiralcel OJ-H, heptane/*i*-PrOH, 9/1, v/v, 1 mL/min), Rt (min): 17.7 (*R*), 22.4 (*S*).

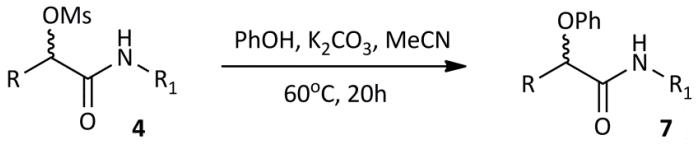

*General procedure D: Synthesis of racemic α-phenoxy-amides **7***

To a solution of α-methanesulfonyloxy-amide **4** (0.20 mmol) and phenol (0.40 mmol, 38 mg) in MeCN (1.5 mL) was added potassium carbonate (0.40 mmol, 55 mg) and the resultant suspension was stirred at 60°C overnight. The volatiles were evaporated and the product was purified by flash chromatography (Silicagel, 40-63 μm, pentane/AcOEt, 9:1 to 4:1, v/v).

7a: *N*-benzyl-2-(phenoxy)propanamide.

Yield: 73%. White crystals. R_f = 0.68 (pentane/AcOEt. 1:1, v/v); mp. 89-90°C (lit.[31] 87.5-88.5); ^{1}H NMR (400 MHz, $CDCl_3$): δ 1.60 (d, ^3J = 6.8 Hz, 3H, C**H$_3$**CH), 4.40-4.53 (m, 2H,

NHC**H**$_2$), 4.74 (q, ^3J = 6.8 Hz, 1H, C**H**O), 6.77 (br s, 1H, N**H**), 6.89 (d, ^3J = 6.0 Hz, 2H, Ar**H**), 7.00 (app t, ^3J = 6.0 Hz, 1H, Ar**H**), 7.15 (d, ^3J = 6.0 Hz, 2H, Ar**H**), 7.24-7.30 (m, 5H, Ar**H**); ^{13}C NMR (50 MHz, $CDCl_3$): δ 18.9, 42.9, 75.0, 115.5, 122.1, 127.5, 128.7, 129.8, 137.9, 156.9, 172.2; HRMS (ESI+) calc. for $C_{16}H_{17}NO_2$: 278.1152, found: 278.1143. HPLC (Chiralcel OJ-H, heptane/*i*-PrOH, 95/5, v/v, 1 mL/min), Rt (min): 32.3 (*S*), 33.8 (*R*).

7b: *tert*-butyl 2-(2-phenoxypropanamido)acetate

Yield: 69%. Clear oil. R_f = 0.76 (pentane/AcOEt. 1:1, v/v); ^{1}H NMR (400 MHz, $CDCl_3$): δ 1.45 (s, 9H, (C**H**$_3$)$_3$), 1.58 (d, ^3J = 6.8 Hz, 3H, C**H**$_3$CH), 3.87 (dd, ^2J = 18.0 Hz, ^3J = 5.2 Hz, 1H, NHC**H**$_2$), 4.02 (dd, ^2J = 18.0 Hz, ^3J = 6.0 Hz, 1H, NHC**H**$_2$), 4.71 (q, ^3J = 6.8 Hz, 1H, C**H**O), 6.91-7.31 (m, 6H, Ar**H**, N**H**); ^{13}C NMR (50 MHz, $CDCl_3$): δ 18.9, 28.2, 41.9, 75.2, 82.6, 115.8, 122.3, 130.0, 157.2, 168.7, 172.5; HRMS (ESI+) calc. for $C_{15}H_{21}NO_4Na$: 302.1363, found: 302.1358. HPLC (Chiralcel OJ, heptane/*i*-PrOH, 98/2, v/v, 1 mL/min), Rt (min): 10.6 (*S*), 11.8 (*R*).

7c: *N*-benzyl-2-(phenoxy)butanamide

Yield: 91%. White solid. R_f = 0.74 (pentane/AcOEt. 1:1, v/v); mp. 63-64°C. ^{1}H NMR (400 MHz, $CDCl_3$): δ1.05 (t, ^3J = 7.2 Hz, 3H, C**H**$_3$CH$_2$), 1.92-2.11 (m, 2H, C**H**$_2$CH), 4.40-4.55 (m, 2H, NHC**H**$_2$), 4.60 (dd, ^3J = 6.4 Hz, ^3J = 4.4 Hz, 1H, C**H**O), 6.73 (br s, 1H, N**H**), 6.91 (d, ^3J = 8.0 Hz, 2H, Ar**H**), 7.01 (app t, ^3J = 7.6 Hz, 1H, Ar**H**), 7.15 (d, ^3J = 8.0 Hz, 2H, Ar**H**), 7.24-7.30 (m, 5H, Ar**H**); ^{13}C NMR (75 MHz, $CDCl_3$): δ 9.6, 26.4, 43.1, 80.1, 115.7, 122.3, 127.7, 128.9, 129.0, 138.2, 157.7, 171.8; HRMS (ESI+) calc. for $C_{17}H_{20}NO_2$: 270.1489, found: 270.1473. HPLC (Chiralcel AD, heptane/*i*-PrOH, 95/5, v/v, 1 mL/min), Rt (min): 9.7 (*R*), 11.0 (*S*).

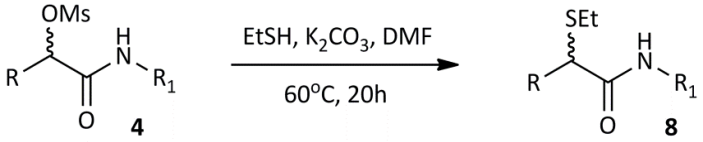

*General procedure E: Synthesis of racemic α-ethylthio-amides **8***

To a solution of α-methanesulfonyloxy-amide **4** (0.20 mmol) and ethanethiol (0.40 mmol, 30 μL) in DMF (0.5 mL) was added potassium carbonate (0.40 mmol, 55 mg) and the resultant suspension was stirred at 60°C overnight. The volatiles were evaporated and the product was purified by flash chromatography (Silicagel, 40-63 μm, pentane/AcOEt, 9:1 to 4:1, v/v).

8a: *N*-benzyl-2-(ethylthio)propanamide

Yield: 70%. Clear oil. R_f = 0.76 (pentane/AcOEt. 1:1, v/v); ^{1}H NMR (400 MHz, $CDCl_3$): δ 1.21 (t, ^3J = 7.6 Hz, 3H, C**H**$_3$CH$_2$), 1.49 (d, ^3J = 7.6 Hz, 3H, C**H**$_3$CH), 2.53 (q, ^3J = 7.6 Hz, 2H, CH$_3$C**H**$_2$), 3.45 (q, ^3J = 7.6 Hz, 1H, C**H**S), 4.46 (d, ^3J = 6.0 Hz, 2H, NHC**H**$_2$), 7.06 (br s, 1H, N**H**), 7.27-7.36 (m, 5H, Ar**H**); ^{13}C NMR (75 MHz, $CDCl_3$): δ 14.7, 19.0, 25.9, 44.0, 44.7, 127.8, 127.9, 129.0, 138.4, 172.8; HRMS (ESI+) calc. for $C_{12}H_{18}NOS$: 224.1108, found: 224.1104. HPLC (Chiralcel OJ, heptane/*i*-PrOH, 95/5, v/v, 1 mL/min), Rt (min): 13.6 (*R*), 14.8 (*S*).

8b: *tert*-butyl 2-(2-(ethylthio)propanamido)acetate

Yield: 45%. Clear oil. R_f = 0.80 (pentane/AcOEt. 1:1, v/v); ^{1}H NMR (400 MHz, $CDCl_3$): δ 1.25 (t, ^3J = 7.6 Hz, 3H, C**H$_3$**CH$_2$), 1.47 (s, 9H, (C**H$_3$**)$_3$), 1.48 (d, ^3J = 6.8 Hz, 3H, C**H$_3$**CH), 2.60 (q, ^3J = 7.6 Hz, 2H, CH$_3$C**H$_2$**), 3.44 (q, ^3J = 6.8 Hz, 1H, C**H**S), 3.88 (dd, ^2J = 18.0 Hz, ^3J = 5.2 Hz, 1H, NHC**H$_2$**), 4.00 (dd, ^2J = 18.0 Hz, ^3J = 5.6 Hz, 1H, NHC**H$_2$**), 7.19 (br s, 1H, N**H**); ^{13}C NMR (75 MHz, $CDCl_3$): δ 14.6, 18.8, 25.9, 28.3, 42.4, 44.4, 82.4, 169.0, 173.0; HRMS (ESI+) calc. for $C_{11}H_{21}NO_3SNa$: 270.1140, found: 270.1135. HPLC (Chiralcel OD, heptane/*i*-PrOH, 98/2, v/v, 1 mL/min), Rt (min): 9.3 (*R*), 10.8 (*S*).

8c: *N*-benzyl-2-(ethylthio)butanamide

Yield: 97%. Clear oil. R_f = 0.75 (pentane/AcOEt. 1:1, v/v); ^{1}H NMR (400 MHz, $CDCl_3$): δ 1.02 (t, ^3J = 7.6 Hz, 3H, C**H$_3$**CH$_2$S) 1.20 (t, ^3J = 7.6 Hz, 3H, C**H$_3$**CH), 1.68-1.82 (m, 1H, CH$_3$C**H$_2$**CH), 1.85-1.98 (m, 1H, CH$_3$C**H$_2$**CH), 2.51 (q, ^3J = 7.6 Hz, 2H, CH$_3$C**H$_2$**S), 3.27 (app t, ^3J = 6.4 Hz, 1H, C**H**S), 4.46 (d, ^3J = 6.0 Hz, 2H, NHC**H$_2$**), 7.07 (br s, 1H, N**H**), 7.27-7.34 (m, 5H, Ar**H**); ^{13}C NMR (75 MHz, $CDCl_3$): δ 12.2, 14.7, 26.0, 26.4, 43.9, 52.2, 127.7, 127.9, 128.9, 138.5, 172.3; HRMS (ESI+) calc. for $C_{13}H_{20}NOS$: 238.1260, found: 238.1248. HPLC (Chiralcel OJ, heptane/*i*-PrOH, 95/5, v/v, 1 mL/min), Rt (min): 12.0 (*R*), 13.1 (*S*).

General procedure F: chemoenzymatic synthesis of α-substituted amides

Production and purification of the haloalkane dehalogenases was performed as described before.[26] Enzyme (see table) was added to a solution of α-bromoamide ***rac*-2** (see table) in 50 mM Tris.SO_4 buffer pH 8.2 (table) and the resultant reaction mixture was incubated at 30°C. After the time indicated in the table the solution was extracted with EtOAc (4 x 50 mL). The combined organic solutions were dried and the solvents were evaporated. The residue was dissolved in DCM (3.0 mL) and cooled in an ice-water bath. Triethylamine (0.50 mmol, 70 μL) was added, followed by the solution of methanesulfonyl chloride (0.12 mmol, 19 μL) in DCM (1.0 mL). The cooling bath was removed and the reaction mixture was stirred for 30 min at rt. The volatiles were evaporated and the residue was reacted further according to **general procedures B-E**.

Substrate	amount	Buffer	enzyme	Reaction time
***rac*-2a**	0.17 mmol	125 mL	0.7 mg DbjA	46 h
***rac*-2b**	0.15 mmol	100 mL	0.84 mg DbjA	20 h
***rac*-2c**	0.15 mmol	175 mL	1.9 mg LinB	44 h

(*R*)-5a: (*R*)-2-Azido-*N*-benzylpropanamide

Yield: 81%. White crystals; mp = 59-59.5°C. $[\alpha]_D^{20}$= -40.0 (c 1.0, $CHCl_3$). Enantiomeric excess: 98%. Other data consistent with the ones obtained for racemic **5a**.

(*R*)-5b: (*R*)-*tert*-butyl 2-(2-azidopropanamido)acetate

Yield: 73%. Clear oil. $[\alpha]_D^{20}$= -42.2 (c 1.0, $CHCl_3$). Enantiomeric excess: 97%. Other data consistent with the ones obtained for racemic **5b**.

(*R*)-5c: (*R*)-2-Azido-*N*-benzylbutanamide

Yield: 80%. Clear oil. $[\alpha]_D^{20}$= -6.0 (c 1.0, $CHCl_3$). Enantiomeric excess: 95%. Other data consistent with the ones obtained for racemic **5c**.

(*R*)-6a: (*R*)-*N*-benzyl-2-(benzylamino)propanamide

Yield: 81%. Clear oil; $[\alpha]_D^{20}$= +4.2 (c 1.0, $CHCl_3$) (lit.[32] $[\alpha]_D^{20}$= -4.2 for the (*S*)-enantiomer) Enantiomeric excess: 97%. Other data consistent with the ones obtained for racemic **6a**.

(*R*)-6b: *tert*-butyl (*R*)-2-(2-phenoxypropanamido)acetate

Yield: 96%. Clear oil; $[\alpha]_D^{20}$= +4.2 (c 1.0, $CHCl_3$). Enantiomeric excess: 91%. Other data consistent with the ones obtained for racemic **6b**.

(*R*)-6c: (*R*)-*N*-benzyl-2-(benzylamino)butanamide

Yield: 85%. Clear oil; $[\alpha]_D^{20}$= +13.8 (c 1.0, $CHCl_3$). Enantiomeric excess: 90%. Other data consistent with the ones obtained for racemic **6c**.

(*R*)-7a: (*R*)-2-Phenoxy-*N*-benzylpropanamide

Yield: 70%. White crystals; mp = 89-90°C. $[\alpha]_D^{20}$= +8.4 (c 1.0, $CHCl_3$). Enantiomeric excess: 95%. Other data consistent with the ones obtained for racemic **7a**.

(*R*)-7b: *tert*-butyl (*R*)-2-(2-phenoxypropanamido)acetate

Yield: 57%. Clear oil. $[\alpha]_D^{20}$= -10.4 (c 1.0, $CHCl_3$). Enantiomeric excess: 93%. Other data consistent with the ones obtained for racemic **7b**.

(*R*)-7c: (*R*)-2-Phenoxy-*N*-benzylbutanamide

Yield: 66%. White crystals; mp = 74-75°C. $[\alpha]_D^{20}$= +20.6 (c 1.0, $CHCl_3$). Enantiomeric excess: 96%. Other data consistent with the ones obtained for racemic **7c**.

(*R*)-8a: (*R*)-*N*-benzyl-2-(ethylthio)propanamide

Yield: 82%. Clear oil; $[\alpha]_D^{20}$= +19.0 (c 1.0, $CHCl_3$). Enantiomeric excess: 28%. Other data consistent with the ones obtained for racemic **8a**.

(*R*)-8b: *tert*-butyl (*R*)-2-(2-(ethylthio)propanamido)acetate

Yield: 76%. Clear oil; $[\alpha]_D^{20}$= +21.5 (c 1.0, $CHCl_3$). Enantiomeric excess: 92%. Other data consistent with the ones obtained for racemic **8b**.

(*R*)-8c: (*R*)-*N*-benzyl-2-(ethylthio)butanamide

Yield: 63%. Clear oil; $[\alpha]_D^{20}$ = +41.0 (c 1.0, $CHCl_3$). Enantiomeric excess: 73%. Other data consistent with the ones obtained for racemic **8c**.

REFERENCES

[1] K. P. Kokko, M. K. Hadden, K. S. Orwig, J. Mazella, T. A. Dix, *J. Med. Chem.* **2003**, *46*, 4141-4148.

[2] W. A. van der Linden, P. P. Geurink, C. Oskam, G. A. van der Marel, B. I. Florea, H. S. Overkleeft, *Org. Biomol. Chem.* **2010**, *8*, 1885-1893.

[3] V. P. Mocharla, B. Colasson, L. V. Lee, S. Röper, K. B. Sharpless, C.-H. Wong, H. C. Kolb, *Angew. Chem. Int. Ed.* **2005**, *44*, 116 –120.

[4] W. Szymanski, R. Ostaszewski, *Tetrahedron Asymmetry* **2006**, *17*, 2667-2671.

[5] W. Szymanski, M. Zwolinska, R. Ostaszewski, *Tetrahedron* **2007**, *63*, 7647-7653.

[6] W. Szymanski, R. Ostaszewski, *Tetrahedron* **2008**, *64*, 3197-3203.

[7] J. F. Fisher, S. Mobashery, *Cancer Metastasis Rev.* **2006**, *25*, 115-136.

[8] S. Hanessian, L. Auzzas, A. Larsson, J. B. Zhang, G. Giannini, G. Gallo, A. Ciacci, W. Cabri, *ACS Med. Chem. Lett.* **2010**, *1*, 70-74.

[9] S. V. Andurkar, J. P. Stables, H. Kohn, *Bioorg. Med. Chem.* **1999**, *7*, 2381-2389.

[10] A. J. Lopez-Farre, D. Sacristan, J. J. Zamorano-Leon, N. San-Martin, C. Macaya, *Cardiovascular Therapeutics* **2008**, *26*, 65-74.

[11] B. Barlaam, T. G. Bird, C. Lambert-van der Brempt, D. Campbell, S. J. Foster, R. Maciewicz, *J. Med. Chem.* **1999**, *42*, 4890-4908.

[12] J. T. Repine, J. S. Kaltenbronn, A. M. Doherty, J. M. Hamby, R. J. Himmelsbach, B. E. Kornberg, M. D. Taylor, E. A. Lunney, C. Humblet, S. T. Rapundalo, B. L. Batley, M. J. Ryan, C. A. Painchaud, *J. Med. Chem.* **1992**, *35*, 1032-1042.

[13] Y. Simeo, W. Kroutil, K. Faber, in *Enzymes in Action: Green Solutions for Chemical Problems*, (Eds: B. Zwanenburg, M. Mikołajczyk, P. Kiełbasiński), Kluwer Academic Publishers, Dordrecht, **2000**, pp. 27-51.

[14] L. Cao, J. T. Lee, W. Chen, T. K. Wood, *Biotechnol. Bioeng.* **2006**, *94*, 522-529.

[15] K. M. Manoj, A. Archelas, J. Baratti, R. Furstoss, *Tetrahedron* **2001**, *57*, 695-701.

[16] E. Y. Lee, M. L. Shuler, *Biotechnol. Bioeng.* **2007**, *98*, 318-327.

[17] S. Hwang, C. Y. Choi, E. Y. Lee, *Biotechnol. Lett.* **2008**, *30*, 1219-1225.

[18] M. I. Monterde, M. Lombard, A. Archelas, A. Cronin, M. Arand, R. Furstoss, *Tetrahedron Asymmetry* **2004**, *15*, 2801-2805.

[19] H. Danda, T. Nagatomi, A. Maehara, T. Umemura, *Tetrahedron* **1991**, *47*, 8701-8716.

[20] K. Lemke, S. Ballschuh, A. Kunath, F. Theil, *Tetrahedron Asymmetry* **1997**, *8*, 2051-2055.

[21] S. Takano, M. Suzuki, K. Ogasawara, *Tetrahedron:Asymmetry* **1993**, *4*, 1043-1046.

[22] S. R. Wallner, M. Pogorevc, H. Trauthwein, K. Faber, *Eng. Life Sci.* **2004**, *4*, 512-516.

[23] P. Gadler, T. C. Reiter, K. Hoelsch, D. Weuster-Botz, K. Faber, *Tetrahedron Asymmetry* **2009**, *20*, 115-118.

[24] M. Schober, P. Gadler, T. Knaus, H. Kayer, R. Birner-Grünberger, C. Gülly, P. Macheroux, U. Wagner, K. Faber, *Org. Lett.* **2011**, *13*, 4296-4299.

[25] D. B. Janssen, *Curr. Opin. Chem. Biol.* **2004**, *8*, 150-159.

[26] Chapter 3 of this thesis.

[27] E. Vänttinen, L. Kanerva, *Tetrahedron Assymetry* **1995**, *6*, 1779-1786.

[28] S. Pedragosa-Moreau, C. Morisseau, J. Baratti, J. Zylber, A. Archelas, R. Furstoss, *Tetrahedron*. **1997**, *53*, 9707-9714.

[29] D. J. Cram, J. *Fundamentals of Carbanion Chemistry*; Academic Press: New York, 165; pp 71-84.

[30] C.F. Bernasconi, K. W. Kittredge, *J. Org. Chem.* **1998,** *63,* 1944-1953.

[31] S. Kushner, R. I. Cassell, R. I., J. Morton II, J. H. Williams, *J. Org. Chem*. **1951**, *16*, ` 1283-1288..

[32] F. D'Angeli, P. Marchetti, G. Cavicchioni, G. Catelani, F. M. K. Nejad, *Tetrahedron Asymmetry*, **1990**, *1*, 155-158

CHAPTER 6

Conclusions and perspectives

Haloalkane dehalogenases are enzymes that cleave carbon-halogen bonds in haloalkanes and produce the respective alcohols. Since the discovery of the first enzyme from this class in 1985,[1] 14 haloalkane dehalogenases have been characterised. Several applications of haloalkane dehalogenases have been described, including the treatment of groundwater and neutralisation of the chemical warfare agent sulfur mustard gas.[2,3] Furthermore, a haloalkane dehalogenase was engineered to function as a protein label that can be applied for cell imaging.[4] Apart from those applications, haloalkane dehalogenases are promising biocatalysts in white biotechnology.

In an industrial context, it is of great importance to achieve high yields of pure products. Furthermore, for the synthesis of pharmaceuticals and their intermediates, it is essential to obtain enantiopure compounds. Haloalkane dehalogenases provide a promising bio-based platform to fulfill these requirements. In this thesis, the diversity of reactions catalysed by haloalkane dehalogenases and their potential use in applied biocatalysis were explored. Moreover, we investigated alternative ways to go beyond kinetic resolution aiming at high yields and high enantiopurity.

CONCLUSIONS

In **chapter 3** of this thesis, activity and stereoselectivity of haloalkane dehalogenases were explored with a group of fourteen α-bromoamides. Optically pure α-haloamides are interesting building blocks in medicinal chemistry and peptide synthesis, because of the presence of a good leaving group. Catalytic activity with eight of the fourteen α-bromoamides was found and for seven compounds the conversion proceeded with high stereoselectivity (E-values of over 200 or high diasteroselectivity yielding diastereomeric excess of > 95%). Preparative-scale experiments were carried out and gave yields of 31-50% for both optically pure substrates and products. A theoretical investigation was conducted to explain the enantioselectivity found for two of the α-bromoamides with haloalkane dehalogenase LinB. The results of substrate docking and subsequent molecular dynamics simulations were in agreement with the enantioselectivity found experimentally. Furthermore, the simulations indicated that the enantioselectivity is caused by the difference in the time that the two isomers exist in a catalytically favorable conformation in the enzyme active site. For a reaction to occur, the following six parameters have to be in a required range: the distances of the substrate to the attacking nucleophile and to the two halogen-stabilising residues, and the angles of the substrate with the attacking nucleophile and with the two halogen-stabilising residues. The percentage of time that these six parameters were in the required range, resulting in a near attack conformation (NAC), was examined by inspecting the simulations. For poorly converted substrates, it was reported earlier that the critical step is the first nucleophilic attack. Therefore, in such cases, the E-value represents the ratio of the NAC percentages

observed for the two enantiomers, assuming that both enantiomers bind similarly well. For five of the six parameters, no distinct differences were found between the two enantiomers. However, for the angle between the oxygen from the attacking nucleophilic aspartate, the attacked carbon atom of the substrate and the halogen atom of the substrate, it was found that the preferred (*R*)-enantiomer resided more often in a NAC, where the angle has to be >157°. The E-values observed in the experiments were in good agreement with the ratio of the NAC percentages found in the simulations. These results show that substrate docking and subsequent molecular dynamics can provide valuable insight into the origins of stereoselectivity. Furthermore, the simulations can be used to predict the preferred enantiomer of a substrate and the E-value of the enzyme. Beyond that, one could think of using the knowledge derived from molecular dynamics and the way it can predict enantioselectivity as a tool to design mutants. This could lead to mutations that increase the enantioselectivity or even invert the enantiopreference, especially in cases where the nucleophilic attack is the rate-limiting step of the reaction that distinguishes the enantiomers.

The high enantioselectivity of haloalkane dehalogenases with α-bromoamides was exploited in **chapter 5** to obtain high yields of α-substituted amides, using an enantioconvergent chemoenzymatic process. The haloalkane dehalogenase-catalysed reaction proceeds via an S_N2 type substitution, which results in an inversion of configuration of the halogen-bearing carbon. Therefore, a kinetic resolution yields two compounds with the same absolute configuration. The bromide of the α-bromoamide is a good leaving group, while the hydroxyl moiety can be easily transformed into a methanesulfonyl ester, also a good leaving group. This activation of the hydroxy-group was performed immediately after extraction of the biocatalysis products, without prior separation of α-bromoamide and α-hydroxyamide. A second reaction, a nucleophilic substitution where different *N*-, *O*- and *S*-nucleophiles were used, generated various α-substituted amides. This process was performed without purification of the intermediates and is therefore highly efficient. Yields up to 96% and e.e.'s up to 98% were observed. In this way, inexpensive racemic substrates can be converted into single enantiomers of valuable products.

A kinetic resolution with an *in situ* chemical racemisation of the substrate can be used to achieve a dynamic kinetic resolution process, as described in **chapter 4**. Different ways to racemise the model substrate methyl-2-bromopropionate, were explored. Simple bromide ions were found to racemise the substrate only at high concentrations, at which the enzyme was inhibited. Two other bromide sources, a lipophilic phosphonium bromide and a polymer-based phosphonium bromide, were found to be more efficient racemising agents. Both compounds were observed to inhibit the enzyme to a certain extent. For the polymer-based compound, we took advantage of the insolubility of the material, which

allows the separation of the enzyme and the racemising agent by a semi-permeable membrane. The α-bromoesters methyl-2-bromopropionate and butyl-2-bromopropionate were found to be converted in an enantioselective manner and were easily racemised. However, these compounds were found to be less stable than the α-bromoamides described in chapters 3 and 5. Therefore the dynamic kinetic resolution was performed on an α-bromoamide, *N*-phenyl-2-bromopropionamide, which was converted to (*S*)-*N*-phenyl-2-hydroxypropionamide with a yield of 63% (95% e.e.) or 78% (88 % e.e.). Chapter 4 presents an example of the preparation of enantiopure alcohols, without using hazardous heavy metal complexes as catalysts.

Chapter 2 describes a method for preparation of chiral haloalcohols by asymmetric transformations. In order to achieve this, a haloalkane dehalogenase-catalysed tandem desymmetrisation of prochiral and *meso* dihaloalkanes and a kinetic resolution of the produced haloalcohol were used. In the first reaction, a chiral center is introduced when a dihaloalkane is converted to the corresponding haloalcohol, while in the tandem kinetic resolution, this product can be converted to the diol. For two substrates, the enantiomeric excess of the haloalcohol increased during the kinetic resolution, as the enantiomer of the haloalcohol that is produced in lower quantity in the first step, is the preferred substrate for the second reaction. Although yields of only 24% and 52% were described, this chapter shows the first applications of haloalkane dehalogenases for a tandem desymmetrisation/kinetic resolution process.

In this thesis it is described that haloalkane dehalogenases can be of great value for production of enantiopure compounds. The fact that the dehalogenation of the substrate proceeds via an S_N2 nucleophilic subsitution, resulting in inversion of configuration at the reactive carbon atom, gives rise to great possibilities. The bromide and hydroxy groups that are present in the products possess the same configuration and can easily be functionalised to other groups, which make haloalkane dehalogenase-catalysed processes versatile, and useful for high-yielding production of haloalkanes and alcohols as well as a range of derived compounds. Furthermore, the configuration of the products can be inverted, which overcomes limitations caused by the homochirality of haloalkane dehalogenases.[5]

PERSPECTIVES

Substrates with bulky hydrophobic groups usually have low solubility in an aqueous environment. Therefore, increasing the yield of biocatalytic reactions often requires the addition of a co-solvent when considering application in an industrial context. In chapter 3 of this thesis, haloalkane dehalogenase DbjA was found to be able to catalyse dehalogenation in the presence of 25 vol% of dimethylsulfoxide, while retaining 50% of its activity. At 50 vol% of dimethylsulfoxide, the activity has dropped to <5% of the original value. This was probably caused by the instability of the biocatalyst. It is likely that a more rigid, thermostable mutant displays higher resistance towards organic solvents.

Since solvent resistance and thermostability are believed to be correlated, we attempted to improve the thermostability of LinB by using FoldX software for calculating the decrease in energy levels caused by mutations. In preliminary experiments, single mutants were selected in two different set ups. In the first one, the region within 9Å from the substrate binding site was left unaffected. In this case, FoldX predicted a decrease of more than 6 kJ per monomer for 40 different mutants. These mutants were visually inspected and subsequently 9 were constructed. In another set up, a region of 8.5Å from the bromide atom of the substrate was left unaffected and additionally only regions within 8Å from flexible parts of the protein, where the B-factor is higher than 20, were selected.[6] All possible mutants were visually inspected and subsequently 12 mutants were constructed.

An improvement in thermostability of LinB was found when a residue located in the cap domain, at the entrance tunnel, was mutated. A melting point increase of 5°C was found for this mutant, D147L, albeit the activity of the mutant had dropped to only 6% of the wildtype activity at 25°C. At 40°C, the activity increased more for the mutant than for the wildtype to a relative activity of 13%. Other mutants that were suggested only gave a rise of 1°C in the melting temperature, but the activity stayed more or less similar to the wildtype enzyme.

From preliminary results of measurements on the influence of the co-solvents dimethylsulfoxide (DMSO) and dimethylformamide (DMF) on the activity, we concluded that mutant D147L is relatively more active in the presence of DMSO and DMF than the wildtype LinB (Figure 1). Remarkably, the activity of the mutant increases with an increasing concentration of co-solvent. The highest activity for mutant D147L is measured in the presence of 50% DMSO and 25% DMF, where for the wildtype the activity already decreased at 10% co-solvent.

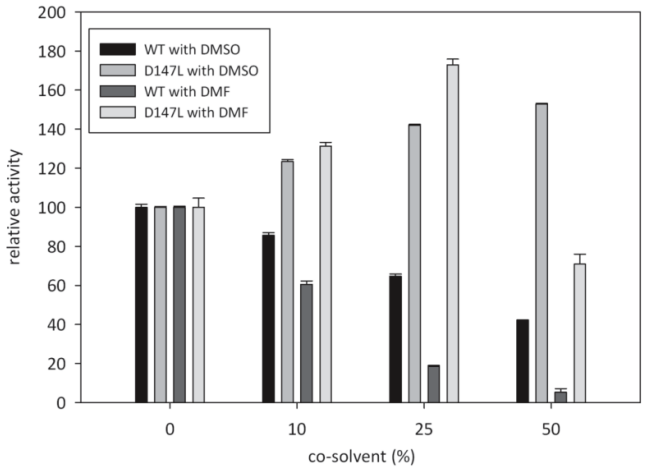

Figure 1: Relative activity of wildtype LinB and mutant D147L with increasing amounts of co-solvents DMSO and DMF. The reactions were performed with 4.5 mM 1,2-dibromoethane in 50 mM Tris.SO_4 with 0, 10, 25 and 50% DMSO, at 30°C, using 0.0025 mg/ml and 0.06 mg/ml enzyme for WT and D147L, respectively. The reactions were carried out for 60 min (DMSO) or 20 min (DMF).

Although the activity of this mutant is much lower than of the wildtype LinB, these results indicate that the thermostability measured indeed correlates to the activity in the presence of a co-solvent. Furthermore, more extensive computational evaluation of the effect of point mutations and the constructions of mutants that carry multiple stabilising mutations is expected to yield improved variants for use with co-solvents. While these experiments have not yielded both an active and stable mutant yet, they provide a promising approach to obtain such mutants. The knowledge that was obtained in chapter 3 regarding the understanding of the structural basis of the enantioselectivity can be of great importance in order to improve or even invert the enantioselectivity. Besides being better applicable for poorly soluble substrates, a thermostable mutant would provide a solid starting point for introducing mutations close to the active site that influence catalytic properties.

In this thesis we found a range of new substrates that are converted by haloalkane dehalogenases. A number of these were converted with high stereoselectivity. The absolute catalytic activity of these enzymes is somewhat limited, the observed rates mostly do not exceed 10 U/mg (see chapter 1 and 2 for more details). However, the excellent soluble expression of these enzymes, the simple single purification step that we employed and the intrinsic stability will make the enzyme the non-limiting factor for biocatalysis. The ever-increasing amount of genome data available provides a great resource to find new haloalkane dehalogenases with high activity towards both existing and novel substrates. A simple protein BLAST search with one of the haloalkane dehalogenases described in this thesis as input already yields many uncharacterised

homologs with at least 40% sequence identity. However, the haloalkane dehalogenases described in this thesis possess sequence identities from as high as 57% to even as low as 17%, when compared. This implies that there are putatively many more haloalkane dehalogenases available in the database that initially are not found by such a blast search, because of this low sequence identity.

I believe that through a combined approach of genome mining, enzyme redesign and directed evolution[7] a wide range of haloalkane dehalogenases with novel applications can be implemented in white biotechnology for the production of important enantiopure building blocks.

REFERENCES

[1] S. Keuning, D. B. Janssen, and B. Witholt. *J. Bacteriol.* **1985**, *163*, 635-639.

[2] G. Stucki and M. Thuer. *Environ. Sci. Technol.* **1995**, *29*, 2339-2345.

[3] Z. Prokop, F. Oplustil, J. DeFrank, and J. Damborsky. *Biotechnol. J.* **2006**, *1*, 1370-1380.

[4] G. V. Los, L. P. Encell, M. G. McDougall, D. D. Hartzell, N. Karassina, C. Zimprich, M. G. Wood, R. Learish, R. F. Ohana, M. Urh, D. Simpson, J. Mendez, K. Zimmerman, P. Otto, G. Vidugiris, J. Zhu, A. Darzins, D. H. Klaubert, R. F. Bulleit, and K. V. Wood. *ACS Chem. Biol.* **2008**, *3*, 373-382.

[5] F. Dangeli, P. Marchetti, and V. Bertolasi. *J. Org. Chem.* **1995**, *60*, 4013-4016.

[6] M. T. Reetz, J. D. Carballeira, and A. Vogel. *Angew. Chem. Int. Ed Engl.* **2006**, *45*, 7745-7751.

[7] J. G. van Leeuwen, H. J. Wijma, R. J. Floor, J. M. van der Laan, and D. B. Janssen. *ChemBioChem.* **2012**, *13*, 137-148.

NEDERLANDSE SAMENVATTING

Ook voor een ieder buiten het vakgebied

Kijk eens goed naar je eigen handen. Aan elke hand zitten precies dezelfde dingen: een duim, wijsvinger, middelvinger, ringvinger en pink, verder zijn alle botjes in je hand hetzelfde. De vorm is hetzelfde en ook zijn ze gelijk in gewicht. Maar kijk nu nog eens iets beter. Wat valt je op? Je handen mogen dan wel uit precies dezelfde onderdelen bestaan, toch zijn ze verschillend, omdat ze elkaars spiegelbeelden zijn.

IJDELE SCHEIKUNDE

Net als met handen lijken sommige moleculen precies op elkaar, maar zijn ze elkaars spiegelbeelden en zijn ze dus niet helemaal hetzelfde. Wel hebben ze dezelfde opbouw, met dezelfde atomen, in dezelfde volgorde en op dezelfde posities. Het gewicht is ook precies gelijk. Zulke spiegelbeelden noemen we *enantiomeren*; er is dan een “linker” en een “rechter” variant. Enantiomeren spelen een belangrijke rol in de biologie en scheikunde en daarmee ook in ons lichaam en in bacteriën, planten en dieren.

Bij bijna alle processen in ons lichaam zijn eiwitten betrokken. Eiwit is het belangrijkste onderdeel van je haar, huid en nagels en eiwitten zijn van groot belang in je afweersysteem. Ook zijn eiwitten betrokken bij het verwerken van je voedsel. In het laatste geval werken eiwitten als katalysatoren, ze versnellen de afbraak van voedingsmiddelen tot nuttige bouwstenen en energiebronnen voor ons lichaam. In zo’n geval wordt een eiwit ook wel een *enzym* genoemd. Er zijn heel veel verschillende soorten enzymen die elk een eigen stofje, ook wel *substraat* genoemd, herkennen en omzetten naar een product.
Eiwitten bestaan uit lange ketens van aan elkaar gekoppelde bouwstenen, zogeheten *aminozuren*. Van deze aminozuren bestaan ook twee varianten, twee enantiomeren. In de natuur wordt echter slechts één van de twee varianten gebruikt, de andere komt niet voor. Om deze reden bestaat er van een eiwit slechts één spiegelbeeld.
Het blijkt dat moleculen die hetzelfde lijken, maar enantiomeren en dus elkaars spiegelbeeld zijn, een verschillend effect kunnen hebben op ons lichaam. Zo kan de biologische uitwerking van de twee enantiomeren, bijvoorbeeld van een medicijn, compleet anders zijn. Een voorbeeld hiervan is de ontstekingsremmer naproxen. Het ene enantiomeer van naproxen geeft het gewenste effect, terwijl het andere maag-darmklachten tot gevolg heeft. In zo’n geval is het erg belangrijk dat slechts één van de enantiomeren wordt toegediend.

PRODUCTIE VAN ENANTIOMEREN

De productie van slechts één enantiomeer, een *enantiozuiver* product, kan uiterst lastig zijn. Enantiomeren lijken op elkaar en hebben dezelfde fysische eigenschappen, zoals bijvoorbeeld kook- en smeltpunt, daarom zijn ze moeilijk van elkaar te scheiden. Slechts één van de enantiomeren maken via een chemisch synthetische route is meestal lastig. In dat geval zijn er vaak giftige en milieuverontreinigende zware metalen nodig voor de productie.
Zoals eerder uitgelegd, bestaan enzymen uit bouwstenen van maar één enantiomeer. Je kunt je voorstellen dat ze daarom ook heel geschikt zijn om onderscheid te maken tussen twee enantiomeren van één substraat. Zoals op elk slot maar één sleutel past. Of vergelijk het met het feit dat je linkerhandschoen niet goed past aan je rechterhand. Deze eigenschap maakt enzymen erg interessant voor de productie van enantiozuivere moleculen.

HALOALKAAN DEHALOGENASES

In dit proefschrift wordt één klasse van enzymen besproken: haloalkaan dehalogenases. Deze enzymen voeren de omzetting van een halogeenatoom in een molecuul, zoals chloor of broom, naar een alcoholgroep uit, bestaande uit een zuurstof- en waterstofatoom. Het eerste enzym uit deze klasse werd ontdekt in 1985 door Groningse wetenschappers, in de bacterie *Xantobacter autotrophicus*. Hoewel we de precieze rol van haloalkaan dehalogenases in de natuur niet weten is het waarschijnlijk dat ze er voor zorgen dat giftige stoffen in de omgeving van de bacterie kunnen worden afgebroken. Op deze manier kunnen ze overleven in een omgeving die vervuild is met giftige halogeenrijke verbindingen. Daarom kunnen deze enzymen bijvoorbeeld ook gebruikt worden bij de sanering van grondwater dat is vervuild met normaalgesproken moeilijk afbreekbare halogeenrijke stoffen.

Dit proefschrift richt zich meer op de toepassingen van haloalkaan dehalogenases in de biokatalyse, in het bijzonder voor de productie van enantiozuivere moleculen. Er zijn verschillende strategieën om slechts één van beide enantiomeren te produceren.

KINETISCHE RESOLUTIE

De meest simpele manier is een zogeheten *kinetische resolutie*, zoals te zien is in figuur 1. De uitgangsstof, het substraat, bestaat uit twee enantiomeren, een “rechter” (R-1) en een “linker” (L-1). Substraat en enzym worden gemengd, waarna de reactie begint. Van de twee enantiomeren wordt alleen het “rechter” R-1 herkend door het enzym en deze

wordt omgezet naar het “linker” product L-2. Het “rechter” substraat wordt hierbij dus ook nog eens gespiegeld. Bij een volledige en perfecte reactie blijft L-1 over (50%) en maak je 50% product L-2. Succesvolle voorbeelden van dergelijke omzettingen door haloalkaan dehalogenases worden beschreven in hoofdstuk 3 van dit proefschrift. Ook wordt ingegaan op hoe het kan dat haloalkaan dehalogenases zo selectief zijn in dit soort reacties.

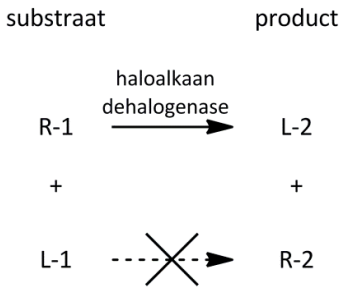

theoretische opbrengst: 50% L-1 en 50% L-2

Figuur 1: Kinetische resolutie met haloalkaan dehalogenases

Het substraat en het product hebben duidelijk andere fysische eigenschappen, waardoor ze relatief eenvoudig kunnen worden gescheiden. Echter, een nadeel van een dergelijke kinetische resolutie is het feit dat je 50% opbrengst krijgt van twee verschillende producten. Het zou economisch gezien aantrekkelijker zijn om een opbrengst van 100% te realiseren van één van beide.

EN VERDER...

Een manier om je opbrengst te verhogen is een zogenoemde *dynamische kinetische resolutie* (figuur 2). In dat geval wordt het enantiomeer L-1 met een extra chemische stap omgezet naar enantiomeer R-1, waarna het enzym het verder kan omzetten naar L-2. In theorie zou hierbij de opbrengst 100% kunnen zijn. In dit proefschrift, in hoofdstuk 4, wordt beschreven hoe een opbrengst van 78% is bereikt.

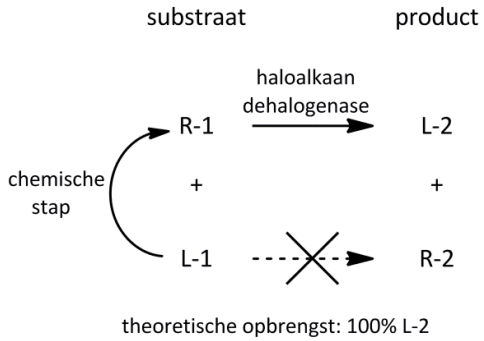

Figuur 2: Dynamische kinetische resolutie met haloalkaan dehalogenases

Een andere manier die is beschreven in hoofdstuk 5 van dit proefschrift is te zien in figuur 3. Zo'n dergelijke methode wordt een *enantioconvergent proces* genoemd. Na een kinetische resolutie, al eerder beschreven in figuur 1, worden extra chemische stappen uitgevoerd, waarbij zowel L-1 en L-2 kunnen worden omgezet naar enantiozuiver product R-3. Ook hierbij is de theoretische opbrengst 100%. In dit proefschrift worden opbrengsten tot 96% behaald. Met verschillende chemische stappen kunnen verschillende producten R-3 worden gemaakt.

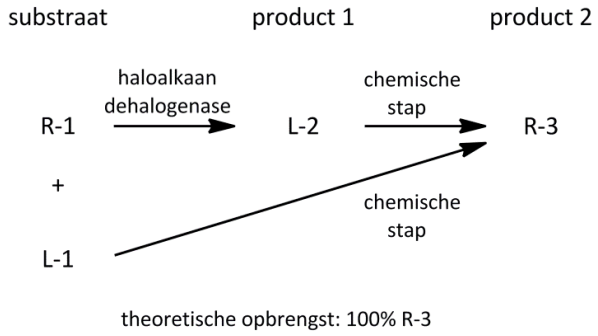

Figuur 3: Enantioconvergent process met haloalkaan dehalogenases

Kortom, in dit proefschrift heb ik aangetoond dat haloalkaan dehalogenases kunnen worden gebruikt voor de productie van enantiozuivere verbindingen, die bijvoorbeeld de basis kunnen vormen voor medicijnen. Echter, de proeven die ik heb gedaan zijn allemaal op laboratoriumschaal uitgevoerd. Voor industriële toepassingen zullen de reacties moeten worden opgeschaald. De experimenten beschreven in dit proefschrift kunnen hierbij een prima basis vormen voor verder onderzoek.

DANKWOORD

Leiden, april 2012

Het is af! Alle experimenten zijn uitgevoerd en alle zinnen getypt! Dan rest mij nog een ieder te bedanken die dit werk mede mogelijk heeft gemaakt. Ik wil een aantal mensen in het bijzonder bedanken.

Dick – Bedankt voor het vertrouwen in me, je praktische hulp en je wetenschappelijk kritische blik. Ik heb ontzettend veel geleerd en ik vind dat we trots mogen zijn op het resultaat.

Wiktor – Dit proefschrift was er, in deze vorm, niet geweest zonder jou. Bedankt voor je steun, zowel op wetenschappelijk als persoonlijk vlak, je geduld en je humor. Het is een eer jou als mijn paranimf te hebben.

Hein – Bedankt voor al je hulp, dankzij jou is hoofdstuk 3 super geworden. Het was zeer prettig samenwerken.

Peter – Bedankt voor al je inzet. Een 'echt' hoofdstuk met de behaalde resultaten zat er helaas niet in, maar dat maakt het niet minder gewaardeerd.

Verder wil ik mijn kantoorgenoten en de vaste koffie- en theeleuten bedanken. Het was enorm fijn om in onze koffiehoek de grote en kleine problemen uit deze wereld op te lossen, dan wel te relativeren. **Hanna –** bedankt voor je vrouwelijke steun tussen de koffiedrinkende mannen ;).

(Oud)bewoners van 'The far east' – Bedankt voor jullie organisch chemische hulp en de gezelligheid. **Alena** – teasing Wiktor was a pleasure with you.

Philana – Hoewel we door afstand zijn gescheiden is het altijd fijn om weer af te spreken. Bedankt voor je steun en relativeringsvermogen. Fijn dat je mijn paranimf wilt zijn.

Papa, **Mama**, **Henja** en **Jarne** – Bedankt voor jullie steun in de kansen die mij zijn gegeven. Oma zou net zo trots zijn geweest als jullie.

Maarten – Zonder jouw onvoorwaardelijke liefde was dit proefschrift er niet gekomen. Ik wil je danken voor je hulp en geduld. Je was er altijd voor me, ook in de moeilijkere tijden. Hopelijk komt ons leven binnenkort weer in een wat rustiger vaarwater.

Naast promoveren is het natuurlijk ook af en toe nodig om te ontspannen. Iedereen bedankt die wilde delen in heerlijke etentjes, bakavonturen, het drinken van wijntjes, theetjes, capu's of andere versnaperingen, zingen bij Roxie (en de drankjes nadien), saunabezoekjes, spelletjes spelen etc. Er gaat niets boven Groningse gezelligheid!

Alja